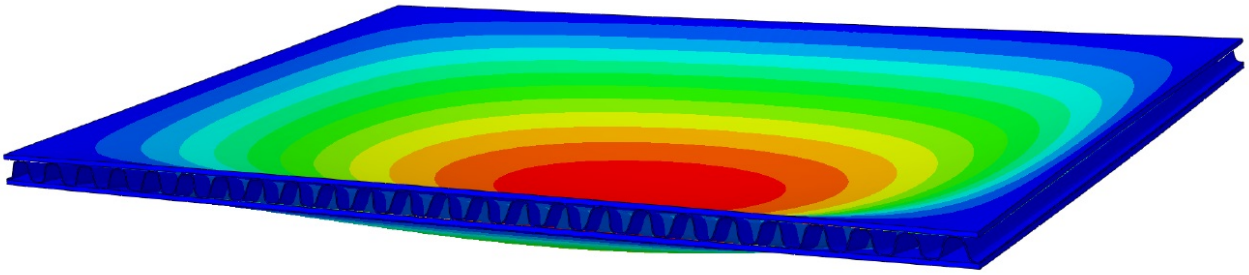

Innovative bio-composite sandwich element as floor system for multi-storey timber buildings

A structural analysis and optimization of the design

Master's thesis in the Master's Programme Structural Engineering and Building Technology

KAJSA FRÖJD
ANDREAS HELLSTRÖM

Department of Architecture and Civil Engineering
Division of Structural Engineering
Steel and Timber Structures
CHALMERS UNIVERSITY OF TECHNOLOGY
Gothenburg, Sweden 2017
Master's thesis 2017:66

MASTER'S THESIS 2017:66

Innovative bio-composite sandwich element as floor system for multi-storey timber buildings

A structural analysis and optimization of the design

Master's thesis in the Master's Programme Structural Engineering and Building Technology

KAJSA FRÖJD
ANDREAS HELLSTRÖM

Department of Architecture and Civil Engineering
Division of Structural Engineering
Steel and Timber Structures
CHALMERS UNIVERSITY OF TECHNOLOGY

Gothenburg, Sweden 2017

Innovative bio-composite sandwich element as floor system for multi-storey timber buildings
A structural analysis and optimization of the design
KAJSA FRÖJD
ANDREAS HELLSTRÖM

Master's thesis 2017:66
ISSN 1652-8557
Department of Architecture and Civil Engineering
Division of Structural Engineering
Steel and Timber Structures
Chalmers University of Technology
SE-412 96 Gothenburg
Sweden
Telephone: +46 (0)31-772 1000

Cover:
Picture from Abaqus, a finite element software, showing the deflection from a uniformly distributed load acting on the floor.

Chalmers Reproservice
Gothenburg, Sweden 2017

Innovative bio-composite sandwich element as floor system for multi-storey timber buildings
A structural analysis and optimization of the design
Master's thesis in the Master's Programme Structural Engineering and Building Technology
KAJSA FRÖJD
ANDREAS HELLSTRÖM
Department of Architecture and Civil Engineering
Division of Structural Engineering
Steel and Timber Structures
Chalmers University of Technology

ABSTRACT

Existing timber floors on the market are, in terms of height, not as competitive as other traditional building materials. The low shear stiffness of timber result in vigorously increasing dimensions as the spans gets longer. The awareness of the environmental issues are greater than ever which has increased the drive for more sustainable solutions which materials from renewable resources or bio-composites can contribute to.

A new type of timber floor, designed as a sandwich floor with a corrugated core has during the past years been under development at Chalmers University of Technology and this thesis is a continuation of the previous work. The scope is to reduce the height of apartment dividing floors in multi-storey buildings, to create less space consuming structures. This is of great importance to achieve the limitations in terms of total height in multi-storey timber buildings. If this could be achieved, the interest of timber as structural material would increase and contribute to a more sustainable future. The focus of the thesis is to improve the accuracy of the calculation model for the structural behaviour to gain the maximum efficiency in design of an optimal floor structure.

An optimization of the rather complex geometry is conducted analytically in this study by using Matlab. The effect of directional material properties and shear deformations, due to low stiffness of timber laminates, are incorporated into the analyses to improve the accuracy of the analytical results. Different timber products are investigated and since the material properties varies between different products, the optimal geometry changes accordingly. A validation in a finite element software, Abaqus, shows that the analytical solution can properly capture the structural behaviour of the floor. Different material combinations are optimized and a simple material cost review is made in order to make a comparison between the material combinations.

The results show that, in terms of structural behaviour, it is possible to significantly reduce the height of timber floors with the proposed design in comparison with existing timber floors on the market.

Keywords: Timber structure, Sandwich plate, Bio-composite, Corrugated core, Shear deformation, Orthotropic material, Finite element method, (FEM).

CONTENTS

PREFACE

The development of a new type of timber floor structure has a great potential to change the market of timber structures which has been very exiting to be a part of. Mathilda Larsson and Henrik Mayor did a great work in 2016 and it has been a pleasure to continue their work.

We want to thank our supervisor and examiner Rasoul Atashipour for the great support and help he provided. Through out the whole project, we have been in close contact with him, which has been of great importance for the work. His knowledge and scientific mindset has been very inspiring and motivating. Also our opponents Rebecca Eliasson and Simon Kastari has been of great importance with feedback of our work along the way. We also want to give a big thanks to "fikagruppen" that every Tuesday provided great pastries to the coffee break.

If the reader is more interested about the subject, we recommend to read Larsson's and Mayor's thesis to get a better understanding of the potential of the floor. Further on, the reader is expected to have basic knowledge in the structural behaviour of timber structures.

Gothenburg, June 2017

Kajsa Fröjd and Andreas Hellström

Nomenclature

Greek letters

α_c	Inclination angle of the core	[°]
ν_{12}	Poisson's ratio corresponding for the given element	[-]
ν_{xy}	Poisson's ratio corresponding to the bending stiffness	[-]
ν'_{xy}	Poisson's ratio corresponding to the stretching stiffness	[-]
ν_{yx}	Poisson's ratio corresponding to the bending stiffness	[-]
ν'_{yx}	Poisson's ratio corresponding to the stretching stiffness	[-]
ω	Angular frequency	[rad/s]
ρ_c	Core density	[kg/m^3]
ρ_f	Face density	[kg/m^3]
σ_{c0d}	Compressive stress parallel to the grain	[Pa]
σ_{c90d}	Compressive stress perpendicular to the grain	[Pa]
σ_{t0d}	Tensile stress parallel to the grain	[Pa]
σ_{t90d}	Tensile stress perpendicular to the grain	[Pa]
σ_x	Stresses parallel to the x-axis	[Pa]
σ_y	Stresses parallel to the y-axis	[Pa]
τ_{Ed}	Shear stress	[Pa]
τ_{Rd}	Shear stress resistance	[Pa]
τ_{xy}	in plane shear stress	[Pa]
ξ	Damping Ratio	[-]

Roman lower case letters

$\hat{m}_{33}$	Total mass of the floor	[kg/m^2]
$\bar{s}_{33}$	Factor calculated from shear stiffness of the plate	
b	Factor from the Swedish annex recommended to 100	[m/Ns^2]
b	Width of cross-section in z-direction	[m]
c_{air}	Velocity of air	[m/s]
f_c	Coincidence frequency	[Hz]
f_1	Fundamental frequency	[Hz]
f_{c0d}	Design compressive strength parallel to the grain	[Pa]
f_{c0k}	Characteristic compressive strength parallel to the grain	[Pa]
f_{c90d}	Design compressive strength perpendicular to the grain	[Pa]
f_{c90k}	Characteristic compressive strength perpendicular to the grain	[Pa]
f_c	Length of intersection between face and core	[m]

f_{mk}	Characteristic bending strength	[Pa]
f_{t0d}	Design tensile strength parallel to the grain	[Pa]
f_{t0k}	Characteristic tensile strength parallel to the grain	[Pa]
f_{t90d}	Design tensile strength perpendicular to the grain	[Pa]
f_{t90k}	Characteristic tensile strength perpendicular to the grain	[Pa]
f_{vk}	Characteristic value for shear strength	[Pa]
f_v	In plane shear strength	[Pa]
f_x	Strength parallel to the x-axis	[Pa]
f_y	Strength parallel to the y-axis	[Pa]
h	Height from center of the top face to the center of bottom face	[m]
h_c	Height of core (center distance)	[m]
k	Circular wave number	[m^{-1}]
k_{c90d}	Factor taking into account load configuration	[-]
k_{def}	Deformation factor	[-]
k_{mod}	Modification factor for duration of load and moisture content	[-]
q	Uniformly distributed load	[kN/m^2]
q_{mn}	Factor for calculating the transverse shear stiffness determined by the load	
t_c	Thickness of core	[m]
t_{fbot}	Thickness of bottom face	[m]
t_{ftop}	Thickness of top face	[m]
v	Unit impulse velocity response	[m/s]
w	Deflection	[m]
w_{inst}	Deflection caused by a point load of 1 kN	[m]
w_{inst}	Deflection caused by a uniformly distributed load	[m]

Roman capital letters

ΔL	Difference in sound pressure	[Pa]
A_2	Equivalent area for calculating SRI	[m^2]
A_c	Area of the core	[m^2]
B	Bulk modulus	[Pa]
B	Total width of the floor in y-direction	[m]
C_{1-10}	Factors for calculating the transverse shear stiffness	
D	Global stiffness matrix	[-]
D_{Qx}	Transverse shear stiffness in plane perpendicular to x-axis	[Pa]
D_{Qx}	Transverse shear stiffness in plane perpendicular to y-axis	[Pa]
D_{xy}	Twisting stiffness	[Pa]
D_x	Bending stiffness, x-direction	[Pa]
D_y	Bending stiffness, y-direction	[Pa]
E_x	Modulus of elasticity in x-direction	[Pa]
E_y	Modulus of elasticity in y-direction	[Pa]
G	Transverse shear modulus	[Pa]
G_{xy}	In plane shear stiffness	[Pa]
I	Second moment of area	[m^4]

I_x	Second moment of inertia in x-direction	[m^4]
I_y	Second moment of inertia in y-direction	[m^4]
K_s	Shear reduction factor	[-]
L	Total length of the floor in x-direction	[m]
L_{cr}	Critical buckling length	[m]
M_{Ed}	Maximum bending moment	[Nm]
P	Resultant compressive point load	[N]
P_{cr}	Critical buckling force	[N]
P_{mn}	Factor for calculating the deflection determined by the load	
R	Sound reduction index	[dB]
R_c	Curvature radius of core	[m]
S	First moment of area	[m^3]
S	Surface area for calculating SRI	[m^2]
T_x	Transverse shear forces in x-direction	[N]
T_y	Transverse shear forces in y-direction	[N]
W	Section modulus	[m^3]
W_{mn}	Factor for calculating the deflection determined by the stiffness	
X_{mn}	Factor for calculating the transverse shear stiffness in x-direction	
Y_{mn}	Factor for calculating the transverse shear stiffness in y-direction	

1 Introduction

The use of timber as a structural material is today limited in multi-storey buildings and not in any way as common as concrete or steel, but the interest from the market increases, primarily due to environmental reasons. Today, timber structures are very space consuming. This thesis, is a continuation of a research project that Chalmers University of Technology started, concerning an apartment dividing timber composite floor. The aim is to provide a timber floor that increases the efficiency of multi-storey buildings.

1.1 Background

Until the early 1990's, a building restriction of maximum two storey timber buildings excited in Sweden. When this restriction was eased in the beginning of the 1990s, the use of timber as building material increased. In terms of height, the excising timber floors are not as efficient as other traditional building materials. A concrete slab for residential buildings has a structural height of 200 mm compared to a traditional timber floor of a height of 480 mm. Therefore the height of timber floors must decrease to make them more competitive. Due to the increased awareness of the environmental issues, the drive for more sustainable solutions increases every year. The interest of including eco-friendly materials has increased and in the development of new products this must be considered. Bio-composite materials from recyclable materials and renewable resources are not as common in the building industry as it could be.

During the past years, a new type of timber floor, designed as a sandwich plate with a corrugated core, has been under development by the Steel and Timber research group at Chalmers University of Technology. During 2016, two master students conducted a thesis where they investigated the potential of implementing the sandwich plate technique on a timber floor, in the same way that has been implemented on steel structures (Larsson and Mayor, 2016). Their goal was to design the face and the core to either optimize the height or the material use of the floor. They made simplifications in their optimization by making some assumptions, such as isotropic material properties and that only bending deformations occur. What was realized was that by making these assumptions the deformation was underestimated and therefore the introduced floor plates are not optimal in terms of both geometric dimensions as well as the constitutive materials. Thus, a further investigation of this floor needed to be done. This thesis is a continuation of their work in order to improve the accuracy of the structural behaviour and introduce optimal innovative timber floor to the market.

The definition of a sandwich plate is that it should be compiled of two thin, stiff and strong faces separated by a thick, light and weaker core that is bonded together with adhesive (Zenkert, 1997). This creates a high stiffness-to-weight ratio and is often used in structures where this is an important factor such as airplanes, trains and boats. Investigations have shown that deflections for a sandwich plate often is underestimated if the shear deformations are neglected. Timber has a low shear stiffness which makes it

even more important to include. The serviceability limit state (SLS) criteria are often governing when designing timber floors. These criteria include deflection, vibration and the dynamic response. Since deformation often is governing, shear deformation must be included in the calculation model to obtain reliable optimal results.

1.2 Aim

In this Master's thesis, the main goal is to provide one suggestion of a design that is considered to be the optimal in terms of two parameters, height and price. The choice of material will influence both the height and the price and therefore, many material combinations will be examined in order to find the best configuration. To achieve a design that is accurate and reliable, a milestone is to write an analytic code in Matlab which is accurate in terms of structural behaviour. When the analytic model is verified and validated with the finite element (FE) modeling software Abaqus, an optimization of the geometry will be made to lower the height as much as possible. In addition to the structural behaviour, the acoustic performance and how it can be implemented as a criteria will be investigated as well.

- Can the real structural behaviour of a laminated timber sandwich plate be captured with the stiffness transformation of a corrugated core to an orthotropic homogeneous plate?
- When a final concept is obtained, can this be competitive on the market?
- Is it possible to implement acoustics as a criteria when optimizing the design?

1.3 Method

To properly capture the structural behaviour of the innovative floor and to validate the results, the process of the work in this thesis was divided into five parts:

a) Verification and investigation of previous work done by Larsson and Mayor

b) Literature study

c) Analytical model verified with finite element method (FEM)

d) Optimization of the geometry for several material combinations

e) A final suggestion and comparison

First, the work from previous thesis (Larsson and Mayor, 2016) are studied and verified. This is done by creating FE models. These models are analysed in terms of static loading, fundamental frequency and buckling to verify the optimal cases that is specified by Larsson and Mayor.

The second part is a literature study to gather necessary information about new and old research on existing timber floors and products. A review is made of current timber floors available on the market, to study their geometrical characteristics, detailed dimensions and material constituents for instance. A review of useful practical findings for timber floors are also made, like the use of bio-foam in the cavities that will appear in the corrugated core. All the necessary regulations and design standards for design of a timber floor are gathered, such as Eurocode.

The third part is to create analytical models of the structural behaviour and modification of the optimization code made by Larsson and Mayor from previous year. This is made by implementing transverse shear deformations and effect of directional material properties of the sandwich sub-elements using new modified formulations and a stiffness transformation to an orthotropic homogeneous plate in the analytic solution and rewriting the whole code in the program Matlab to reduce the risk of being influenced by their code as well as reducing the risk of human errors. When the analytic model is made, it is verified in the FE software Abaqus.

The fourth part consists of making an optimization code for the geometry using the optimization tool in Matlab. With this tool, the geometry for different material combinations is optimized in terms of height. In the same as in previous step, these models are verified using several FE models.

For the last part a final suggestion is made among all the material combinations, grain orientations and size ratios based on material costs and the total structural height. This suggestion is compared with a traditional timber floor in order to see the potential of the new innovative floor.

1.4 Limitations

Calculations and analyses from an earlier master thesis of this type of innovative floor is used as a starting point. The optimization is therefore made by only changing the code from calculating on an isotropic to an orthotropic material behaviour. For verification of previous work FE analyses are made in Abaqus, modelled in both shell and solid elements.

Only a symmetric cross-section is studied due to the advantages in the analytical solution. This makes the thickness of the top and bottom face equal to each other. No consideration about the total length of the corrugation have been made. This means that the corrugation can abruptly end in a corrugation. Therefore, a practical geometry would be the most similar possible geometry to the obtained optimal case. Geometrical dimensions and constraints of the corrugated web and the size of the floor, are chosen after requests from meetings with the industry. Therefore, the thesis only conclude analyses of a floor of the dimensions 4x6 m and 6x4 m. The SLS criteria are often governing when designing timber floors which is why the focus in this thesis is on those when designing the floor.

Only one main category of insulation for the floor is researched, bio-foam filling. This is to contain a sustainable and eco-friendly profile of the new innovative timber floor. The effect of the filling material in terms of structural behaviour are not considered.

The FE analyses used for the verification of the modified analytic solution are made in both 3D shell and 3D solid models. Because of inaccurate results a decision is made to make the FE analyses for the 20 optimal cases only in shell elements. This is because of needing a finer mesh of the model which significantly increases the computational time. Only a global analysis of the floor is made which means that no details or joists of the floor are investigated.

The fire resistance of the floor is not investigated. A prototype of the floor should be used to make a comprehensive investigation of the fire resistance.

2 Literature study

In this chapter the literature study is made for the thesis. The chapter will focus on products that are available in the market today, in terms of different engineering wood products (EWP) that are seen as appropriate materials for the development of the floor, as well as an investigation of current timber floor systems. Next part of the literature study, a review of different bio-foam fillings material is made followed by additional issues that can occur when dealing with timber floors, such as stiffness and acoustics. The last part explains the design process for residential buildings and the regulations from Eurocode (EC), European Construction Standards (EKS) and the Swedish Building Regulations (BBR).

2.1 Engineered wood products

Engineered wood products (EWP) started to be developed when wood products were required to be larger in dimensions than what is possible with sawn timber. EWP are made out of saw dust, veneers, sawn timber boards, fibers or particles. A lot of different EWP have been developed since the beginning of the 20th century. Below four different kinds of EWP that are used for the innovative floor namely, plywood, laminated veneer lumber (LVL), particle board and magnesium oxide board will be introduced.

2.1.1 Plywood

Plywood is produced by gluing thin veneers together by hot pressing them together for curing to a plate. Plywood was invented in the beginning of the 20th century in North America (Swedish Wood, 2015). The veneers are placed perpendicular to each other in each layer and always have an odd number of veneers to create symmetry. The thin veneers creates a higher reliability and lower variability due to defect elimination. Plywood has different stiffness in different direction which makes it an orthotropic material. Plywood can be made by different types of veneers, such as birch and conifer, which creates plywood with different material properties.

Birch plywood have very thin veneers, 1.4 mm thin, and is made out of processed high strength hardwood (Finnish Plywood, 2002). This is the best product for advanced construction that have varying demands. The company Finnish Plywood makes birch plywood in thicknesses between 4-50 mm with a density of 630 kg/m^3. Plywood made out of spruce, so called conifer plywood, is less dense with a density of 410 kg/m^3 and is a more economical choice than birch plywood. The material properties, for instance modulus of elasticity and shear, are lower than those of birch plywood.

2.1.2 Laminated veneer lumber

Kerto-Q is a laminated veneer lumber (LVL) product and consists of veneers glued together where four layers are glued together in the same grain orientation, followed by a fifth layer perpendicular to those (MetsäWood, 2017). The pattern is repeated until the desired thickness is reached. Kerto-S is a similar product but places all the layers in the same orientation. Due to the placement of the veneers, Kerto-Q is considered highly orthotropic. Just as for plywood, the production process generates an element with a low amount of defects. The thickness varies from 21-69 mm and the density is 480 kg/m^3.

2.1.3 Particle board

Particle boards are hot pressed in the same way as plywood, but instead of veneers they are built up by small wood chips and sawdust (Swedish Wood, 2015). The core is usually made by course chips while the outer layer is made of finer chips to create a nice finish. Particle boards have the same material properties for the two in plane directions while the out of plane direction is different. Particle board can be found in thicknesses between 6-40 mm and has a density around 550 kg/m^3. In an economical point of view particle board is a better choice than plywood.

2.1.4 Magnesium oxide board

Different types of bio-composite products exist on the market today; one of them is the magnesium oxide board. This board is mainly made out of magnesium oxide, magnesium chloride, wood chips and perlite (Manalo, 2012). These boards are pressed in the same way as particle boards. These boards are mainly used as sheathing to improve the fire-resistance of structural elements and where high level of sound insulation is required. Available thicknesses on the market are between 4-50 mm with a density of 1000 kg/m^3 (MGO, 2014). This is a density twice as large as an ordinary particle board, which makes it more preferable from an acoustic point of view.

2.2 Market review

In order to make a comparison and relate the results obtained, a market review has been made where recent products have been investigated. The review will cover the most traditional designs used and also the latest, more innovative products.

2.2.1 Traditional timber floors

What in this thesis is considered to be a traditional timber floor is consisting of either rectangular joists with a top board or solid timber floors such as cross laminated timber (CLT).

SSP - Stressed skin panel

A stressed skin panel (SSP) can be done in two different ways, either as an H-section or a T-section. Both cases includes webs made by for instance sawn timber or LVL (Swedish Wood, 2015). The difference is that the T-section only includes a top face while the H-section includes both top- and bottom faces, see Figure 2.1. The face is usually a board made of plywood, particle board or oriented strand board (OSB). An OSB is very similar to a particle board but it is made with larger strands.

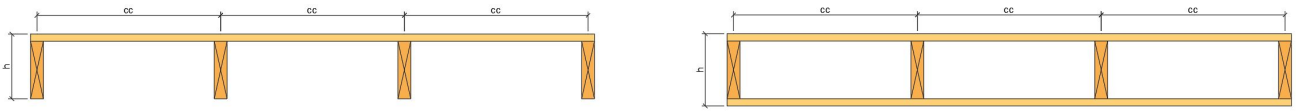

(a) *T-section* (b) *H-section*

Figure 2.1: Illustration of two different kinds of traditional Stressed Skin Panel.

I-joist floors

An I-joist floor is designed in the same way as the T-section in Figure 2.1(a) but the traditional joists are replaced with I-joists, see Figure 2.2. The I-joist beam was introduced in the 1970's and provides a more effective use of material. The web is made of a thin board material, either plywood or OSB. The flanges are glued to the webs and are usually made of LVL or sawn timber (Swedish Wood, 2015). Typical heights of I-joists are 200-650 mm depending on span and the spacing between the joists. Companies that produce the joists provide tables with predefined span lengths and loads to obtain the suitable dimensions so that the costumer easily can find what type of joist is required for a project.

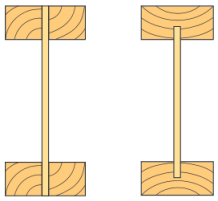

Figure 2.2: Examples of different I-joist sections (Swedish Wood, 2015).

For concentrated loads, web stiffeners might be required to prevent the web from buckling. In order to place the installations inside the floor, holes can be made in the web and can often be manufactured so that the strength can be guaranteed.

CLT solid floors

CLT floors are solid structures with at least three layers, bonded with adhesives of sawn timber with different grain orientation. If more than three layers are used, the orientations can be placed in the most beneficial way for the purpose of the slab. For a 6 meter long span, a height of 160-220 mm is required depending on loading condition (StoraEnso, 2013). These solid floors do not have any cavities or opportunities for installation inside the cross-section.

2.2.2 Innovative timber floors on the market

There is an increased interest of timber floors that are thinner and uses less material. Therefore the market is under development to satisfy these demands. Except from the development of the traditional timber floors, there are an expansion of new products. For multi-storey buildings SSP have high potential to be a great alternative to the traditional concrete slabs in terms of height, cost and sustainability. In this chapter four new innovative timber floors will be introduced.

Kielsteg

Kielsteg is an Austrian prefabricated lightweight composite product made by EWP (Kielsteg, 2016). As seen in Figure 2.3 it has an S-shaped zigzag web made of either Plywood or OSB and repeated strips of spruce makes the top and bottom faces. This design was made to get a high material utilization by placing wood where it contributes most to the static performance. The S-shape appearance can be explained by simple beam theory; it is the same shape as the buckling mode for a clamped-guided beam. The buckling behaviour analysis shows that the web has a self-stabilizing phenomenon when buckles due to its shape. Finger joints are used between the web and the flange and are placed lengthwise, fastened with melamine urea adhesive, also called MUF. This adhesive is commonly used in wooden based panels such as particle boards and plywood (Lopes, Rocco, Donizeti, Luis, and Roberto, 2015). The produced floor has a height between 228-800 mm for the structural part, can reach a span between 5-27 m and has a production width between 0.42-1.2 m (Jeffree, 2016). Kielsteg is most cost effective for longer spans and is not competitive for the shorter spans in terms of cost. The floor can easily be transported because of its light weight and dimensions. The slab can be combined and fastened with concrete, steel and timber.

Figure 2.3: Illustration of a Kielsteg floor (Kielsteg, 2016).

Kielsteg reaches the acoustic requirements by using a floor layup consisted of loose fill insulation, acoustic insulation board, screed and soft seals (Kielsteg, 2016). These layers adds to the thickness with 140-230 mm.

Kielsteg has been used in hundreds of buildings since it was first used in 2008 in Schäffern, Austria. The implemented roof elements have a height of 200 mm and 250 mm and a maximum length of 24.1 m. Periodic inspection has been made to check the SLS state and so far,until year 2017, no severe damages have occurred.

Lignatur

Lignatur is a SSP product for roofs and floor from Switzerland (Lignatur, 2014). The floor is hollow and made by repetitive rectangular cross-sections seen in Figure 2.4, similar to an SSP H-section shown in Section 2.2.1. The structural parts of the floor is made out of C24 graded softwood and bonded together with adhesive. Stiffeners for the web are arranged at different distances to create a high structural stiffness. Lignatur can reach a span up to 12 m with a structural height of 320 mm. Suspension connections are attached to each floor in production for easier lifting and assembling. The floor can be assembled with any conventional building material. For service channels and installation inside the floor, measurements needs to be performed in production due to the transverse stiffeners.

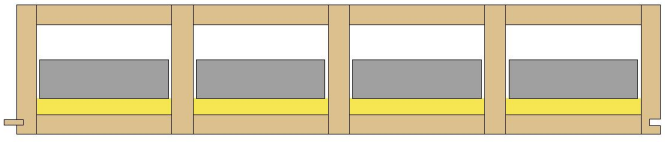

Figure 2.4: Illustration of a Lignatur cross-section with added concrete and sound insulation (Lignatur, 2014).

The acoustic performance of the floor can be improved by adding weight, for instance ballast, inside the hollow core. Lignatur have also developed their own kind of tuned mass-dampers called silent12, the layer between the ballast and the wooden part in Figure 2.4, to improve the acoustic performance of the floor even more. If the floor still does not reach the requirements a cement screed and impact

insulation can be added on top of the floor in combination with the ballast and the silent12. This adds about 150-190 mm to the structural height.

The floor is designed according to guideline for European technical approval (ETA) and has a 50 years design life and no maintenance should be required during this time (ETA, 2014). Lignatur got their ETA approval from the Austrian Institute of Construction Engineering in 2014 and has been used since then.

Pryda

Pryda is an Australian company that 2014 launched a prefabricated truss-system based sandwich slab for roof and floor structures (Pryda, 2016). It is a development of their traditional beam trusses that they have used for decades. It compounds of a sheathing made out of particle board for the top and bottom faces and the traditional truss-beams as the core. The trusses are either made out of timber or steel. The structural part of the floor has a height between 250-450 mm, reaches spans between 4.4-6.6 m and has a production width of 2.7 m. The production width is constrained by the sheathings' product length except for the last cassette, which is specially designed for each case. To lift the cassettes into place, a lifting bracket is installed during the production. The sheathings are designed to meet the acoustics and fire criterion for each separate case.

Because of the hollow core, installation can easily be put inside the floor and then no extra ceiling is needed, see Figure 2.5. The dimensions and design of the floor have been made with calculations and laboratory tests according to the Building Code of Australia.

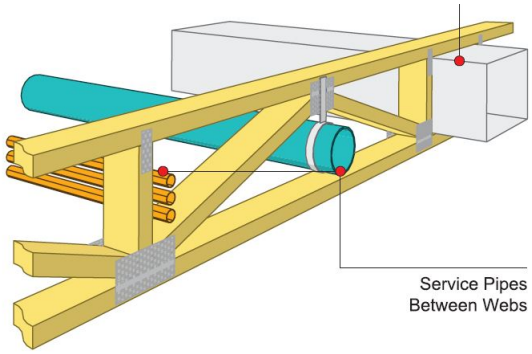

Figure 2.5: Illustration of a Pryda floor with timber trusses and how installation easily can be placed inside the hollow core (Pryda, 2016).

A Swedish company called Derome have recently, in march 2016, launched a product similar to the Pryda beam trusses (Derome, 2016). But they have not yet launched a total solution of a prefabricated floor product with this kind of solution for the core.

TECslab

TECslab is also an Australian product that have been developed from their product TECbeam. It is a steel and timber composite floor that looks like the traditional I-joist timber floor, but with webs made out of thin steel plates with punched circles and flanges in LVL. So called "strongbacks" beams are added perpendicular to the web through the punched holes to get higher rigidity. It reaches a span up to 7 m and has a structural height between 250-400 mm (TECbuild, 2010).

The acoustic requirements can be reached by adding furring in the same way as the traditional floors or with a product called Hebel (TECbuild, 2017). Hebel is a lightweight steel-reinforced autoclave aerated concrete with a thickness of 75 mm or more, that TECbuild have developed to enhance the market value of their product. The TECslab can only be used in buildings with four storeys or less and has been designed according to the Australian code. The first ones using this product was an Australian company called Express Two Storey Living. They started to implement this product in the end of year 2016 (Building NEWS, 2014).

2.2.3 Bio-foam filling material

The cavities of cores in any of the previously introduced innovative floors, like present corrugated core sandwich floor in this thesis, will be filled with insulation material. Due to the shape of the cavities the most practical way to fill these is with expanded foam. When foam like products arrived in the 80's, they included a lot of fossil as well as chemical substances (Tan and Khoo, 2014). Today, the most commonly used product is the expanded polystyrene (EPS) and even though the product is 100% recyclable and have an approximate content of air around 95-98%, all the materials used to make EPS are fossil, which makes this material less attractive on the market. Alternatives to the fossil based foam materials are now excising on the market. Bio-foam can be produced from sugar canes, soybeans, vegetable oil or recycled plastics instead of polystyrene (Biofoam spray insulation, 2017). This make the products more sustainable and is a good choice for the environment.

These expanding bio-foam fillings can expand up to 100 times its original size when it is applied, this will fill the cavities and provide a sealed thermal and airtight building (Econstruction, 2007). When filling up the cavities with bio-foam this also provides to the improvement of the acoustic behaviour of the structure due to its elimination of leakage areas. When using an organic material there is always a risk of mould growth and fungi but there are no research showing that bio-foam would be less resistant than EPS. The most interesting material properties of the bio-foam filling materials are the compressive strengths since this can reduce the local deflection between the corrugation tops and the density due to improve the acoustic performance. The compressive strength and density are shown in Table 2.1 for different bio-foam filling materials. Noticeable is that the compressive strength is highly dependent on the density.

Table 2.1: Material properties for different biofoam filling materials (Biofoam spray insulation, 2017)

Filling material	Compressive strength [kPa]	Density [kg/m^3]
Biofoam 800	12.1	14.4
Biofoam 1600	42.3	24
Biofoam 2700	115.4	34.4
Biofoam moulded	4000	40

2.3 Stiffening techniques for residential comfort

If a discomfort of a timber structure is apparent, this might be due to a low stiffness. To create a higher stiffness, the most common solution for traditional timber floors is to add a layer of concrete on top of the floor. This is, except for the vibrations, also favourably for the acoustic and deflection performance of the floor (Hasníková and Kuklík, 2013). Other stiffening techniques that have been investigated is the strengthening with CLT and carbon fiber reinforced polymers (CFRP). These are added to the faces of the sandwich floor to create a higher stiffness for the in-plane bending. There are also different techniques to increase the stiffness of the core. That can be done by adding stiffeners perpendicular to the directions of the webs or adding a type of reinforcement system inside the floor, usually made out of steel. The two latest techniques can be implemented without loosing any room-height (Valluzzi, Garbin, and Modena, 2006). The present innovative corrugated-core sandwich floor will be shown that has high potential in increasing the stiffness by optimally design the geometric dimensions without need of increasing the floor height.

2.4 Acoustics

A floor structure that is heavy, with a low stiffness and a high damping, has in general very good sound insulating properties (Wennhage, 2001). Timber has a high strength-to-weight ratio which is not beneficial regarding the acoustic performance and that is one of the reasons why for instance concrete is more preferable in this matter. As for other timber floors on the market, the sound insulation of the floor structure is likely to be one of the biggest obstacles. To be competitive with other timber floors on the market, the acoustic performance must be sufficient.

Prediction of the sound performance is hard since in the end, factors like for instance assembly and workmanship will influence. Most of the acoustic models that exists today have been developed for heavy materials, such as concrete, which cannot be used for a complex orthotropic light-weight sandwich structure. Even though models for concrete floors can not be used, some basic acoustic principles can be useful to know such as what parameters improves and impairs the acoustic performances. Nilsson conducted a PHD thesis where a simple structure of a single leaf panel made of concrete was studied (Nilsson, 1974). Conditions such as room dimensions, acoustic coupling and boundary conditions were taken into account. Nilsson further developed a model to evaluate acoustic performance of a sandwich

structure (Nilsson, 1989). A short introduction to the findings in the two reports will be briefly explained in this section.

Another way to predict the sound insulation can be useing finite element calculations, it can give a relatively good correlation to experimental measurements but is very time consuming and requires a lot of data space (Brunskog and Hammar, 2000).

2.4.1 Traditional handling of acoustic problems

For timber floors as the ones described in Section 2.2, the sound insulation performance is often tested experimentally and additional sound insulation layers are added until the result is satisfactory. Usually a floating floor is used above of the structural member and below a ceiling can be attached. It has been shown that for an certain amount of mass, m, it is beneficial to place half of the mass on either side of the structure (Emms, Chung, McGunnigle, and Dodd, 2006). When additional sound insulating layers are added above and below the structural members, the height of the floor is unfortunately increased but this might be necessary to meet the requirements. If cavities exist in the structure, this can be used in order to improve the sound insulation without increasing the height. The cavities in the corrugated core will be used to improve the acoustic performance which is described in Section 2.2.3. Bio-foam filling is a sustainable way that is expected to improve the acoustic which reduces the need of additional insulation above and below the floor.

2.4.2 Sound reduction index

The sound insulation between two rooms is often measured with a Sound Reduction Index (SRI), R [dB], and is defined as (Nilsson, 1974):

$$R = \Delta L - 10 \log \frac{A_2}{S} \tag{2.1}$$

where

ΔL	Difference of sound pressure between both sides of the dividing panel, [Pa]
A_2	Equivalent area in the receiving room, [m^2]
S	Surface area of the entire dividing panel, [m^2]

Equation (2.1) implies that the sound reduction index does not only involve the panel itself but also how the entire structure functions from one room to another, the size of the panel and also the receiving room is affecting the result. ΔL is the pressure difference between the rooms, which means that the term does include flanking sound as well. Flanking sound is the sound that is transmitted through other elements that is not the dividing part investigated, for instance connected walls, and can not be neglected.

2.4.3 Coincidence frequency

To fully understand what the coincidence frequency is, also known as the critical frequency, the concept of a wave number must be understood. The wave number, k [m^{-1}], is defined as the number of cycles of a wave per unit distance, described as circular wave number k is defined as (Nilsson, 1974):

$$k = \frac{2\pi}{\lambda} = \frac{2\pi f}{\upsilon} = \frac{\omega}{\upsilon} \tag{2.2}$$

where

f	Frequency, [Hz]
λ	Wavelength, [m]
ω	Angular frequency, [Hz]
υ	Phase velocity, velocity of the wave in the direction of propagation, [m/s]

As an example, the phase velocity for air is the same as the velocity of sound in air $\upsilon_a = 343$ m/s but varies with for instance temperature and humidity. Each medium has a specific velocity of propagation and in the same way, different design and material choices will affect the phase velocity of the floor and hence, the wave number. Stiffness, or rather the bulk modulus, B, and density ,ρ, will affect the phase velocity, where an increased stiffness leads to an increased phase velocity but in contrast, an increased density decreases the velocity according to the following formulation:

$$\upsilon = \sqrt{\frac{B}{\rho}} \tag{2.3}$$

where

B	Bulk modulus [Pa]
ρ	Density [kg/m^3]

It can be shown that even though the bulk modulus and the density tend to increase simultaneously for materials, the stiffness is dominant compared to the density.

The frequency where the bending wave number of the floor is matching the wave number of the surrounding air, $k_{air} = k_{floor}$, is called the coincidence frequency, f_c [Hz]. This is a critical frequency since for this frequency, the bending waves will coincide with the sound waves in the air. This means that all sound would theoretically be transmitted without any losses, hence SRI would approach zero. In reality there will always be losses and the SRI is instead reduced around the critical frequency. The coincidence frequency for a sandwich plate, is defined as (Nilsson, 1974):

$$f_c = \frac{c_{air}}{2\pi} \frac{k_{plate}^2}{k_{air}} \tag{2.4}$$

For a sandwich structure, the wave number is a function of frequency, f. This means according to Equation 2.4 that the coincidence frequency is frequency dependent as well.

For frequencies below the coincidence frequency the sound radiation is subsonic, which means that for free vibrations, if the plate would be infinitely large, there would be no sound radiation from the plate (Nilsson, 1974). For frequencies above the coincidence frequency, if there would be no power flow in the edges to the supports, the transmission loss would be independent of the boundary conditions. Although, in reality such losses occur in terms of e.g friction. Sound waves above the coincidence radiates even for infinite plates and is instead called supersonic. Of course, no infinite floors are investigated, therefore sound will be transmitted for both subsonic and supersonic frequencies. The heavier and stiffer the floor is, the greater is the power flow at the edges. For lighter structures, the assembly and workmanship can have great influence of the power flow.

Low frequency sound are especially critical for light-weight structures as the one investigated and it is in the low frequency region the greatest differences can be found compared to heavy-weight floors like concrete (Emms et al., 2006). Unfortunately impact noise such as footsteps lays within the low frequency range and is probably the most common impact sound in residential buildings, which can appear to be very annoying.

2.5 Regulations and codes

Not only a floor must have sufficient load capacity, but there are also other criteria for instance deflection, dynamic response and fire safety that needs to be fulfilled. Fire safety is not considered in this thesis but are explained below. In the following sections, criteria from Eurocode, EKS and BBR will shortly be explained.

2.5.1 Eurocode

The Eurocodes work as standard for all members of the European Union and were established to create a common design among the member states (Eurocode, 2017). The codes are produced to fulfill the following general criteria:

- Serviceability requirement – the structure during its intended life, with appropriate degrees of reliability and in an economic way, will remain fit for the use for which it is required.
- Safety requirement – the structure will sustain all actions and influences likely to occur during execution and use.
- Fire requirement – the structural resistance shall be adequate for the required period of time.
- Robustness requirement – the structure will not be damaged by events such as explosion, impact or consequences of human errors, to an extent disproportionate to the original cause.

The codes are based on a limit state which means that the capacity of a structure should be higher than the load effects that are likely to occur, in combination with safety factors (Eurocode, 2017). Some national differences can occur, for instance due to different climates, which is individual to every member state. These differences are treated in a national annex which every member state is obligated to design. The codes are continuously getting updated as new research and findings are made.

2.5.2 European Construction Standards

European Construction Standards (EKS) is a regulation that the administrative authority, Boverket, in Sweden is providing in addition to Eurocode which gives rules and guidance how to interpret Eurocode (EKS, 2017). Different safety classes are defined in EKS where a building component can get either 1, 2 or 3, where 3 is the highest. The building component investigated in this report is regarded as safety class 3 since the result of a collapse of a floor could possibly lead to serious personal damages.

2.5.3 Swedish Building Regulations

Apart from Eurocode, Boverket has created another regulation with rules that does not concern the design of the structural behaviour, called BBR (Boververkets byggregler). It is providing rules related to for example fire safety, hygiene, sound insulation, moisture, health and environment which is not critical for the resistance or the structural behaviour.

3 Design

In order to create a floor that is competitive on the market, many aspects must be considered. The economic aspect is among the most crucial and there are a number of ways of optimizing the cost. To reduce the total height of the floor by using strong materials can possibly add an extra storey to the building, which of course is attractive to the client even if the price of the floor elements increases. The choice of materials influences the total price considerably and choices like this will be bared in mind when designing the floor. The materials used will also strongly effect the environment and that is something that needs to be considered for a sustainable development. Another aspect is the assembly of the floor, as a design with as few joints and connections as possible is desirable.

3.1 Description of sandwich floor

To create an integrated floor that is effective in terms of material use and has a high stiffness-to-weight ratio, a sandwich structure has been chosen. The definition of a sandwich plate is that it should be compiled of two thin, stiff and strong faces separated by a thick, light and weaker core bonded together with adhesive (Zenkert, 1997). This solution creates a very high stiffness-to-weight ratio and is today used in applications for airplanes, trains and boats where this ratio is a very important factor.

The core of the sandwich element can be designed in many ways. It can be solid or use a more complex and effective structure. There are a lot of different core structures that can be used; the one selected for this project is the corrugated structure. This is mainly due to the rather simple assembly since the core is continuous and only intersect with the top and bottom face. This decrease the risk of a poor assembly and reduces the number of joints. Moreover, manufacturing process is much simpler than other efficient configurations like honeycomb sandwich.

The cross-section of the floor can be seen in Figure 3.1 and can be explained by seven variables, where some of them are dependent on each other.

h_c	height of core
t_{ftop}	thickness of top face
t_{fbot}	thickness of bottom face
t_c	thickness of core sheet
α_c	inclination angle of corrugated core
f_c	interaction length between core and face
R_c	curvature of the corrugated corners

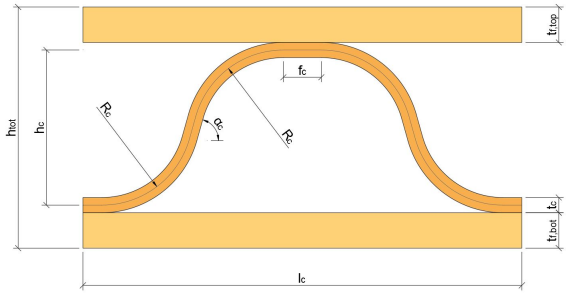

Figure 3.1: Design of floor.

All the variables can vary within a certain range (lower- and upper bound) that are defined beforehand. As there are numerous of design criteria, a change of one variable might affect one criterion positive while another negative. This makes it very hard to obtain an optimal cross-section, therefore a very complicated iterative process is needed. For this problem, Matlab has been used which is further described in Section 4.3.

There are not only variation of the cross-section geometry that affects the design, also the planar length and the width of the total floor can be set to different dimensions. According to the industry, the most common dimensions for a floor is a rectangular slab with a size of 4x6 m. As seen in Figure 3.2, the corrugation of a rectangular floor can be extruded in two different directions, along the short side or along the long side. These will from now on be referred to as *4x6 floor* and *6x4 floor*.

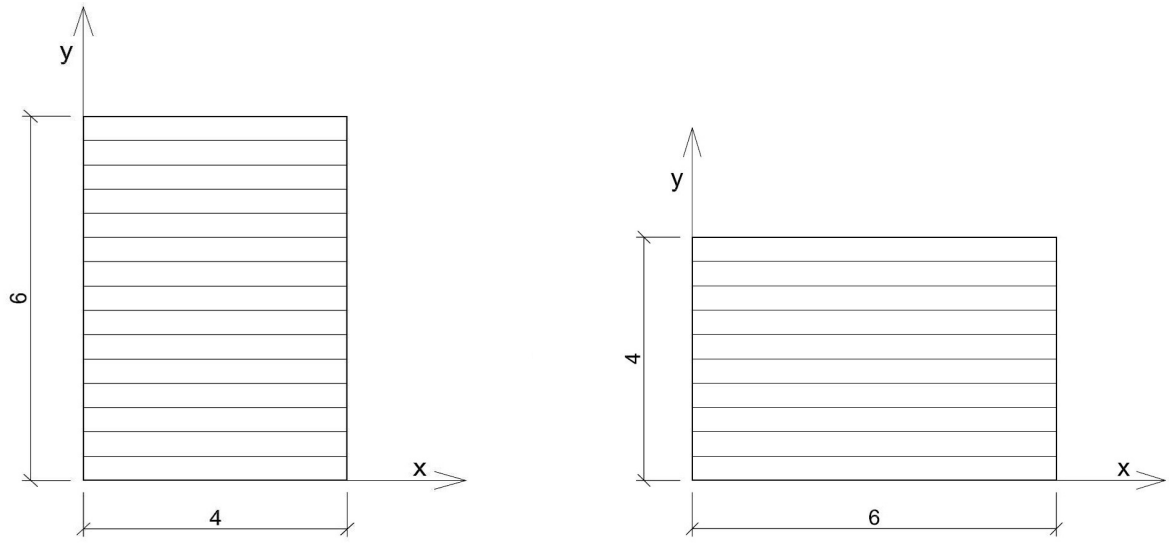

(a) *4x6 floor, corrugation extruded along the short side.* (b) *6x4 floor, corrugation extruded along the long side.*

Figure 3.2: Different corrugation directions.

3.2 Geometric constraints

Two categories of constraints will be dealt with, performance and geometric constraints which all needs to be fulfilled. The performance constraints from Eurocode, EKS and BBR are described in Chapter 5 and covers the most common design criteria. The geometrical constraints, which relates to the shape of the cross-section, are either based on the manufacturing limitations received from the industry or to create a geometry that is mathematically possible.

All the constraints listed in Equations (3.1-3.7) below are all due to different reasons. In order to use the analytic model described in Chapter 5, the thicknesses of the faces need to be equal (symmetric cross-section). Regarding the angle α_c, lower and upper bound has been set to 55° and 89°. The lower due to the risk of local buckling or crushing of the inclined part of the core and the higher is restricted to 89° to not reach singularity problems in the calculations, which happens at 90°. Obviously, the results of a web-core sandwich panel is obtained when the inclination angle approaches 90 degrees. Since adhesives will be used in the interface between the face and the core, f_c has a lower bound of 30 mm to create a sufficient connection. To obtain a structure that includes timber products that are within the range of standard dimensions on the market, upper and lower bounds have been added to the thicknesses of the core, t_c and the thickness of the faces, t_{ftop} and t_{fbot}. The lower bound of R_c is dependent of the thickness, the thicker the core is, the greater the radius must be due to the curvature that is possible for manufacturing. The ratio constraint given in Equation (3.7) is due the assumption of a thin face sandwich structure and needs to be fulfilled in order to use the calculation model. Notice that h is the height from the center of the top face to the center of the bottom face.

$$t_{ftop} = t_{fbot} \tag{3.1}$$

$$55° \leq \alpha_c \leq 89° \tag{3.2}$$

$$f_c \geq 30mm \tag{3.3}$$

$$6.5mm \leq t_f \leq 50mm \tag{3.4}$$

$$6.5mm \leq t_c \leq 50mm \tag{3.5}$$

$$R_c \geq 6t_c \tag{3.6}$$

$$5.77 \leq \frac{h}{t_{ftop}} \leq 100 \tag{3.7}$$

The following constraints, Equations (3.8-3.13), are set to create a geometry that is mathematically possible. All the distances can be seen in Figure 3.3.

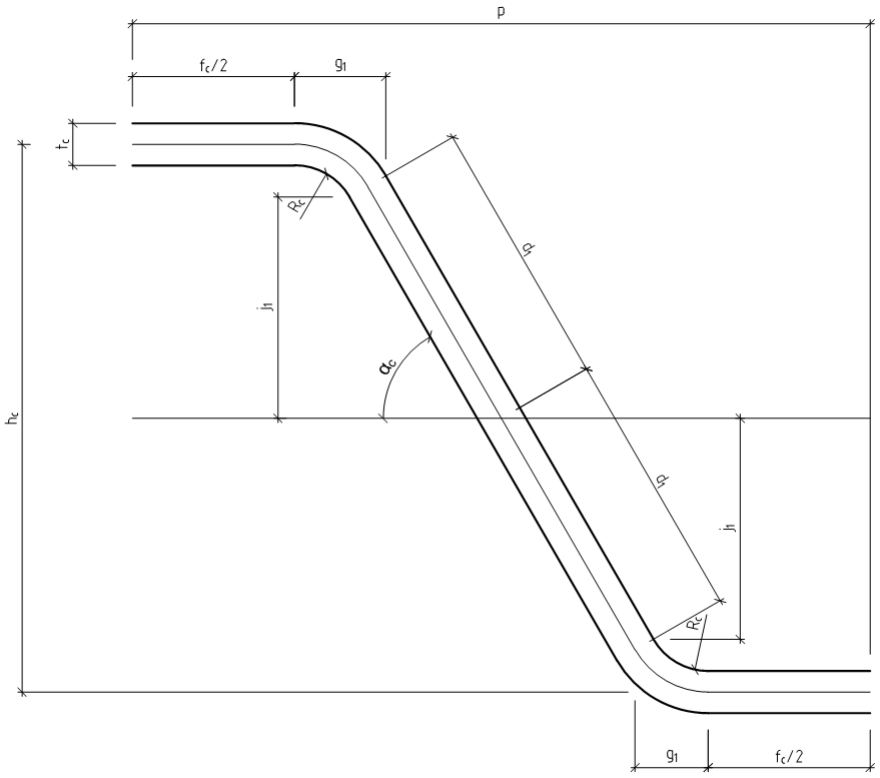

Figure 3.3: Geometry of cross-section, notations according to (Libove and Hubka, 1951)

$$0 \leq j_1 \leq \frac{h_c}{2} \tag{3.8}$$

$$d_1 \geq 0 \tag{3.9}$$

$$2t_c \leq h_c \tag{3.10}$$

$$2g_1 \leq p \tag{3.11}$$

$$2d_1 = \frac{h_c - 2R_c(1 - \cos\ \alpha_c)}{\sin\ \alpha_c} \tag{3.12}$$

$$f_c = p - 2d_1 \cos\alpha_c - 2R_c \sin\alpha_c \tag{3.13}$$

No consideration of the total amount of corrugation periods have been taken into account. This means that the corrugation can end abruptly after four or six meters. Additional constraint could be added so that the corrugation ends either at the top or bottom face. This constraint is disregarded in order to see the optimal structural behaviour of the corrugation. Clearly, the real optimal case would be the nearest possible geometry to the one obtained from the optimization.

3.3 Material combinations

The faces and the core can be assembled with different timber products with different grain orientation. For face and core respectively, the materials in Table 3.1 has been considered.

Table 3.1: Materials investigated to be used for the sandwich structure

Material	Face	Core
Plywood, birch (B)	✓	✓
Plywood, conifer (C)	✓	✓
Particle board (P)	✓	✗
Magnesium board (M)	✓	✗
Kerto-Q (K)	✓	✗

The products applicable for the core are fewer than for the face due to manufacturing of the curved parts. Particle board and Magnesium board are more brittle materials and are not applicable for being curved. Kerto-Q is only produced in plates of very thick cross-sections and is therefore not applicable to be used as core material. Furthermore, the top and bottom faces will always be considered to be the from same material.

The grain orientation can be placed parallel to the global x-axis, referred to as parallel to the corrugation (∥), or rotated 90° which is referred to as perpendicular to the corrugation (⊥). All the grain combinations can be seen in Figure 3.4. The grain direction of the top and bottom face is kept the same. With the materials used in Table 3.1 with all possible grain orientations, a total of 32 combinations can be found.

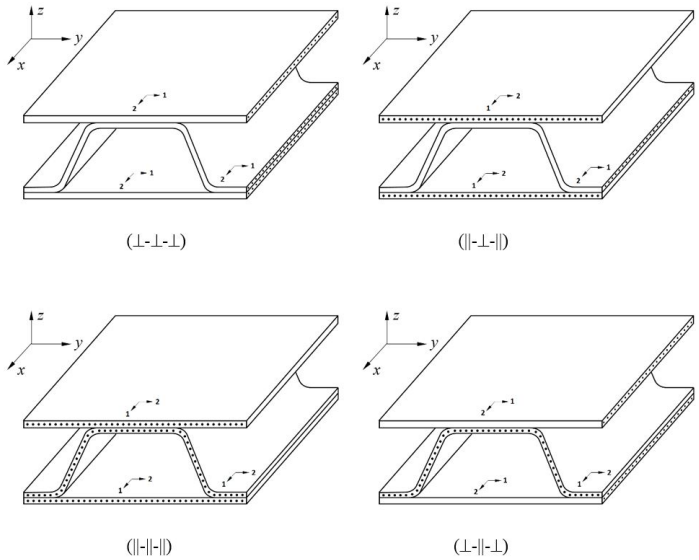

Figure 3.4: Different combinations of material orientation in different sub-elements and global coordinate system of the corrugated core sandwich element (x,y,z) and local coordinate system corresponding to the orthotropic material orientation (1,2,3).

4 Method of analyses

To make a reliable structural analysis of the sandwich floor with corrugated core with adequate accuracy, three different approaches are used namely analytical solutions, FE modeling and simulations, and a final optimization via Matlab code. The design of the floor is optimized by using the *Optimization Tool* in Matlab, considering both performance and geometrical constraints. It is taken into account the effect of directional material properties of timber in order to obtain results as accurate as possible. After the optimal geometries are generated numerically, the resulting geometries are modelled in Abaqus to validate and compare the results.

In the literature study the acoustics were investigated but considered to complex to include in the analyses. Therefore, as mentioned earlier, almost all of the new floors have been first designed structurally and tested experimentally on-site to measure their acoustic performance and fixing the probable acoustic problems by applying practical solutions. No suitable acoustic model has been found for a sandwich structure like the one investigated in this thesis, therefore such a model will not be evaluated in this thesis but needs to be fundamentally developed for further studies.

4.1 Analytical solutions

Analyses of sandwich plates with corrugated core have been done since the beginning of the 1950's (Libove and Hubka, 1951). Applications of these theories require knowledge about the type of material and certain elastic constants. This advanced technology has been implemented for steel elements in other industries. These theories are not accurate to be implemented for composite timber products and therefore needs to be improved and refined in more detail to create proper analysis. This is made by doing a stiffness transformation from a corrugated aluminum core to an orthotropic homogeneous plate. Significant shear deformations due to low shear stiffness of laminated timber and directional material properties due to the grain orientation are the two main effects that needs to be incorporated into the analysis of a light-weight timber structure. Details of formulations, for instance elastic constants and shear stiffness, can be found in Chapter 5.

4.2 Finite element analysis

To verify the analytical solutions the comercially avaliable FE software Abaqus CAE, version 6.13-3, is used. There are two types of elements that are appropriate for the modeling of this sandwich structure, shell and solid elements. To get the most accurate results a model of solid elements is preferred, also called continuum elements. Solid elements on the other hand, are very mesh-sensitive and requires a very fine mesh to be accurate for such a complicated thin-wall structure. Recommendations about the mesh is to include about 10 elements in the thickness direction of the element, which makes the mesh

very fine for thin elements. Apparently, a global analysis requires a lot of computational effort and time. With a rather simple structure in terms of FE-modelling, the solid model is not preferable for this kind of global analysis. The result from the solid model is much more difficult to tell if it is trustworthy or not because of the mesh-sensitivity the results changes for every different mesh. Models made by shell elements are usually more accurate for very thin elements, and does not acquire the same amount of computational time as solid models. Apart from the computational time, also the modeling time is longer with solid elements than with shell elements. More details about how the models are created in Abaqus are given in Appendix C.

4.2.1 Material properties

Timber is an orthotropic material which means the results of the analyses are highly dependent of the orientation of the material. The material properties for the solid were made by using *engineering constants*, which makes it possible to enter different properties in the different axes of the local coordinate system. Nine parameters including moduli of elasticity, Poisson's ratios and shear moduli are valued for each sub-element of the floor structure: i.e., E_1, E_2, E_3, ν_{12}, ν_{13}, ν_{23}, G_{12}, G_{13} and G_{23}. The subscripts of the material properties describe the assigned local orientation for each part, which were assigned by a *datum CYS axis*. For shell models the elastic material behaviour can be set as *lamina constants* then only six input values are needed, these are E_1, E_2, ν_{12}, G_{12}, G_{13} and G_{23} for each layers of the sandwich structure.

4.2.2 Boundary conditions and interactions

The sandwich structure consists of three parts, two faces and one core, bonded with adhesives to create a full-composite interaction and keep the parts in place. To assemble and constrain these parts in Abaqus, a *tie constraint* is used at the interfaces between the core and the face sheets to simulate the adhesive connections. This constraint makes sure that there are no partial slip and relative motion between the separate parts.

The floor supports are modelled as hard simply supported type of boundary conditions along the four edges. This is modelled by a *displacement/rotation* boundary condition constraining; the displacements of the floor parallel to the edges as well as in the z-direction are set to zero.

4.3 Optimization

For the optimization of the geometry, a programming code via Matlab software version R2015b is used. The optimization target is defined to reduce the height as much as possible while fulfilling all the criteria. For the specific problem, the command *fmincon* was chosen, which minimizes a certain

objective function $f(x)$, while satisfying constraints in the following way:

$$\min f(x) \text{ such that } = \begin{cases} lb \leq x \leq ub & \text{Upper and lower bound} \\ Ax \leq b & \text{Linear Inequality Constraint} \\ A_{eq}x = b_{eq} & \text{Linear Equality Constraint} \\ C(x) \leq 0 & \text{Non-linear Inequality Constraint} \\ C_{eq}(x) = 0 & \text{Non-linear Equality Constraint} \end{cases} \tag{4.1}$$

As described in Section 3.1, there are seven variables that together generates the cross-section. The following variables are put into a vector x for the optimization:

$$\{x\} = \{x_1, x_2, x_3, x_4, x_5, x_6, x_7\} = \{h_c, t_{ftop}, t_{fbot}, t_c, \alpha_c, f_c, R_c\} \tag{4.2}$$

In this case, the objective function is the total height of the floor:

$$f(x) = x_1 + x_2 + x_3 + x_4 \tag{4.3}$$

The constraints from Section 3.2 are inserted in the form of vectors (lower case letters) and matrices (capital letters) in a form that can be seen in the cases in Equation (4.1).

Before starting the optimization, an initial guess vector, x_0 must be provided, including values for all seven variables, x_1-x_7. It is noticeable that the command *fmincon* only finds a local minimum which is dependent on the initial guess, x_0. As an example, Figure 4.1 is used to visualize the problem. If the initial guess is to the right of the local maximum, it will only find the local minimum. If the initial guess instead is a point to the left of the local maximum, it will find the global minimum. This means that there is a risk that the global minimum is missed.

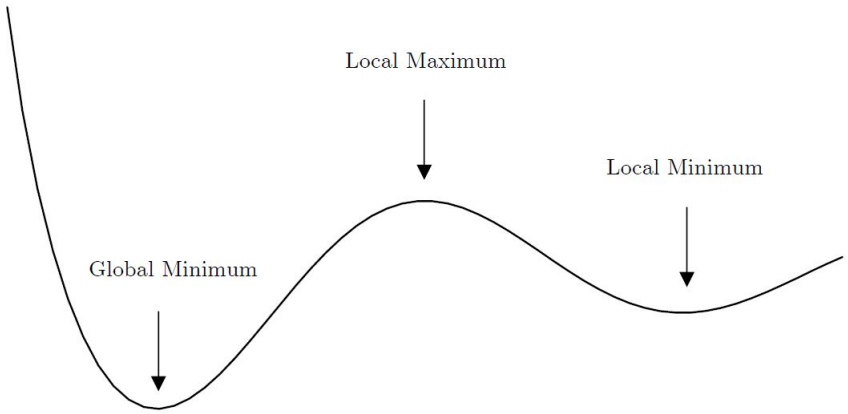

Figure 4.1: Visualization of the process of finding a global minimum by using the command GlobalSearch.

To solve this issue, the process should be repeated with different trial points to cover a wider range of the domain which increases the chances to find the global minimum. To do so, the command *GlobalSearch* is used which repeats the solver *fmincon* with different trial points and returns the lowest local minimum that is found. To increase the possibility of finding the global minimum even more, the *GlobalSearch* is repeated with a for-loop.

There are default options set for the optimization tool but can be changed if needed. The algorithm type is among the most important option and the default setting 'interior-point' can solve large problem rather quickly but requires more memory space and the result might not be as accurate as with other algorithms (MathWorks, 2017a). Instead, 'sqp' (sequential quadratic programming) is used which has several advantages. It satisfies bounds at all iterations and can recover from NaN (Not a Number) and Inf (Infinite) results. Studies have shown that this method is better than the other algorithms for non-linear problems in terms of accuracy and efficiency (MathWorks, 2017b). Other examples of options that can be set are maximum number of iterations, maximum iteration time and constraint tolerance for instance. The entire Matlab code are given Appendix B.

5 Mathematical modeling and analysis

By experience, the design of timber structures are usually governed by Serviceability Limit State (SLS) rather than Ultimate Limit State (ULS). Therefore the focus in the design will be on the SLS criteria primarily and on the ULS criteria secondarily. The SLS criteria include deflection and dynamic response, which are related to comfort rather than safety. The ULS criteria on the other hand, is related to the failure criteria but are in general fulfilled if the SLS criteria are fulfilled.

For all given equations in Sections 5.1-5.5, the sub notations f, c, x, and y corresponds to parameters for the face sheets, the corrugated core, x-direction and y-direction, and all calculations are made per unit length.

5.1 Elastic constants

Elastic constants are translated from a corrugated aluminum core to an orthotropic homogeneous floor with equations derived from the theory made by Libove and Hubka (Libove and Hubka, 1951). The stiffness parameters are crucial when analysing the structural behaviour of the sandwich structure. Bending and stretching stiffness parameters have different equivalent Poisson's ratio values, which is related to the material properties of the core and the faces. All the stiffness parameters can be inserted into the stiffness matrix D as follows:

$$D = \begin{bmatrix} E_x & E_{xy} & 0 & 0 & 0 & 0 \\ E_{yx} & E_y & 0 & 0 & 0 & 0 \\ 0 & 0 & G_{xy} & 0 & 0 & 0 \\ 0 & 0 & 0 & D_x & D_{xy} & D_{Qx} \\ 0 & 0 & 0 & D_{yx} & D_y & D_{Qy} \\ 0 & 0 & 0 & 0 & 0 & 0 \end{bmatrix} \tag{5.1}$$

Libove and Hubka, derived formulas for the elastic constants D_x, D_y, D_{xy}, D_{Qx} and D_{Qy} for a corrugated-core sandwich element with isotropic sub-elements (Libove and Hubka, 1951). D_x and D_y are the bending stiffness components, D_{xy} is the twisting stiffness, and D_{Qx} and D_{Qy} are the transverse shear stiffness which are important in the consideration of shear deformations. In the following, an extension of the formulation of stiffness parameters are represented when the corrugated plate is made of orthotropic sub-elements. In other words, each of the faces and the core individually made of orthotropic materials. Moreover, the new representation of the stiffnes formulation compensates for the error due to ignoring the transverse shear deformations by taking into account those effects; for more details see (Atashipour and Al-Emrani, 2017).

E_x, E_{xy}, E_{yx} and E_y corresponds to the stretching stiffness and D_x, D_{xy}, D_{yx}, D_y corresponds to the bending stiffness. These stretching and bending entries involves different Poisson's ratios, one for stretching ν' and one for bending ν. These are defined as (Atashipour, Al-Emrani, Fröjd, and Hellström, 2017):

$$\nu'_{xy} = \nu_{12} \tag{5.2}$$

$$\nu'_{yx} = \nu_{12}\frac{E_y}{E_x} \tag{5.3}$$

$$\nu_{xy} = \nu_{12} \tag{5.4}$$

$$\nu_{yx} = \nu_{12}\frac{D_y}{D_x} \tag{5.5}$$

When the Poisson's ratios are defined, the stretching stiffness parameters are calculated as:

$$E_x = \frac{E_{xf}A_{xf}}{1-\nu'_{xyf}\nu'_{yxf}} + \frac{E_{xc}A_{xc}}{1-\nu'_{xyc}\nu'_{yxc}} \tag{5.6}$$

$$E_y = \frac{E_{yf}A_{yf}}{1-\nu'_{xyf}\nu'_{yxf}} + \frac{E_{yc}A_{yc}}{1-\nu'_{xyc}\nu'_{yxc}} \tag{5.7}$$

$$E_{xy} = E_y\nu'_{xyc} \tag{5.8}$$

$$E_{yx} = E_x\nu'_{yxc} \tag{5.9}$$

and the bending stiffness parameters as:

$$D_x = \frac{E_{xf}I_{xf}}{1-\nu_{xyf}\nu_{yxf}} + \frac{E_{xc}I_{xc}}{1-\nu_{xyc}\nu_{yxc}} \tag{5.10}$$

$$D_y = \frac{E_{yf}I_{yf}}{1-\nu_{xyf}\nu_{yxf}\frac{1-E_{yf}I_{yf}}{D_x}} \tag{5.11}$$

$$D_{xy} = 2\left[\left(G_{xyf}t_{ftop}k_{GJ}^2 + \frac{G_{xyc}t_c^2}{A_{cx}}(k_{GJ}-k_c)^2 + G_{xyf}t_{fbot}(1-k_{GJ})^2\right)h^2\right] \tag{5.12}$$

$$D_{yx} = D_{xy} \tag{5.13}$$

The in plane shear stiffness, G_{xy} is calculated as:

$$G_{xy} = GA = 2G_{xyf}t_f + \frac{G_{xyc}t_c^2}{A_c} \tag{5.14}$$

The transverse shear stiffness, D_{Qx} and D_{Qy} are calculated as:

$$D_{Qx} = \frac{G_{xyc}t_c^2}{A_c}\left(\frac{h}{p}\right)^2 \tag{5.15}$$

$$D_{Qy} = \frac{1}{\left[\frac{2C_1C_5C_6+(C_6-C_1)(C_2C_3-C_5C_9)}{C_3C_7-C_4C_8}\right]\frac{1}{h} + \left[\frac{C_1C_3C_6}{C_3C_7-C_4C_8}\right]\frac{1}{p} + \left[C_{10} + \frac{C_5^2C_7-C_2C_5(C_1-C_4)-C_2(C_2C_3-C_5C_9)}{C_3C_7-C_4C_8}\right]\frac{p}{h^2}} \quad (5.16)$$

where

ν_{12}	Poisson's ratio parameter for given element, [-]
E	Modulus of elasticity, [Pa]
A	Cross-section area, [m^2]
I	Second moment of inertia, [m^4]
G_{xy}	In plane shear stiffness, [Pa]
t	Thickness, [m]
p	Length of one half corrugation period, see Figure 3.3, [m]
$C_1 - C_{10}$	Factors depending on the geometry and different stiffness parameters, for derivation see Appendix A

and k_c and k_{GJ} are calculated as:

$$k_c = \frac{1}{2}\left(1 + \frac{A_{fbot} - A_{ftop}}{l_c h}\right) \quad (5.17)$$

$$k_{GJ} = \frac{\frac{G_{xyc}t_f^2\ k_c}{A_c} + G_{xyf}A_{fbot}}{GA} \quad (5.18)$$

5.2 Deflection

Deflection is an SLS requirement and can not alone lead to collapse but is very important for comport and appearance (Swedish Wood, 2015). Deflection is often governing in the design phase for structures with low stiffness and long spans. Investigations have shown that the deformation, caused by both transverse and vertical loads, are usually underestimated for sandwich floors (Dias, Monteiro, and Martins, 2013). Zenkert mention that for any kind of sandwich structure, it should consist of deformations caused by both the bending moments and transverse shear forces (Zenkert, 1997). These two types of deflections are visualized in Figure 5.1. The shear deformations are often only a small fraction of the total deflection and are usually neglected, which is the case in Euler-Bernoulli beam theory. But for a sandwich plate, with rather low shear stiffness, the shear deformation can not be neglected and needs to be considered in order to receive a more accurate result.

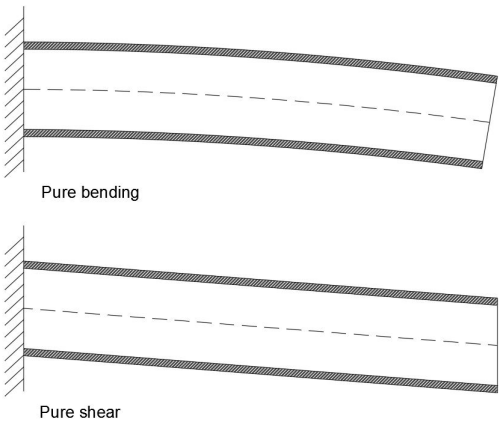

Figure 5.1: Visualization of deformations caused by pure bending and pure shear of a cantilever beam.

Timoshenko beam theory is a first order shear deformation theory which takes into account both the bending deformations and the shear deformations. Compared to Euler-Bernoulli theory where plane sections remain straight and normal to the longitudinal axis, Timoshenko theory do not stay normal to the longitudinal axis. Calculation of the deflection w [m], according to Timoshenko theory, of an orthotropic sandwich floor is quite complex and according to Zenkert (1997) it can be written as:

$$w = \sum_{n=1}^{\infty} \sum_{m=1}^{\infty} W_{mn} P_{mn} \ \sin(\alpha x) \sin(\beta y) \tag{5.19}$$

where

α	Equals $m\pi/L$, where L is the length of the floor along the x-axis
β	Equals $n\pi/B$, where B is the length of the floor along the y-axis
x, y	Coordinates (x,y) on the plate where the deflection is investigated, [m]
W_{mn}	Factor determined by the stiffness, proportion and the Poisson's ratio of the floor, for derivation see Appendix A
P_{mn}	Factor determined by the load acting on the structure, see Equations (5.20- 5.21)

For a uniformly distributed load q [kN/m^2],

$$P_{mn} = \frac{16q}{mn\pi^2} \tag{5.20}$$

For a point load P [kN],

$$P_{mn} = \frac{4P}{mn\pi^2} \tag{5.21}$$

The allowed deformations differ from case to case and is up to the structural designer to determine what is acceptable. Eurocode gives recommendations for the deflection of a timber beam which says that the instantaneous deflection should be less than a value between $L/300$ and $L/500$, where L is the span of

the beam. In this thesis the most strict criterion is used for the global deflection of the floor as:

$$w_{inst} \leq \frac{min(B, L)}{500} \tag{5.22}$$

The local deflection between the corrugation periods shown in Figure 5.3 is considered to be restrained by the filling material in the cavities and is therefore not investigated in this thesis. If the cavities for some reason would not be restrained, the local deflection also needs to be investigated.

5.3 Dynamic performance

The dynamic response of a floor, for instance vibrations, arise when it is exposed to loads that vary over time (Ohlsson, 1988). Light-weight structures are sensitive to transient loading (i.e. loading caused by human activities) and for residential buildings this is often the governing factor causing disturbing vibrations. These vibrations are causing discomfort for the users. The discomfort is, in the same way as acoustics, subjective and it is therefore difficult to create a good design code. Eurocode has set three criteria that need to be fulfilled in order to create comfort when using timber floors in residential buildings which are:

$$f_1 \geq 8 Hz \tag{5.23}$$

$$w_{1kN} \leq 1.5\, mm \tag{5.24}$$

$$v \leq b^{(f_1 \zeta - 1)} \tag{5.25}$$

where

f_1	Fundamental frequency, [Hz]
w_{1kN}	Deflection caused by a point load of 1 kN, [m]
v	Unit impulse velocity response, [m/s]
b	Factor taken from the Swedish Annex recommended to 100 m/Ns^2 for Swedish conditions
ζ	Modal damping ratio, [-]

The fundamental frequency is the frequency at which a system tends to oscillate in the absence of any driving or damping force. This is of interest to know if the system is classified as low or high frequency floor. Low frequency floors, below 8-10 Hz, are sensitive to walking with resonant vibration and high frequency floors, above 8-10 Hz, are sensitive to the individual step (Jarnerö, 2014). For the analytic solution simplifications are made to calculate the fundamental frequency in terms of using a single degree of freedom (SDOF) system. The floor element is a continuous system and its complete behaviour can not be captured by an SDOF-system. This only consider the first mode shape and assumes that only this exist. When the floor structure is demonstrated in a SDOF system, f_1, for an orthotropic high frequency

floor, can be calculated with the Reissner-Mindlin plate theory. When removing all the zero expressions and not accounting for the in-plane vibration that model can be simplified as (Reissner, 1945):

$$f_1 = \frac{1}{2\pi}\sqrt{\frac{\bar{s}_{33}}{\hat{m}_{33}}} \tag{5.26}$$

where

$\bar{s}_{33}$ Factor calculated from the shear stiffness, for derivation see Appendix A
$\hat{m}_{33}$ Total mass of the floor including permanent load, [kg/m^2]

This simplified expression can be used for a sandwich floor when only frequencies of flexural vibrations are of interest. Other modes are not fundamental for a floor with a thin core and moderately thick plate. Seen in Equation (5.26), the dynamic resistance is dependent of the stiffness and the mass of the floor. A high fundamental frequency is preferable to achieve good dynamic performance. If none of the parameters stiffness and mass can be changed to improve the vibrations, implementation of a vibration/damping elastic interlayer can be added, which also contributes to the acoustic performance (Jarnerö, Bolmsvik, Brandt, and Olsson, 2012).

5.4 Shear stress

The highest shear stresses of the floor will occur in the middle of the core for a sandwich plate with corrugated core (Zenkert, 1997). When designing a structure with faces with lower shear strength than the core, the interface between core and face also needs to be controlled. The adhesive connection between the face and the core is considered to have a higher shear strength than the timber itself, which means that the timber will fail before the adhesive and is therefore not controlled. To calculate the transverse shear forces T_x [N] and T_y [N], the following equations are used:

$$T_x = \sum_{n=1}^{\infty}\sum_{m=1}^{\infty} -\frac{X_{mn}q_{mn}}{Z_{mn}} \cos\left(\frac{m\pi x}{L}\right) \sin\left(\frac{n\pi y}{B}\right) \tag{5.27}$$

$$T_y = \sum_{n=1}^{\infty}\sum_{m=1}^{\infty} -\frac{Y_{mn}q_{mn}}{Z_{mn}} \sin\left(\frac{m\pi x}{L}\right) \cos\left(\frac{n\pi y}{B}\right) \tag{5.28}$$

where

X_{mn}	Factor determined by the stiffness, size and the Poisson's ratios of the plate used for T_x, for derivation see Appendix A
Y_{mn}	Factor determined by the stiffness, size and the Poisson's ratios of the plate used for T_y, for derivation see Appendix A
Z_{mn}	Factor determined by the stiffness, taking into account both X_{mn} and Y_{mn}, see Appendix A
q_{mn}	Factor determined by the load acting on the structure, uniformly distributed load or point load, see Equations (5.20-5.21) in Section 5.2
x, y	Coordinates (x,y) on the plate where shear force is investigated, [m]
L, B	Total length of the plate in x- and y direction respectively, [m]

The shear stresses, τ_{Ed} [Pa], acting on the structure can then be calculated according to simple beam theory (Zenkert, 1997):

$$\tau_{Ed} = \frac{TS}{Ib} \tag{5.29}$$

where

T	Transverse shear force, see Equation (5.27-5.28), [N]
S	First moment of area, [m^3]
I	Second moment of area, [m^4]
b	Width of the cross-section at the investigated z-coordinate, [m]

According to Eurocode the shear stresses should for all parts of the cross-section fulfill the following demand:

$$\tau_{Ed} \leq \tau_{Rd} = \frac{k_{mod} f_{vk}}{\gamma_M} \tag{5.30}$$

where

f_{vk}	Characteristic value for shear strength, [Pa]

5.5 Principal stresses

In the design of a timber cross-section the stresses in different principal directions need to be evaluated. This is made by fulfilling the following four requirements (Eurocode, 2017):

$$\sigma_{t0d} \leq f_{t0d} = k_{mod} \frac{f_{t0k}}{\gamma_M} \tag{5.31}$$

$$\sigma_{t90d} \leq f_{t90d} = k_{mod} \frac{f_{t0k}}{\gamma_M} \tag{5.32}$$

$$\sigma_{c0d} \leq f_{c0d} = k_{mod} \frac{f_{c0k}}{\gamma_M} \tag{5.33}$$

$$\sigma_{c90d} \leq f_{c90d} = k_{c90} k_{mod} \frac{f_{c0k}}{\gamma_M} \tag{5.34}$$

where

σ_{t0d}	Tensile stress parallel to the grain, [Pa]
f_{t0k}	Characteristic tensile strength parallel to the grain, [Pa]
σ_{t90d}	Tensile stress perpendicular to the grain, [Pa]
f_{t90k}	Characteristic tensile strength perpendicular to the grain, [Pa]
σ_{c0d}	Compressive stress parallel to the grain, [Pa]
f_{c0k}	Characteristic compressive strength parallel to the grain, [Pa]
σ_{c90d}	Compressive stress perpendicular to the grain, [Pa]
f_{c90k}	Characteristic compressive strength perpendicular to the grain, [Pa]
k_{c90d}	Factor taking into account load configuration, [-]

For an orthotropic material another criterion is also required to be fulfilled (Norris, 1962). According to Norris (1962) the failure in wood would occur under plane stress if this criteria is fulfilled:

$$\left(\frac{\sigma_x}{f_x}\right)^2 - \frac{\sigma_x \sigma_y}{f_x f_y} + \left(\frac{\sigma_y}{f_y}\right)^2 + \left(\frac{\tau_{xy}}{f_v}\right)^2 = 1 \tag{5.35}$$

where

σ_x	Stress parallel to the x-axis, [Pa]
f_x	Strength parallel to the x-axis, [Pa]
σ_y	Stress parallel to the y-axis, [Pa]
f_y	Strength parallel to the y-axis, [Pa]
τ_{xy}	In plane shear stress, [Pa]
f_v	In plane shear strength, [Pa]

These criteria are only checked with a FE model after the design is made. They are not involved in the design process and for that reason not affecting the design of the cross-section.

5.6 Local bending of top plate

Just as a top board of a traditional timber floor needs to have sufficient strength to distribute the load to the joists, a corrugated sandwich floor needs to have sufficient strength between each top of the corrugated core as well. When checking the top face bending capacity, a load P of 1 kN, will be distributed on a 50x50 mm surface in the middle of a corrugation span, see Figure 5.2. In order to create a realistic

calculation model, the closest neighbouring spans will be included in the model as well, hence three periods of corrugation will be included. The bending will be modelled as a simply supported continuous beam with three spans, see Figure 5.3. The width of the beam will be considered to be the full width of the plate, hence 4 or 6 m and the height is the thickness of the top plate.

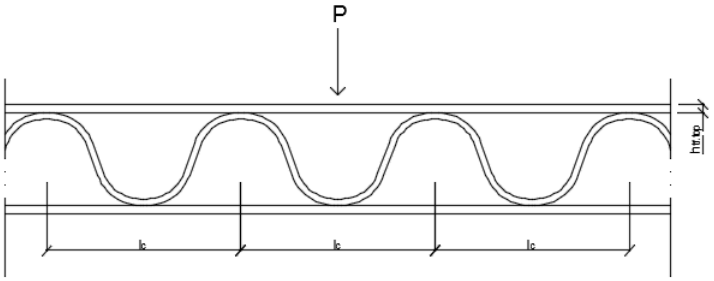

Figure 5.2: Model for analytic model.

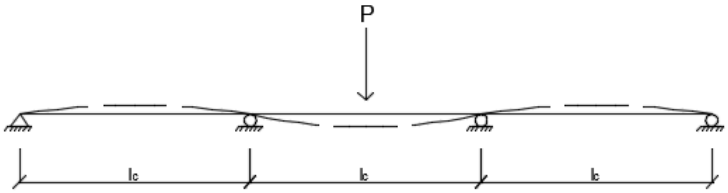

Figure 5.3: Simplified calculation model for local bending.

As explained in Section 5.2, the shear deformations cannot be neglectable for a material with low shear modulus. The maximum moment $M_{Ed.local}$ [Nm] is therefore derived based on Timoshenko theory which includes the effects of shear deformations:

$$M_{Ed.local} = \frac{3}{8}\,\frac{n}{5n+6} \tag{5.36}$$

$$n = \frac{K_s G A L^2}{EI} \tag{5.37}$$

where

K_s	Shear reduction factor, equals to 5/6 [-]
G	Transverse shear modulus, [Pa]
L	Length of a single span, [m]
EI	Flexural stiffness for the top plate, [Nm^2]
A	Area of cross-section, [m^2]

According to Eurocode, the following demand must be satisfied:

$$M_{Ed.local} \leq M_{Rd.local} = f_{md} W = k_{mod} \frac{f_{mk}}{\gamma_M} W \tag{5.38}$$

where

$M_{Rd.local}$ Local bending resistance, [Nm]
k_{mod} Strength modification factor, [-]
f_{mk} Characteristic value for bending strength, [Pa]
γ_M Partial coefficient for the material, [-]
W Section modulus, [m^3]

5.7 Local buckling

For a sandwich element the local buckling can occur in the faces or in the core. When investigating a sandwich plate with corrugated core the local instability mainly occurs in the core. This is due to the resultant compressive force from the ultimate load, P [N], acting on the plate, is acting directly on the corrugated core and is calculated as:

$$P = \frac{P_{ULS}}{sin(\theta)} \tag{5.39}$$

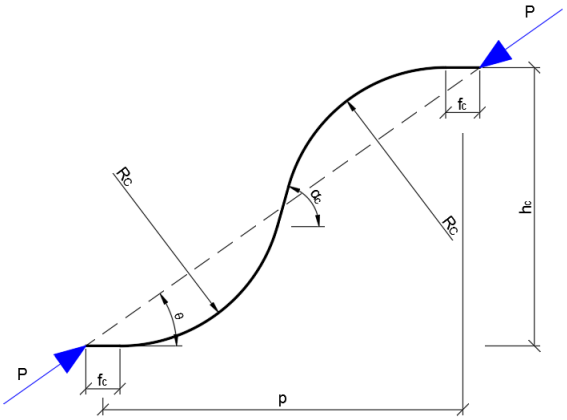

Figure 5.4: Simplification of calculating the local buckling of the corrugated core.

The corrugated core has a shape of the second buckling mode of a straight simply supported beam. For calculation of the critical buckling force P_{cr} [N], Euler buckling theory is assumed, see Equation (5.40). To calculate the critical buckling length L_{cr} [m], see Equation (5.41). Assumptions are made that the critical length is the extended length of the part in Figure 5.4.

$$P_{cr} = \frac{EI\pi^2}{L_{cr}^2} \tag{5.40}$$

where

$$L_{cr} = 2f_c + d + 2R_c\alpha_c \tag{5.41}$$

The failure criterion that need to be fulfilled is stated in Eurocode as:

$$P \leq P_{cr} \tag{5.42}$$

6 Validation

Before finding the optimal cross-sections, a verification and comparison between the analytic solution and the FE analyses were made. The verification has been done with a fixed reference geometry due to the time consuming process of modelling in 3D-solid. With a fix geometry, the results can be achieved rather quick by only changing the material properties. As can be seen in Table 6.2, all the material combinations and all possible grain directions result in 32 cases. In this early phase, only deflection from uniformly distributed load and fundamental frequency will be validated since the SLS criteria often are governing. In future steps, when the optimization is done, further controls will be made. For the verification, a *4x6 floor* with the following geometry has been used, for visualization see Figure 6.1:

Table 6.1: The geometry of the floor used for the validation, also visualized in Figure 6.1.

Variable	h_c[mm]	t_f[mm]	t_c[mm]	α_c[°]	f_c[mm]	R_c[mm]
Geometry	90	21	15	55	30	100

Before analysing all the variations of materials in Abaqus, a convergence study of the mesh was made for both shell and solid elements, see Appendix C. The mesh size chosen for the verification are both for shell and solid elements 0.04 m. The obtained results are presented first as bar charts, see Figure 6.2 and 6.3, and later the same results are presented in Table 6.2.

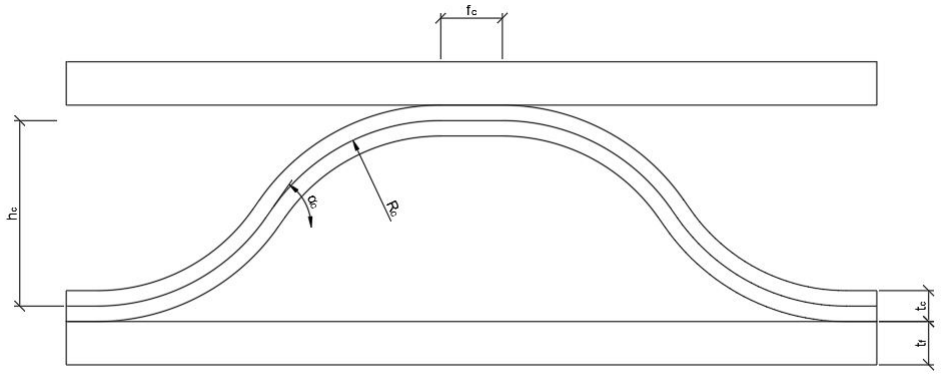

Figure 6.1: Visualization of the geometry used in the validation.

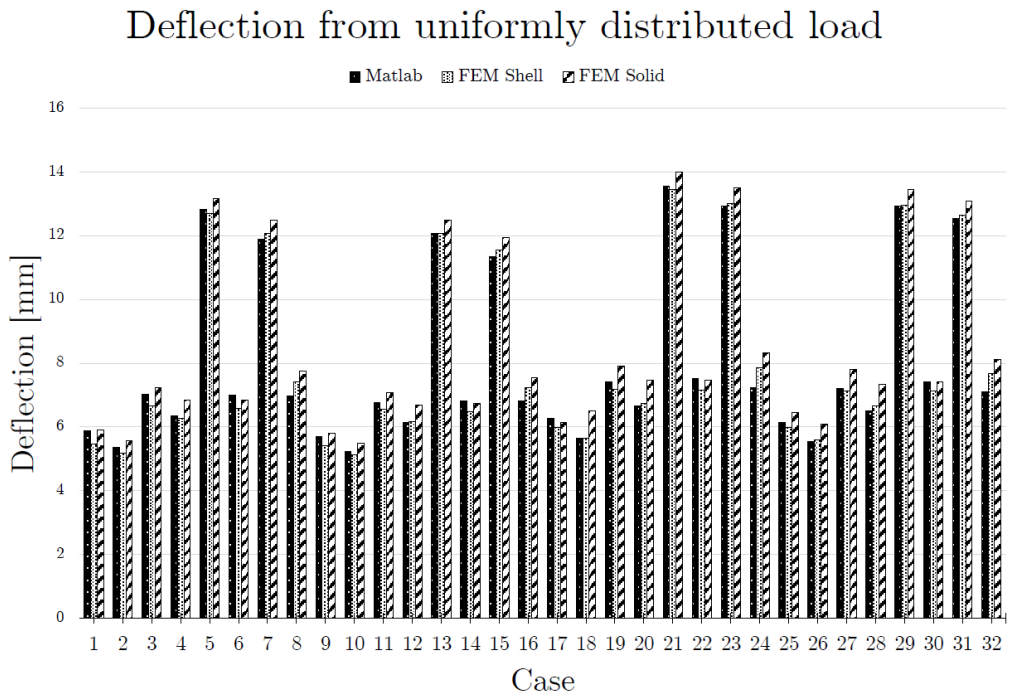

Figure 6.2: Bar chart showing the deflection comparison between the different methods of analyses, the analytic solution (Matlab), the finite element method with both shell (FEM shell) and solid (FEM solid) of all 32 cases stated in Table 6.2.

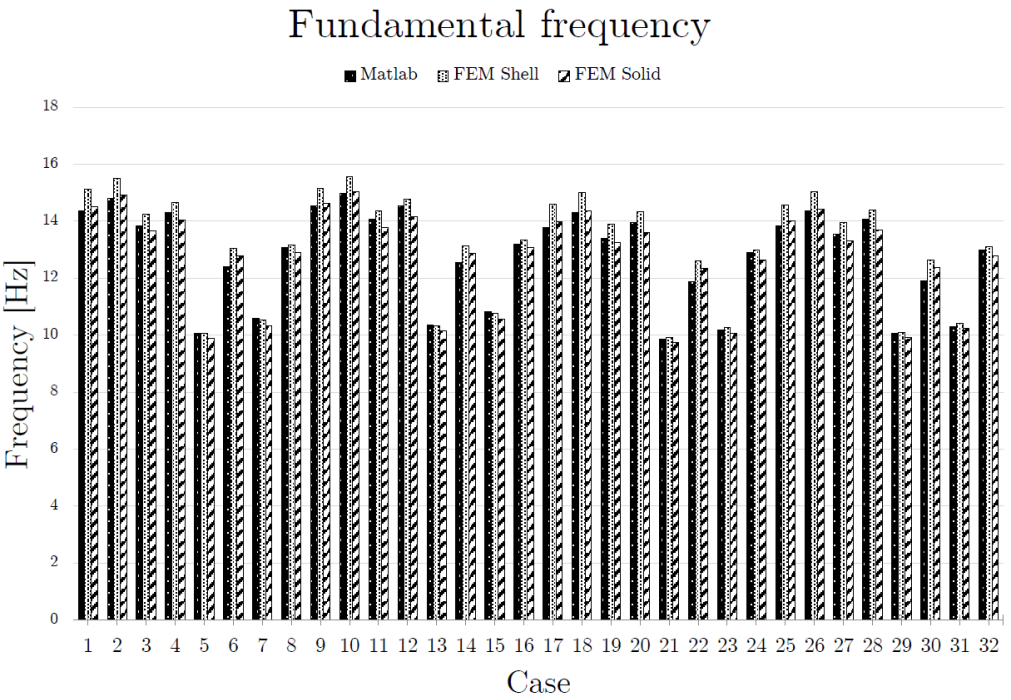

Figure 6.3: Bar chart showing the fundamental frequency comparison between the different methods of analyses, the analytic solution (Matlab), the finite element method with both shell (FEM shell) and solid (FEM solid) of all 32 cases stated in Table 6.2.

When using shell elements in Abaqus, the analytic solution corresponds relatively well and generates results that are on the safe side, except when using Kerto-Q as face material. The error is likely due to the approximation of the assumptions made when obtaining the transverse shear stiffness. The error is although rather small and the model is considered trustworthy. Apart from the case with Kerto-Q, the deflection calculated analytically is overestimated and the natural frequency is underestimated, which is desirable.

The reasons for rather poor results obtained when using solid elements are described in Section 4.2 and will further on not be used.

Table 6.2: Comparison of deflection and fundamental frequency between analytic (Matlab) and FE analyses (shell and solid elements). The geometry is constant according to Table 6.1

			Criteria							
			Deflection [mm]				Fundamental Frequency [Hz]			
Core	Face	Case	Matlab	FEM Shell	FEM Solid	Discrepancy Matlab and FE shell [%]	Matlab	FEM Shell	FEM Solid	Discrepancy Matlab and FE shell [%]
B⊥	B⊥	1	5.88	5.47	5.90	7.57	14.35	15.12	14.52	-5.06
	B‖	2	5.35	5.17	5.57	3.40	14.81	15.51	14.94	-4.49
	C⊥	3	7.02	6.66	7.23	5.36	13.82	14.26	13.67	-3.04
	C‖	4	6.34	6.27	6.83	1.19	14.32	14.67	14.03	-2.36
	P	5	12.84	12.70	13.16	1.10	10.06	10.07	9.90	-0.06
	M	6	7.00	6.57	6.85	6.44	12.41	13.05	12.78	-4.9
	K⊥	7	11.90	12.07	12.50	-1.37	10.60	10.53	10.33	0.67
	K‖	8	6.98	7.41	7.76	-5.89	13.07	13.18	12.90	-0.81
B‖	B⊥	9	5.71	5.42	5.80	5.30	14.55	15.17	14.64	-4.07
	B‖	10	5.22	5.12	5.50	1.82	14.99	15.57	15.04	-3.73
	C⊥	11	6.76	6.56	7.08	3.06	14.08	14.36	13.79	-1.91
	C‖	12	6.14	6.17	6.69	-0.40	14.55	14.77	14.17	-1.5
	P	13	12.07	12.07	12.49	-0.04	10.37	10.32	10.15	0.47
	M	14	6.82	6.49	6.75	5.11	12.55	13.12	12.86	-4.34
	K⊥	15	11.35	11.54	11.93	-1.62	10.81	10.76	10.57	0.53
	K‖	16	6.80	7.22	7.54	-5.79	13.20	13.34	13.07	-1.02
C⊥	B⊥	17	6.26	5.99	6.49	4.57	13.78	14.60	14.00	-5.56
	B‖	18	5.65	5.63	6.15	0.36	14.31	15.02	14.36	-4.71
	C⊥	19	7.42	7.19	7.91	3.14	13.41	13.91	13.24	-3.58
	C‖	20	6.65	6.73	7.47	-1.18	13.97	14.34	13.61	-2.63
	P	21	13.55	13.46	14.01	0.70	9.86	9.92	9.73	-0.67
	M	22	7.52	7.15	7.48	5.11	11.88	12.62	12.34	-5.84
	K⊥	23	12.94	13.02	13.51	-0.59	10.17	10.28	10.08	-0.98
	K‖	24	7.24	7.86	8.33	-7.92	12.91	12.98	12.63	-0.53
C‖	B⊥	25	6.14	5.98	6.46	2.68	13.84	14.58	14.02	-5.05
	B‖	26	5.55	5.6	6.09	-0.88	14.37	15.03	14.41	-4.36
	C⊥	27	7.21	7.13	7.79	1.18	13.54	13.95	13.32	-2.91
	C‖	28	6.49	6.66	7.34	-2.48	14.09	14.40	13.70	-2.16
	P	29	12.93	12.95	13.44	-0.17	10.06	10.10	9.92	-0.35
	M	30	7.41	7.12	7.42	4.17	11.91	12.63	12.37	-5.72
	K⊥	31	12.55	12.64	13.08	-0.68	10.28	10.42	10.23	-1.26
	K‖	32	7.10	7.68	8.11	-7.59	13.00	13.11	12.78	-0.88
Average Discrepancy			-	0.43	-5.11	-		-2.77	-12.1	-

7 Numerical results and discussion

The optimization code is validated and in this chapter it is used to develop twenty optimal cases by combining all different material combinations, grain orientations and floor size ratios (i.e 4x6 and 6x4). None of the combinations were disregarded in the process even though studies and conclusions were made by Larsson and Mayor (2016) of different combinations. They concluded that the optimal case for a rectangular floor with dimension of the ratio 2:1, corresponding to the same extrusion of corrugation that we use in *6x4 floor*, were obtained by having a grain orientation ($\perp - \perp - \perp$), and for a floor of dimension ratio of 1:2, corresponding to the *4x6 floor*, the grain orientation should be placed ($\| - \| - \|$). They also stated that for all cases the instantaneous deflection is less for the 1:2 floor. This was conclusions made with other assumptions than used in this thesis. The analytic solution now includes shear deformations and orthotropic material behaviour, therefore such a conclusion cannot be made and both the *4x6 floor* and the *6x4 floor* must be optimized before disregarding any of the alternatives.

7.1 Case study

In order not to miss out on any case that possibly could be the optimal one, the following combinations were optimized:

- Two variations of the corrugation extrusion, (*4x6 floor* and *6x4 floor*).
- Ten different material combinations (five face materials and two core materials).
- Four different grain orientation combinations, see Figure 3.2.
- Five different thicknesses of the core (6.5 mm, 9 mm , 12 mm, 15 mm, 18 mm).

The core thicknesses are standard dimensions available on the market and are fixed for every optimization due to the shape of the curved parts of the core. All the other variables are free to move within a certain upper and lower bound in order to find the optimal geometry that minimizes the height. All together, 320 cases are optimized analytically. See Appendix D to see graphs over how the variables change for the optimal cases when the thickness of the core changes.

The material properties for the different products change with various thicknesses. Since the thickness of the core is fixed, there are no problems inserting the properties, but for the face, an initial guess of the thicknesses will decide the properties. If the optimization returns with a face thickness that differs from the initial guess, the new properties must be inserted. This has to be done as an iteration until the material properties match with the optimized thickness. For the given materials, the material properties that have been used are shown in Table 7.1.

Table 7.1: Material properties for the material used for the 20 optimal cases.

Material	Thickness [mm]	Density [kg/m^3]	E_1 [MPa]	E_2 [MPa]	ν_{12} [-]	G_{12} [MPa]	G_{13} [MPa]	G_{23} [MPa]
Birch Plywood	6.5	630	12737	4763	0.5	620	169	123
Birch Plywood	9	630	11395	6105	0.5	620	206	155
Birch Plywood	12	630	10719	6781	0.5	620	207	170
Birch Plywood	15	630	10316	7184	0.5	620	207	178
Birch Plywood	18	630	10048	7452	0.5	620	206	183
Conifer Plywood	6.5	410	9462	3529	0.5	530	66	41
Conifer Plywood	9	410	8465	4535	0.5	530	69	52
Conifer Plywood	12	410	7963	5037	0.5	530	69	57
Conifer Plywood	15	410	7663	5337	0.5	530	69	59
Conifer Plywood	18	410	7464	5536	0.5	530	69	61
Conifer Plywood	21	410	7323	5677	0.5	530	69	62
Kerto-Q	21-24	480	10000	2400	0.02	600	600	600
Particle board	25-32	550	2400	2400	0.2	680	680	680
Magnesium board	20	1000	5560	5560	0.35	2059	2059	2059

By studying the analytic results it was found that the governing criteria was solely the global deflection from a distributed load. Equation (7.1) shows that the maximum allowed deflection for the investigated slab always is 8 mm.

$$w_{inst} \leq \frac{min(B, L)}{500} = \frac{4000\ mm}{500} = 8\ mm \tag{7.1}$$

After a process with meetings with companies from the industry some requests about the dimensions were brought up. Requests about that the thickness of the core should not be too thin (6.5 mm) or too thick (15-18 mm) were broached and also that the inclination angle α_c should, if possible, be somewhere in the middle of the constraint range of 55° and 89°. By taking all of these requests into consideration, 10 cases for the *4x6 floor* and 10 cases for the *6x4 floor* were selected from graphs showing the variation of how the variables h_{tot}, α_c, V, p, t_f, h_c, R_c and f_c varies when the core thickness t_c varies, see Appendix D.

By studying these graphs it was found that for all the combinations made for the *4x6 floor* the grain orientation placed ($\| - \| - \|$) always made the optimal case. For the *4x6 floor* the core thickness was chosen to be either 9 mm or 12 mm and the inclination angle between 60°-80°. For the *6x4 floor* the study shows that for this case the opposite grain direction is the optimal one ($\perp - \perp - \perp$). For this floor all the cases that were chosen have a core thickness of 12 mm. The optimal inclination angle for these cases were about 55° for every case and were accepted even though it was lower than desired.

To create 20 cases with products with standard dimensions, the face thickness is also set to a standard dimension close to the optimized thickness. A new optimization were then carried out to optimize the remaining variables. All of these 20 cases are presented in Table 7.2 and the most important parameter, the total height, is visualized in Figure 7.1. It shows that the lowest height obtained with the analytic model is obtained with a *4x6 floor* with pure birch plywood with grain orientation ($\parallel - \parallel - \parallel$).

Table 7.2: 20 optimal cases. The material combinations are referred as Face material/Core material/Face material where B-Birch plywood, C-Conifer plywood, K-Kerto-Q, M-Magnesium board, P-Particle board

Material	LxB	Grain Orientation	Height [mm]	Volume [m^3]	h_c [mm]	t_f [mm]	t_c [mm]	α_c [°]	f_c [mm]	R_c [mm]
B/B/B	4x6	$\parallel - \parallel - \parallel$	123.6	1.14	78.6	18	9	74.1	30	54
	6x4	$\perp - \perp - \perp$	132.3	1.21	84.3	18	12	55.0	30	72
C/B/C	4x6	$\parallel - \parallel - \parallel$	133.1	1.21	85	18	12	65.8	30	72
	6x4	$\perp - \perp - \perp$	142.2	1.36	88.2	21	12	64.2	30.8	73.3
K/B/K	4x6	$\parallel - \parallel - \parallel$	142.2	1.28	91.2	21	9	70.0	50	61
	6x4	$\perp - \perp - \perp$	142.2	1.34	88.2	21	12	58.4	35	92.7
M/B/M	4x6	$\parallel - \parallel - \parallel$	138.0	1.31	86.0	20	12	66.2	30	72
	6x4	$\perp - \perp - \perp$	146.6	1.31	94.6	20	12	55.0	30	72
P/B/P	4x6	$\parallel - \parallel - \parallel$	179.7	1.63	115.7	26	12	78.6	30	72
	6x4	$\perp - \perp - \perp$	196.3	1.77	126.3	29	12	60.7	30	72
B/C/B	4x6	$\parallel - \parallel - \parallel$	127.4	1.14	82.4	18	9	76.3	30	54
	6x4	$\perp - \perp - \perp$	144.1	1.36	90.1	21	12	55.0	30	72
C/C/C	4x6	$\parallel - \parallel - \parallel$	136.6	1.22	88.6	18	12	67.3	30	72
	6x4	$\perp - \perp - \perp$	160.4	1.37	106.4	21	12	55.0	30	72
K/C/K	4x6	$\parallel - \parallel - \parallel$	142.2	1.29	91.2	21	9	70.5	30	54
	6x4	$\perp - \perp - \perp$	162.4	1.51	102.5	24	12	55.0	30	72
M/C/M	4x6	$\parallel - \parallel - \parallel$	144.9	1.31	92.9	20	12	56.8	30	72
	6x4	$\perp - \perp - \perp$	164.6	1.32	112.6	20	12	55.0	30	72
P/C/P	4x6	$\parallel - \parallel - \parallel$	187.1	1.69	121.1	27	12	80.8	30	72
	6x4	$\perp - \perp - \perp$	211.0	1.86	137.0	31	12	55.0	30	72

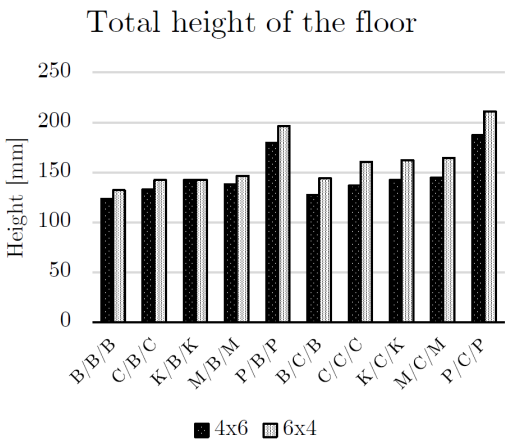

Figure 7.1: Comparison of the total height of the 20 optimal cases.

These 20 optimal cases were modelled with shell elements in Abaqus the same way as the verification of the analytic solution in Chapter 6. All of the cases have been analysed with regard to deflection, dynamic performance, principle stresses and buckling, which is summarized in the Sections 7.1.1-7.1.4. Some of the criteria are not analysed in Abaqus, since the analytic solution is considered to be sufficient for these criteria.

7.1.1 Deflection

The governing criterion for the optimization is the deflection caused by a uniformly distributed load and the result can be seen in Figure 7.2. As expected the analytical solution in Matlab and the FE model are in good agreement. It can be noticed that for the *6x4 floor* the analytic solution and the FEM solution does not corresponds as well as the *4x6 floor*. This could mean that the analytic solution is sensitive for either the extrusion length (L) or the total length of the corrugation (B). This should be investigated further in order to draw conclusions.

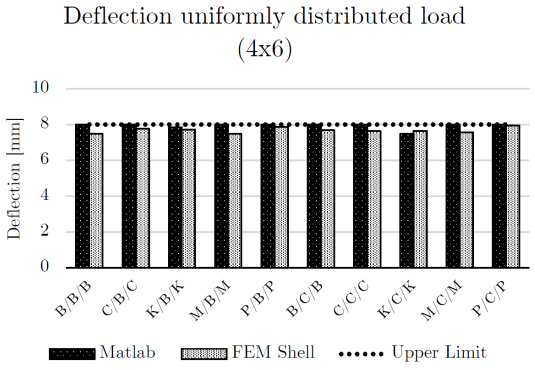

(a) *4x6 floor for 10 material combinations, average error 3.2%.*

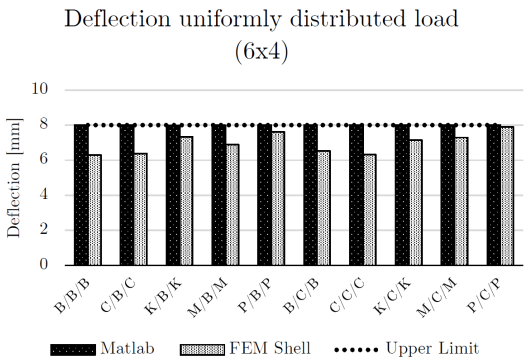

(b) *6x4 floor for 10 material combinations, average error 12.9%.*

Figure 7.2: Deflection for a uniformly distributed load, 4x6 and a 6x4 floor.

The optimized cases in Matlab always reach the maximum deflection of 8 mm except for the K/C/K and K/B/K case for a *4x6 floor*, see Figure 7.2. This is due to the criteria in Equation (3.7), which needs to be fulfilled for the assumption of thin faces in the sandwich theory. In other words, the governing criterion for these cases is

$$5.77 \leq \frac{h}{t_{f\,top}} \leq 100 \tag{7.2}$$

Since the thinnest Kerto-Q board of 21 mm was used, the total height can not be less than 142.2 mm which is reached for both K/C/K and K/B/K for a *4x6 floor*, see Table 7.2. The total height of the floor can therefore not be lower, even though none of the performance constraints are fully utilized.

As noticed from the validation in Chapter 6, the case when Kerto-Q is used it can lead to a higher deflection in the FE model than expected from the analytic solution. This behaviour was obtained when K/C/K was used for the *4x6 floor*. Luckily, since none of the performance constraints were fully utilized in the analytic solution, the total deflection does not exceed the limit of 8 mm.

7.1.2 Dynamic response

Only the first two criteria from the dynamic response have been analysed in the FE model, the fundamental frequency and the deflection caused by a point load of 1 kN:

$$f_1 \geq 8\,Hz \tag{7.3}$$

$$w_{1kN} \leq 1.5\,mm \tag{7.4}$$

When investigating the fundamental frequency, only the self-weight and a dead load of 50 kg/m^2 are considered. The dead load is added to be a part of the self-weight. This is done by converting the dead load to an increased density of the parts of the floor. The extra density is distributed to both the faces and the core proportional to the face-core volume ratio. The results can be seen in Figure 7.3. When doing a FE model, a multiple degrees of freedom (MDOF) system describes the mode shapes of the floor the best. In this case all mode shapes for each frequency can be seen and investigated compared with the analytic solution using a SDOF system.

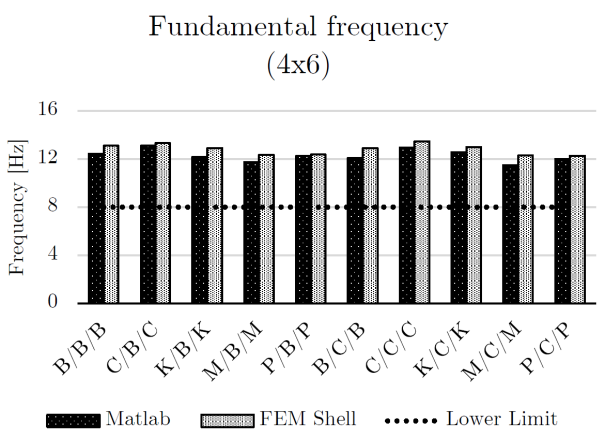

(a) *4x6 floor for all 10 material combinations, average error 4.2%.*

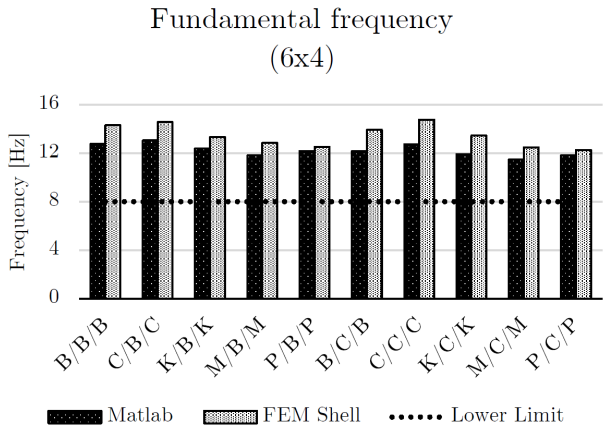

(b) *6x4 floor for all 10 material combinations, average error 9.9%.*

Figure 7.3: Fundamental Frequency for a 4x6 and 6x4 floor.

In the same way as the local bending analysis in Section 5.6, the point load of 1 kN is converted to a load acting on a surface of 50x50 mm square. On this area, a pressure load of 400 kPa is applied. This load is placed at the middle of the plate and the resulting deflection can be seen in Figure 7.4.

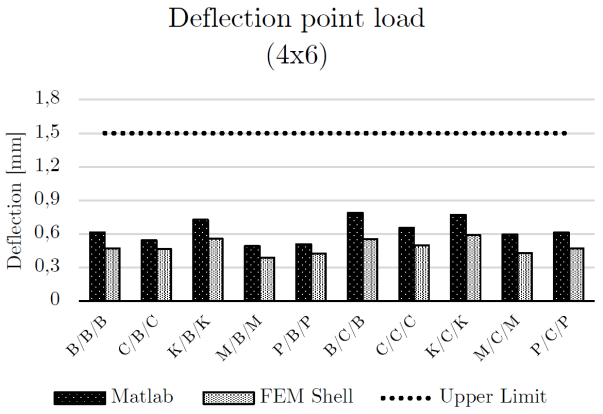

(a) *Deflection from 1 kN point load for the 4x6 floor, average error 22.6%*

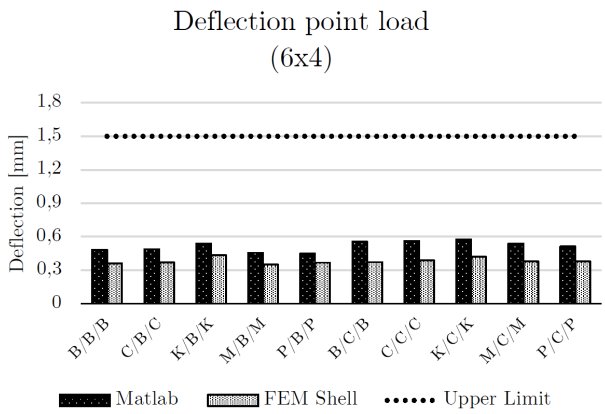

(b) *Deflection from 1 kN point load for the 6x4 floor, average error 25.7%*

Figure 7.4: Deflection from 1 kN point load for a 4x6 and 6x4 floor.

7.1.3 Principal stresses

The tensile and compressive stresses in Equations (5.31-5.34) are controlled and the utilization ratio for this criteria is higher than the Norris criteria. The highest utilization ratio is 69.1 %, which is obtained in the core for the M/C/M *6x4 floor* case. For the maximal stresses in all parts of the floor and in all directions, see Appendix E.

In order to find the location where Norris criteria should be controlled, the Von Mises stresses are used. By using Abaqus, it is easy to find where the highest Von Mises stresses occur and this is where σ_x, σ_y, and τ_{xy} are investigated. As expected, the utilization ratio is rather low with a maximum of 17.0%, which again occur for M/C/M *6x4 floor*. For all utilization ratios for all optimal cases see Appendix E.

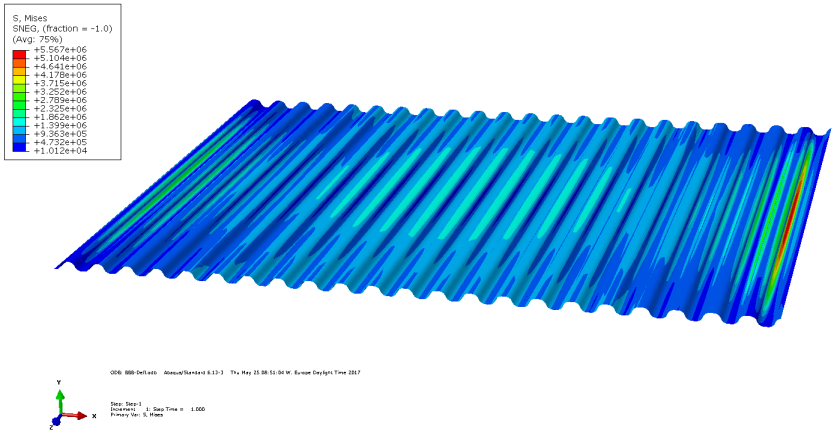

Figure 7.5: Von Mises stress in the core

The location of the highest stress is obtained close to the edge where the corrugation abruptly ends, see Figure 7.5. Since the corrugation does not end at an intersection with the face, the stresses are higher than what would be expected if it ended with an intersection. When the design of the floor will be further developed, this is not likely to be an issue since this result is on the safe side.

7.1.4 Linear buckling analyses

For the linear buckling analyses, the same load as for deflection of the uniformly distributed load is used. The buckling analyses is performed in Abaqus where the three first buckling modes are analysed. Lanczos eigensolver is used and the three first buckling modes are similar for all 20 cases. As the linear buckling analyses is used, a material without any imperfections are considered which is not realistic, especially since timber products are used.

The load factor, which is the ratio between the buckling load and the applied load, always exceeds a value of 22 which is considered safe even though the linear analysis is used. The worst case is shown above in Figure 7.6 with the three first buckling modes.

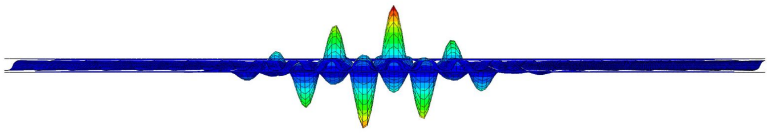

(a) *First mode shape.*

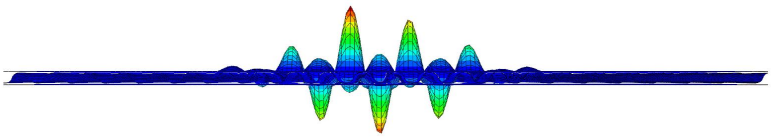

(b) *Second mode shape.*

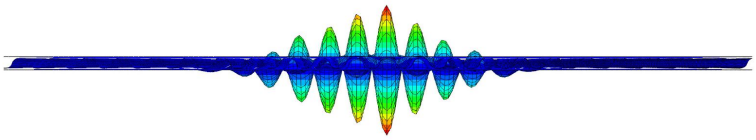

(c) *Third mode shape.*

Figure 7.6: Three different mode shapes of the floor.

7.1.5 Price list

A price comparison has been made where only the material cost is included. In table 7.3, a price list from lowest to highest is made for all the five materials used.

Table 7.3: Price list of the different material used for the optimal cases (Angard, 2017).

Material	Price [SEK/m^3]
Particle board	2500
Conifer Plywood	4500
Kerto-Q	6000
Birch Plywood	7700
Magnesium board	9500

The material price for each of the 20 cases per m^2 can be calculated and the results can be seen in Table 7.4, again the price is sorted from lowest to highest.

Table 7.4: Price per square meter for every optimal case sorted by price, from lowest to highest.

	4x6		6x4	
	Material	Price [SEK/m^2]	Material	Price [SEK/m^2]
1	P/C/P	208.4	P/C/P	225.5
2	C/C/C	228.2	C/C/C	256.0
3	P/B/P	253.2	P/B/P	266.7
4	C/B/C	273.7	C/B/C	301.4
5	K/C/K	305.6	K/C/K	354.6
6	B/C/B	329.4	K/B/K	359.0
7	K/B/K	338.2	B/B/B	388.1
8	B/B/B	365.0	B/C/B	388.7
9	M/C/M	446.2	M/C/M	448.0
10	M/B/M	492.4	M/B/M	492.4

7.2 Concept suggestion

Initially the industry requested a solution with magnesium board or particle board as face material. Particleboard used as face material was expected to outperform the other options in terms of price (without loosing substantially in height) but it turned out that this was not the case and since the height of the floor increases substantially, particle board is not the best choice. Magnesium board has some acoustical and fire safety advantages compared to the other materials but the price is to high to be considered as compatible. Birch plywood is the strongest material which result in the lowest total height but the material price is rather high. Kerto-Q is more expensive than conifer plywood and the total height is not lower. Therefore, there is no reason to consider Kerto-Q as face material.

After investigating all the cases, combining the height of the floor and the price, the case with pure conifer plywood with grain orientation (⊥-⊥-⊥) is considered as the best material choice. The *4x6 floor* is both lower and cheaper than *6x4 floor* which makes it the obvious choice between the two. Conifer has the advantage of being strong relatively to the price and is therefore considered to be the best material choice for both the core and the face, see Figure 7.7 for chosen suggestion of design. The core thickness of 12 mm was chosen since this provide a low total height in combination with a desired inclination angle. For a core thickness of 12 mm, the optimal face thickness is 19.8 mm. Due to the standard dimensions available, the face is set to both 18 mm and 21 mm in order to find the lowest total height which is obtained with 18 mm.

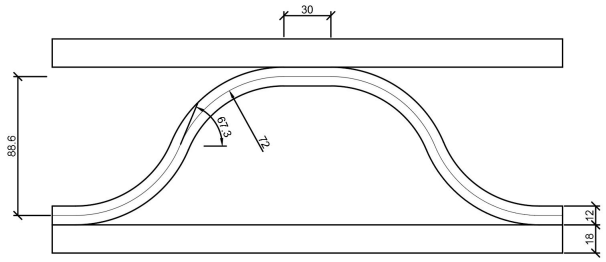

Figure 7.7: Geometry with given dimensions in mm and degrees of chosen optimal case, C/C/C.

The optimal case for the material combination C/C/C is explained more in detail to see how different variables affect each other and the total height, this can be seen in Figure 7.8. At a first glance, it can be seen that the curves follow each other in pairs depending on the grain orientation of the face. This indicates that the orientation of the face is the governing orientation direction. The two pairs have the same trend just a small offset from each other.

A criteria that is fully utilized for all thicknesses is the deflection of 8 mm from the uniformly distributed load. Furthermore, for the thinnest core (6.5 mm) the deflection from the point load is also fully utilized. This explains the big difference in inclination angle.

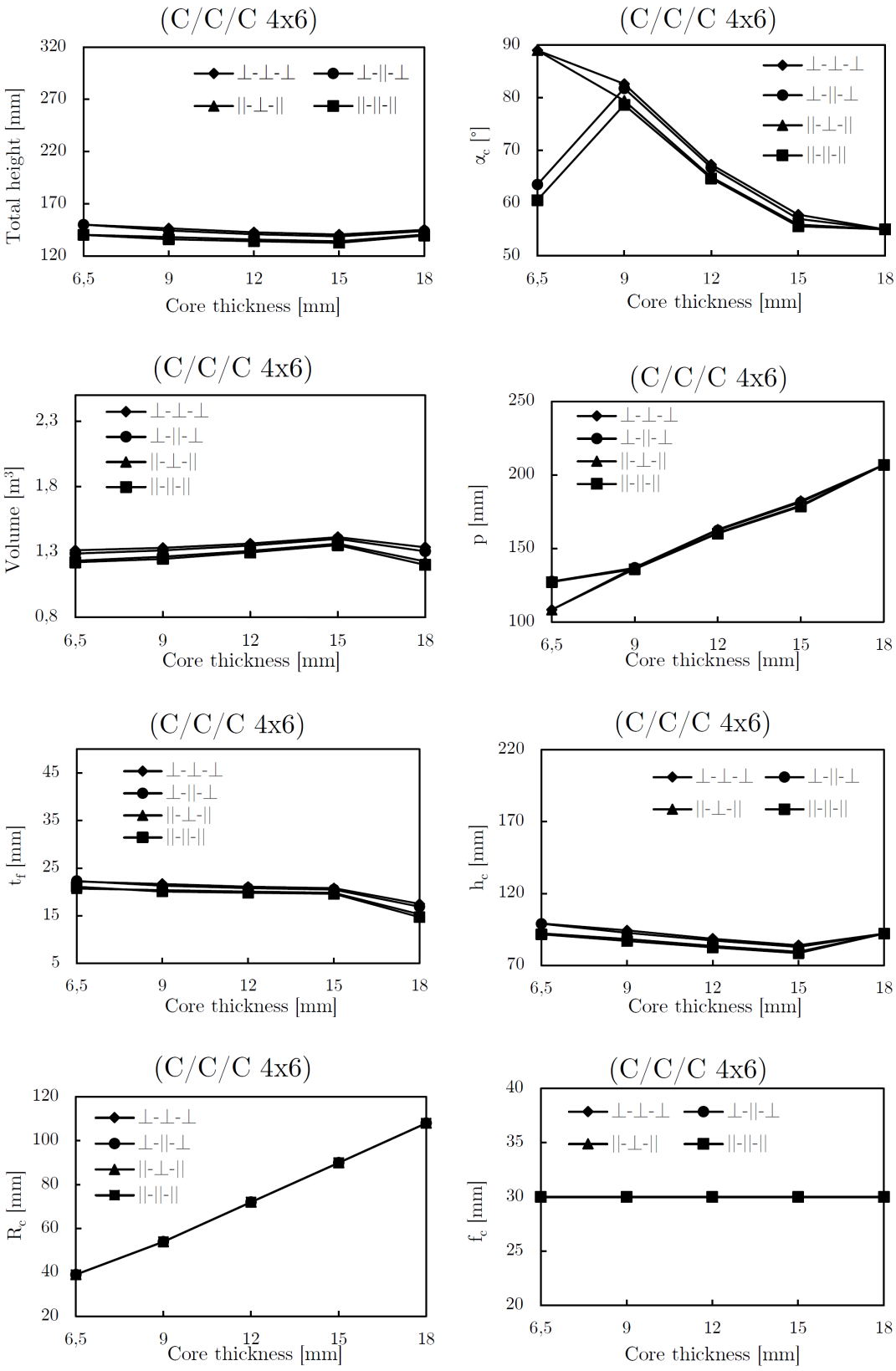

Figure 7.8: How different parameters varies for the optimal case when the core thickness and grain orientation varies.

7.3 Comparison between a traditional floor and the suggested floor

The optimal case which is considered to be the *4x6 floor* with pure conifer plywood, has a total height of approximately 137 mm, see Table 7.2. This is only the height of the structural part and will therefore only be compared with the structural part of the traditional floor. This traditional floor is similar to the one explained in Section 2.2.1.

The compared traditional floor is a traditional SSP (T-section), explained in Section 2.2.1, taken from a five storey residential building with spans of 6.2 meters. The floor is built up with 360 mm LVL-beams (spacing 600 mm) with a 22 mm particle board on top which gives a total structural height of 382 mm. This is the traditional way of building multi-storey timber buildings in Sweden today. By using the new innovative sandwich floor with corrugated core 245 mm can be saved for each storey. What must be taken into consideration is that this is only the structural part and the acoustic and fire resistance is left out of the equation for both of the floors.

8 Concluding remarks

- By implementing shear deformations and a stiffness transformation to an orthotropic homogeneous plate the analytic and the FE analyses corresponds well to each other.
- All analytic calculations are on the safe side with a margin with an average of 10%.
- The error between the analytic solution and the FEM is higher for the *6x4 floor* than for the *4x6 floor*.
- The governing criteria is, as expected, the deflection caused by a uniformly distributed load.
- Solid elements in Abaqus are not suitable for this kind of analyses.
- To obtain the highest stiffness for *4x6 floor* a grain orientation of (∥-∥-∥) should be used.
- To obtain the highest stiffness for *6x4 floor* a grain orientation of (⊥-⊥-⊥) should be used.
- Between the *4x6 floor* and *6x4 floor*, the lower deflection is for the *4x6 floor*. This explains why the orientation of grains as well as the corrugation direction should be along the shorter edge of the floor plate. Therefore, as a general conclusion, it could be expected that the most optimal design of any innovative sandwich type of floor is the one that the highest stiffnesses are gained along the shorter edges, like the concept of beam floors.
- The suggested floor is a pure conifer floor with dimensions of 4x6 m and a grain direction (∥-∥-∥).
- 245 mm/storey can be saved in term of height if using the suggested floor.

As a conclusion, the development of a sandwich floor is worth to continue since the potential is obvious. There are numerous of ways of seeing this as beneficial, the most obvious is if an additional floor could be inserted into a building with a constant height. If this is not possible, the height of the building could be lowered for the same amount of floors which of course is beneficial. If neither of these suggestions are desirable, the extra space could be used for other purposes, either by improving the acoustic insulation, which often is an issue for timber structures or increase the ceiling height of each apartment, which is considered as luxury, which increase the value of the apartment. It is evident from the industry demand that any new floor system that can lead to saving more space is preferred and welcome.

9 Further research

The floor that have been investigated has a size of 4x6 m with support on all four edges, which creates a plate action. If these boundary conditions changes the design procedure of the floor will be completely different. There are assumptions that must be considered as uncertainties that must be investigated. Explained in Section 7.1.1 the analytic solution is sensitive for either the extrusion length (L) or the total length of the corrugation (B). To know for sure why a larger error for the *6x4 floor* is obtained, more analyses need to be made. The adhesive connection is expected to have sufficient strength not to fail, but the shear deformations in the mechanical connectors might result in a slip action between the face and the core and should be investigated. Both in the analytic model and the FE model, this connection is considered to be tied together without any slip.

Since there are no standard dimensions of plywood that could be used for the entire floor, the structural effect of joints should be considered which might decrease the stiffness if assembled poorly. If the connections between these elements are not made to create a plate action the design procedure will change and the calculations made in this thesis will not be applicable. To make this floor competitive on the market these connections needs to be further investigated to create an easy assembly that creates plate action.

There was a first attempt in this thesis to implement the acoustics criteria in the analytic calculations. Section 2.4 shows that there were no fundamental research to be found about this type of sandwich structure and similar research did all have empirically produced equations. Due to this, the implementation of the acoustic behaviour of the structural floor was determined to be too complicated at this state. Without any experiments on this type of structure there are no reference criterion that can be used for the specific timber sandwich plate. An empirical study and laboratory test of a prototype of this kind needs to be made to measure the sound reduction index of the structural floor, without any fillings. When this is made the equation can easily be implemented and seen as a constraint when analyzing the structural behaviour of the floor.

An investigation about how the bio-filling material affect the structural and acoustic behaviour of the floor should be made. The bio-filling might contribute to the global stiffness and make the structure more slender or on the contrary make it only heavier and thicker. But, there are some evidences from the latest research studies in literature that show that any filling material like foams will result in an increase in structural stiffness and performance. Also, definitely those filling will increase the acoustic performance. But, all bio and environmentally-friendly filling choices should be listed and studies to select the best choice from points of view of price and the practical issues related to implementation and filling procedure. Those parts together with the fire performance is out of the scope of this thesis and should be studied in future.

Only the structural part is investigated and installation areas are disregarded which might be an issue since the sandwich structure is a closed system. Possibilities to place it within the height of the structural part should be investigated to not lose any unnecessary height. Fundamental research and empirical laboratory test of a prototype need to be to verify the results from the analytic solution and the FE-analyses.

References

Angard, A. B. (2017). *Price list*. Email conversation with the product manager at Derome in May 2017. (Cited on page 48).

Atashipour, S. & Al-Emrani, M. (2017). *A realistic model for transverse shear stiffness prediction of composite corrugated-core sandwich element*. Int J Solid Struct. (Cited on page 26).

Atashipour, S., Al-Emrani, M., Fröjd, K., & Hellström, A. (2017). *An innovative bio-composite sandwich structure as floor system in multi-storey timber buildings – structural analysis and optimal design*. Compos Struct. (Cited on page 27).

Biofoam spray insulation. (2017). Biofoam. Retrieved May 9, 2017, from http://www.biofoamsprayinsulation.ie/index.html. (Cited on pages 11, 12)

Brunskog, J. & Hammar, P. (2000). *Prediction medels of impact sound insulation on timber floor structures; a literature survey*. Lund University, Sweden, Engineering Acustics. (Cited on page 13).

Building NEWS, S.-N. (2014). Floor cassettes - express two storey living with tecbeam. Retrieved March 29, 2017, from http://www.spec-net.com.au/press/1016/tec_191016/Floor-Cassettes-Express-Two-Storey-Living-Tecbeam. (Cited on page 11)

Derome. (2016). Derome lanserar effektiv lösning för bjälklag. Retrieved March 29, 2017, from http://www.derome.se/nyheter/nyhetsarkiv/2016/derome-lanserar-effektiv-losning-for-bjalklag. (Cited on page 10)

Dias, A., Monteiro, S., & Martins, C. (2013). *Reinforcement of timber floors - transversal load distribution in timber-concrete systems*. Trans Tech Publications Switzerland. (Cited on page 28).

Econstruction. (2007). Energy efficient soy-based foam insulation. Retrieved May 9, 2017, from http://www.abbeyinsulation.ie/downloads/Biofoam.pdf. (Cited on page 11)

EKS. (2017). Eks – boverkets konstruktionsregler [Boverket]. Retrieved March 14, 2017, from http://www.boverket.se/sv/lag--ratt/forfattningssamling/gallande/eks---bfs-201110/. (Cited on page 16)

Emms, G., Chung, H., McGunnigle, K., & Dodd, G. (2006). *Improving the impact insulation of light timber*. University of Auckland, New Zeeland. (Cited on pages 13, 15).

ETA, E. T. A. (2014). European technical assessment. Retrieved March 29, 2017, from http://www.lignatur.ch/fileadmin/ablage/downloads/produkte/2014-06-20_electronic_copy_eta_11_0137_lignatur.pdf. (Cited on page 10)

Eurocode. (2017). Eurocodes: Building the future - the european commission website on the eurocodes - home. Retrieved March 14, 2017, from http://eurocodes.jrc.ec.europa.eu/home.php. (Cited on pages 15, 16, 32)

Finnish Plywood. (2002). *Handbook of finnish plywood*. Lahti, Finland: Kirjapaino Markprint Oy. (Cited on page 5).

Hasníková, H. & Kuklík, P. (2013). *Use of composite timber-concrete structure while timber floor reconstruction in existing buildings*. Faculty of Civil Engineering CTU Prague. (Cited on page 12).

Jarnerö, K. (2014). *Vibrations in timber floors - dynamic properties and human perception*. Linnaeus University Dissertations. (Cited on page 30).

Jarnerö, K., Bolmsvik, Å., Brandt, A., & Olsson, A. (2012). *Effect of flexible supports on vibration performance of timber floors*. Euronoise Prague. (Cited on page 31).

Jeffree, M. (2016). Much more from a lot less. *Timber Trades Journal; Tonbridge*, (6798), 48, 50, 52. (Cited on page 8).

Kielsteg. (2016). Workbook for architects and planners_v05n üa_2016. Retrieved March 13, 2017, from http://www.kielsteg.at/wp-content/epaper_en_kielsteg2016/index.html. (Cited on pages 8, 9)

Larsson, M. & Mayor, H. (2016). *Innovative timber floor - development of a timber sandwich structure* (Master's thesis, Chalmers University of Technology, Divison of Structural Engineering). (Cited on pages 1, 3).

Libove, C. & Hubka, R. E. (1951). *Elastic constants for corrugated-core - sandwich plates*. Langley Aeronautical Laboratory. (Cited on pages 20, 22, 26).

Lignatur. (2014). Workbook. Retrieved March 29, 2017, from http://www.lignatur.ch/fileadmin/ablage/downloads/workbook_a4_en/2014-06-04_workbook_a4_en.pdf. (Cited on page 9)

Lopes, S. D. A., Rocco, L. F. A., Donizeti, V. L., Luis, C. A., & Roberto, O. A. (2015, June). Environmental performance assessment of the melamine-urea-formaldehyde (MUF) resin manufacture: A case study in brazil. *Journal of Cleaner Production*, *96*, 299–307. Retrieved March 14, 2017, from http://linkinghub.elsevier.com/retrieve/pii/S0959652614002248. (Cited on page 8)

Manalo, A. (2012). *Structural behaviour of a prefabricated composite wall system made from rigid polyurethane foam and magnesium oxide board*. University of Southern Queensland Australia. (Cited on page 6).

MathWorks. (2017a). *Optimization toolbox, user's guide*. The MathWorks Inc. (Cited on page 25).

MathWorks. (2017b). Constrained nonlinear optimization algorithms - matlab & simulink - mathworks nordic. Retrieved June 3, 2017, from https://se.mathworks.com/help/optim/ug/constrained-nonlinear-optimization-algorithms.html. (Cited on page 25)

MetsäWood. (2017). Characteristics of kerto-q. Retrieved June 15, 2017, from http://www.metsawood.com/global/Products/kerto/Pages/Kerto-Q.aspx. (Cited on page 6)

MGO. (2014). Evaluation report for mgo corpoation. Retrieved May 19, 2017, from http://mgoboard.com.au/wp-content/uploads/2015/07/MgO-Corp-America-ER31004-Report.pdf. (Cited on page 6)

Nilsson, A. C. (1974). *Sound transmission through single leaf panels* (Doctoral dissertation, Chalmers University of Technology, Department of Building Acoustics). (Cited on pages 12–15).

Nilsson, A. C. (1989). *Wave propagation in and sound transmission through sandwich plates*. Royal Institute of Technology, Sweden, Department of Technical Acoustics. (Cited on page 13).

Norris, C. B. (1962). *Strength of orthotropic materials subjected to combined stresses*. Forest Products Laboratory, U.S. Department of Agriculture. (Cited on page 33).

Ohlsson, S. (1988). *Springiness and human-induced floor vibrations - a design guide*. Gothenburg, Sweden: Swedish Concil for Building Research. (Cited on page 30).

Pryda. (2016). Pryda floor cassette manual 2016. Retrieved March 13, 2017, from http://www.pryda.com.au/wp-content/uploads/2016/10/Pryda-Floor-Cassette-Manual-2016.pdf. (Cited on page 10)

Reissner, E. (1945). *The effect of transverse shear deformation on the bending of elastic plate*. (Cited on page 31).

StoraEnso. (2013). Technical specifications. Retrieved May 11, 2017, from http://www.clt.info/en/product/technical-specifications/. (Cited on page 8)

Swedish Wood. (2015). *Design of timber structures*. Stockholm, Sweden: ProService. (Cited on pages 5–7, 28).

Tan, R. B. & Khoo, H. H. (2014). *Life cycle assessment of eps and cpb inserts: Design considerations and end of life scenarios*. National University of Singapore. (Cited on page 11).

TECbuild. (2010). Tecslab floor joist span tables. Retrieved March 29, 2017, from http://www.tecbuild.com.au/wp-content/uploads/2014/12/TECSLAB+Floor+Joist+Span+tables+-+1.5+kPa+Houses+2.0+kPa+Residential+_26+Apartments-ID80878.pdf. (Cited on page 11)

TECbuild. (2017). Fire, thermal & acoustic performance. Retrieved March 29, 2017, from http://www.tecbuild.com.au/wp-content/uploads/2014/12/FIRE_2c+THERMAL+_26+ACOUSTIC+PERFORMANCE+-+Decorative+Timber+Flooring-ID80881.pdf. (Cited on page 11)

Valluzzi, M. R., Garbin, E., & Modena, C. (2006). *An intrados technique for flexural strengthening of timber floors*. University of Padua Italy. (Cited on page 12).

Wennhage, P. (2001). Weight minimization of sandwich panels with acoustic and mechanical constraints. *Journal of Sandwich Structures & Materials*, *3*(1), 22–49. Retrieved March 28, 2017, from http://journals.sagepub.com/doi/abs/10.1106/CM4M-7JAY-VBTP-37JE. (Cited on page 12)

Zenkert, D. (1997). *The handbook of sandwich construction*. West Midlands, UK: Engineering Materials Advisory Services Ltd. (Cited on pages 1, 17, 28, 31, 32, 61).

A Equations for analytic solution

For all equations in Appendix A the following sub-notations are used:

x	x-direction, parallel to the corrugation
y	y-direction, perpendicular to the corrugation
f	face
c	corrugated core

A.1 Transverse shear stiffness, DQy

To calculate D_{Qy} Equation (5.16), the following equations are needed.

$$C_1 = \left(\frac{p^2}{3EI_{yf}} + \frac{1}{K_s G A_{yf}}\right)p \tag{A.1}$$

$$C_2 = -\frac{1}{EI_{yc}}\left(\frac{1}{2}(t_f + t_c)\Lambda_1 + \Lambda_3\right)p \tag{A.2}$$

$$C_3 = -\left(\frac{1}{EI_{yc}}\Lambda_4 + \frac{1}{EA_{yc}}\Lambda_5 + \frac{1}{K_s G A_{yf}}\Lambda_6\right) \tag{A.3}$$

$$C_4 = \left(\frac{p^2}{3EI_{yf}} + \frac{1}{EA_{yc}}\Lambda_2 + \frac{1}{K_s G A_{yf}}\right)p \tag{A.4}$$

$$C_5 = \frac{1}{EI_{yc}}\left(\frac{1}{2}(t_f + t_c)\Lambda_2 + \Lambda_8\right) - \left(\frac{1}{EA_{yc}} + \frac{1}{K_s G A_{yc}}\right)\Lambda_7 \tag{A.5}$$

$$C_6 = \left(\frac{p^2}{3EI_{yf}} + \frac{1}{K_s G A_{yf}}\right)p \tag{A.6}$$

$$C_7 = \left[\frac{1}{3}p^2\left(\frac{1}{EI_{yf}} + \frac{1}{EI_{yf}}\right) + \left(\frac{1}{K_s G A_{yf}} + \frac{1}{K_s G A_{yf}}\right) + \frac{p}{EI_{yc}}\Lambda_1\right]p \tag{A.7}$$

$$C_8 = \left(\frac{p^2}{3EI_{yf}} - \frac{1}{EA_{yc}}\Lambda_2 + \frac{1}{K_s G A_{yf}}\right)p \tag{A.8}$$

$$C_9 = \frac{p}{EI_{yc}}\Lambda_2 \tag{A.9}$$

$$C_{10} = \frac{1}{EI_{yc}}\left[\frac{1}{4}(t_f + t_c)^2\Lambda_1 + (t_f + t_c)\Lambda_3 + \Lambda_9\right] + \frac{1}{EA_{yc}}\Lambda_6 + \frac{1}{K_s GA_{yc}}\Lambda_5 \tag{A.10}$$

$$\Lambda_1 = f_c + 2R_c\theta + 2l_a \tag{A.11}$$

$$\Lambda_2 = \Lambda_1\frac{p}{2} \tag{A.12}$$

$$\Lambda_3 = \Lambda_1\frac{h_c}{2} \tag{A.13}$$

$$\begin{aligned}\Lambda_4 = {} & \frac{1}{2}R_c^3(2\alpha_c - \sin(2\alpha_c)) + \frac{1}{2}R_c\alpha_c(p^2 + (p - f_c)^2) - 2R_c^2(1 - \cos(\alpha_c))(p - f_c) + \\ & \frac{1}{12}2l_a\left[3p^2 + (2l_a\cos(\alpha_c))^2\right] + \frac{1}{3}\left[\left(p^3 + \frac{1}{8}f_c^3\right) - \left(p - \frac{1}{2}f_c\right)^3\right]\end{aligned} \tag{A.14}$$

$$\Lambda_5 = \frac{1}{2}R_c(2\alpha_c - \sin(2\alpha_c)) + 2l_a\sin^2\alpha_c \tag{A.15}$$

$$\Lambda_6 = \frac{1}{2}R_c(2\alpha_c + \sin(2\alpha_c)) + 2l_a\cos^2\alpha_c + f_c \tag{A.16}$$

$$\Lambda_7 = R_c\sin^2(\alpha_c) + \frac{1}{2}2l_a\sin(2\alpha_c) \tag{A.17}$$

$$\begin{aligned}\Lambda_8 = {} & R_c^3(1 - \cos(\alpha_c))^2 + R_c\left(\frac{1}{2}p2l_A - R_c h_c\right)(1 - \cos(\alpha_c)) - R_c^2(p - f_c)(\alpha_c - \sin(\alpha_c)) + \\ & \frac{1}{12}(2l_a)^2(3p + 2l_a\cos(\alpha_c))\sin(\alpha_c) + \frac{1}{2}R_c h_c(2p - f_c)\alpha_c + \frac{1}{8}h_c f_c(4p - f_c)\end{aligned} \tag{A.18}$$

$$\begin{aligned}\Lambda_9 = {} & 2R_c^3\left(\frac{3}{2}\alpha_c - \sin(\alpha_c) + \frac{1}{4}\sin(2\alpha_c)\right) - 2h_c R_c^2(\alpha_c - \sin(\alpha_c)) + h_c^2 R_c\alpha_c + \\ & \frac{1}{12}(2l_a)^3\sin^2(\alpha_c) + \frac{1}{4}h_c^2(2l_a + 2f_c)\end{aligned} \tag{A.19}$$

A.2 Equations for deflection

Equation W_{mn} required for deflection calculation in Chapter 5.2, derived by Rasoul Atishapour.

$$W_{mn} = \frac{\begin{array}{r} -D_x D_{xy}\alpha^2\beta^2\nu_{yx} - D_{xy}D_y\alpha^2\beta^2\nu_{xy} + D_x D_{xy}\alpha^4 + 2D_x D_y\alpha^2\beta^2 - D_{xy}D_{Qx}\alpha^2\nu_{xy}\nu_{yx} \\ + D_{xy}D_y\beta^4 - D_{xy}D_{Qy}\beta^2\nu_{xy}\nu_{yx} + 2D_x D_{Qy}\alpha^2 + D_{xy}D_{Qx}\alpha^2 + D_{xy}D_{Qy}\beta^2 \\ + 2D_{Qx}D_y\beta^2 - 2D_{Qx}D_{Qy}\nu_{xy}\nu_{yx} + 2D_{Qx}D_{Qy} \end{array}}{\begin{array}{r} -D_x D_{xy}D_{Qx}\alpha^4\beta^2\nu_{yx} - D_x D_{xy}D_{Qy}\alpha^2\beta^2 - D_{xy}D_{Qx}D_y\alpha^4\beta^2\nu_{xy} - D_{xy}D_y D_{Qy}\alpha^2\beta^4\nu_{xy} \\ + D_x D_{xy}D_{Qx}\alpha^6 + D_x D_{xy}D_{Qy}\alpha^4\beta^2 + 2D_x D_{Qx}D_y\alpha^4\beta^2 + 2D_x D_y D_{Qy}\alpha^2\beta^4 \\ + D_{xy}D_{Qx}D_{Qy}\alpha^2\beta^4 - 4D_{xy}D_{Qx}D_{Qy}\alpha^2\beta^2\nu_{xy}\nu_{yx} + D_{xy}D_y D_{Qy}\beta^6 + 2D_x D_{Qx}D_{Qy}\alpha^2\beta^2\nu_{yx} \\ + 2D_{Qx}D_y D_{Qy}\alpha^2\beta^2\nu_{xy} + 2D_x D_{Qx}D_{Qy}\alpha^4 + 4D_{xy}D_{Qx}D_{Qy}\alpha^2\beta^2 + 2D_{Qx}D_y D_{Qy}\beta^4 \end{array}} \tag{A.20}$$

where

α	$m\pi/L$, where L is the plate length along the x-axis
β	$n\pi/B$, where B is the plate length along the y-axis

A.3 Equations for shear stress

To calculate T_x and T_y, the following equations are required (Zenkert, 1997):

$$X_{mn} = \left[\frac{1}{2}\alpha^5\,\frac{D_x D_{xy}}{1-\nu_{xy}\nu_{yx}} + \alpha^3\,\beta^2\left[\frac{D_x D_y}{1-\nu_{xy}\nu_{yx}} - \frac{D_{xy}(\nu_{xy}D_y + \nu_{yx}D_x)}{2(1-\nu_{xy}\nu_{yx})}\right] + \frac{1}{2}\alpha\beta^4\frac{D_y D_{xy}}{1-\nu_{xy}\nu_{yx}} + D_{Qy}\alpha\left[\alpha^2\frac{D_x}{1-\nu_{xy}\nu_{yx}} - \beta^2\left(D_{xy} + \frac{\nu_{yx}D_x}{1-\nu_{xy}\nu_{yx}}\right)\right]\right]/D_{Qy} \tag{A.21}$$

$$Y_{mn} = \left[-\frac{1}{2}\beta^5\,\frac{D_y D_{xy}}{1-\nu_{xy}\nu_{yx}} + \alpha^2\,\beta^3\left[\frac{D_x D_y}{1-\nu_{xy}\nu_{yx}} - \frac{D_{xy}(\nu_{xy}D_y + \nu_{yx}D_x)}{2(1-\nu_{xy}\nu_{yx})}\right] - \frac{1}{2}\alpha^4\beta\frac{D_x D_{xy}}{1-\nu_{xy}\nu_{yx}} - D_{Qx}\beta\left[\beta^2\frac{D_y}{1-\nu_{xy}\nu_{yx}} + \alpha^2\left(D_{xy} + \frac{\nu_{xy}D_y}{1-\nu_{xy}\nu_{yx}}\right)\right]\right]/D_{Qx} \tag{A.22}$$

$$Z_{mn} = \alpha X_{mn} - \beta Y_{mn} \tag{A.23}$$

A.4 Equations for the fundamental frequency

$$s = \begin{bmatrix} s_{11} & s_{12} & 0 & 0 & 0 & 0 \\ 0 & s_{22} & 0 & 0 & 0 & 0 \\ 0 & 0 & s_{33} & s_{34} & s_{35} & 0 \\ 0 & 0 & 0 & s_{44} & s_{45} & 0 \\ 0 & 0 & 0 & 0 & s_{55} & 0 \\ 0 & 0 & 0 & 0 & 0 & s_{66} \end{bmatrix} \tag{A.24}$$

where

$$s_{11} = E_x \alpha_c^2 + G_{xy} \beta^2 \tag{A.25}$$

$$s_{12} = E_y \nu'_{xy} G_{xy} \beta \alpha \tag{A.26}$$

$$s_{22} = G_{xy} \alpha^2 + E_y \beta^2 \tag{A.27}$$

$$s_{33} = K_s (D_{Qx} \alpha^2 + D_{Qy} \beta^2) \tag{A.28}$$

$$s_{34} = K_s D_{Qx} \alpha \tag{A.29}$$

$$s_{35} = K_s D_{Qy} \alpha \tag{A.30}$$

$$s_{44} = D_x \alpha^2 + \frac{D_{xy}}{2} \beta^2 + K_s D_{Qx} \tag{A.31}$$

$$s_{45} = (D_y \nu_{xy} + \frac{D_{xy}}{2}) \alpha \beta \tag{A.32}$$

$$s_{55} = \frac{D_{xy}}{2} \alpha^2 + D_y \beta^2 + K_s D_{Qy} \tag{A.33}$$

$$s_{66} = s_{44}s_{55} - s_{45}^2 \tag{A.34}$$

For calculation of the the fundamental frequency f_1, in Chapter 5.3, a factor $\bar{s}_{33}$ is derived as:

$$\bar{s}_{33} = s_{33} - (s_{34}s_{55} - s_{35}s_{45})\frac{s_{34}}{s_{66}} - (s_{35}s_{44} - s_{34}s_{45})\frac{s_{35}}{s_{66}} \tag{A.35}$$

B The Matlab code

The Matlab code with all related function files can be found in this appendix. To use the code, do the following steps:

- Copy and paste the code into the editor
- Change to desired indata, both in line 11-18 and 67-77 (They should be same), see possible indata below
- Run the code

To change the indata, only certain choices can be made. The following rows are the indata:

```
%%%%- input for Indata file -%%%%
B=6;                %Length in y-dir (perp to extrusion of corrugation)
L=4;                %Length in x-dir (parallel to extrusion of corrugation)
dif=0;              %Face, Grain angle relative to extrusion of corrugation
dic=0;              %Core, Grain angle relative to extrusion of corrugation
FaceThickness=18;   %Face thickness
CoreThickness=12;   %Core thickness
FaceMat='C' ;       %Face material
CoreMat='C' ;       %Core material
% 'B'- Birch plywood (Possible for core and face)
% 'C'- Conifer plywood (Possible for core and face)
% 'P'- Particle board (Possible for face)
% 'M'- Magnesium Board (Possible for face)
% 'K'- Kerto-Q (Possible for face)
%%%%- End Input -%%%%
```

Figure B.1: Material input

Where L (x-axis) and B (y-axis) can vary from 0-infinity (plate dimensions). Dif and dic are the grain orientation relative to the x-axis and can only be either 0° or 90°. FaceMat (face material) and CoreMat (core material) with corresponding possible thicknesses can be seen in the following table:

Table B.1: Possible material choices for the Matlab code

Material	FaceMat	CoreMat	Thickness
Birch Plywood	'B'	'B'	6.5, 9, 12, 15, 18, 21, 24, 27, 30, 35, 40, 45, 50
Conifer Plywood	'C'	'C'	6.5, 9, 12, 15, 18, 21, 24, 27, 30
Particle board	'P'	Not possible	6(6-13), 13(13-20), 20(20-25), 25(25-32), 32(32-40), 40(>40)
Magnesium board	'M'	Not possible	10, 18, 20, 50
Kerto-Q	'K'	Not possible	21(21-24), 27(27-69)

```
%%%%%%%%%%%%%%%%%%%%%%%%%%%%%%%%%%%%%%%%%%%%%%%%%%%%%%%%%%%%%%%%%%%%%%%%%%%%
% Optimization of cross-section geometry (x-vector) of corrugated sandwich
% floor using global search/fmincon.
% x={x1,x2,x3,x4,x5,x6,x7}={hc,tftop,tfbot,tc,alphac,fc,Rc}
% Before running the code, copy the input below (row 16-23) to the function
% ConstraintFunction(x)
% Then Run this file to start the optimization
% Made by: Kajsa Fröjd and Andreas hellstrom - 2017
%%%%%%%%%%%%%%%%%%%%%%%%%%%%%%%%%%%%%%%%%%%%%%%%%%%%%%%%%%%%%%%%%%%%%%%%%%%%
%%%%- input for Indata file -%%%%
B=6;                %Length in y-dir (perp to extrusion of corrugation)
L=4;                %Length in x-dir (parallel to extrusion of corrugation)
dif=0;              %Face, Grain angle relative to extrusion of corrugation
dic=0;              %Core, Grain angle relative to extrusion of corrugation
FaceThickness=18;   %Face thickness
CoreThickness=12;   %Core thickness
FaceMat='C' ;       %Face material
CoreMat='C' ;       %Core material
% 'B'- Birch plywood (Possible for core and face)
% 'C'- Conifer plywood (Possible for core and face)
% 'P'- Particle board (Possible for face)
% 'M'- Magnesium Board (Possible for face)
% 'K'- Kerto-Q (Possible for face)
%%%%- End Input -%%%%

%Number of times to repeat the code
n=1;

% Insert lower bound (lb), upper bound (ub), and initial guess, x0
lb=[0.00,   0.0065, 0.0065, 0.0065, 55*pi/180,  0.03,   0.02];
x0=[0.09,   0.0450, 0.0450, 0.0090, 70*pi/180,  0.05,   0.04];
ub=[0.40,   0.0500, 0.0500, 0.0250, 89*pi/180,  0.20,   0.20];

% Insert linear constraints
Aineq= [0,0,0,6,0,0,-1];
bineq=[0];
Aeq=[0,1,-1,0,0,0,0];
beq=[0];

%Options for the iterations
options = optimset('display','iter','Algorithm','sqp',...
    'MaxFunEvals',5000,'TolCon',1e-5);

%Defining the problem using 'fmincon'
problem=createOptimProblem('fmincon','objective',@ObjectiveFunction,...
    'x0',x0,'Aineq',Aineq,'bineq',bineq,'Aeq',Aeq,'beq',beq,'lb',lb,'ub',ub,...
    'nonlcon',@ConstraintFunction,'options',options);

for i=1:n
    % Run the optimization using GlobalSearch
    [x,height] = run(GlobalSearch,problem);
    % Saving the optimized x-vector from loop #i into a matrix
    xRun(i,:)=x;
    % Saving the height from the optimized x-vector fro loop #i into a vector
    heightRun(i)=height;
end
```

```
% Finding the lowest height found from the loop
[M,N]=min(heightRun);

% Display the optimal x-vector and the corresponding height
x=xRun(N,:)
height=heightRun(N)

% Plot the cross-section
[lc, ls, la, l1,h,g1,c1,d1,b1,p,theta,k1,e1,j1,a1] = calculate_geometry(x);
plot_corr(x,lc,d1)
%%%%%%%%---------End of code----------%%%%%%%%%%%
```

```
function [ height ] = ObjectiveFunction(x)
% Objective Function which is to be minimized (hc+tftop+tfbot+tc)
height = x(1)+x(2)+x(3)+x(4);
end
```

```
function [ c,ceq ] = ConstraintFunction(x)
% Indata below should be the same as the ones in row 16-23
%-------------------------------------------------------------------------
%%%%- input for Indata file -%%%%
B=6;                %Length in y-dir (perp to extrusion of corrugation)
L=4;                %Length in x-dir (parallel to extrusion of corrugation)
dif=0;             %Face, Grain angle relative to extrusion of corrugation
dic=0;             %Core, Grain angle relative to extrusion of corrugation
FaceThickness=18;   %Face thickness
CoreThickness=12;  %Core thickness
tcmax=CoreThickness/1000;
tfmax=FaceThickness/1000;
FaceMat='C' ;       %Face material
CoreMat='C' ;       %Core material
% 'B'- Birch plywood (Possible for core and face)
% 'C'- Conifer plywood (Possible for core and face)
% 'P'- Particle board (Possible for face)
% 'M'- Magnesium Board (Possible for face)
% 'K'- Kerto-Q (Possible for face)
%%%%- End Input -%%%%
%-------------------------------------------------------------------------
% Input file for different materials, thickness and grain orientation
[ L,B,nu12f,nu12c,rhoc,rhof,Exc,Eyc,Exf,Eyf,Gxyc,Gxyf,...
    G23c,G23f,fm,fvkc,fvkf,gammaM,gammaGsls,gammaQsls,...
    gammaGuls,gammaQuls,qk,Qk,qdw,Q1kN,kmod,alphaA,Excc] = ...
    Indata(FaceMat,dif,FaceThickness,CoreMat,dic,CoreThickness,B,L);

%Calculating the geometry
[lc, ls, la, l1,h,g1,c1,d1,b1,p,theta,k1,e1,j1,a1] = calculate_geometry(x);

%Sectional constants
[Acu,Afu,Ac,V,Ix,Iy,Ixf, Ixc,mcshear]=calculate_crossconst(x,lc,ls,la,h,B,L,a1,d1);

%Stiffness
[Dxf,Dxc,Dyf,Dyc, D,Dx,Dy,DQy,DQx,Dxy,nuxy,nuyx,nuxypf,nuyxpf, Ks ] = ...
    calculate_Stiffness( x,h,Eyc,Exc,Eyf,Exf,nu12f,nu12c,Gxyf,Gxyc,...
    G23c,G23f,la,p,Acu,Afu,Ixf,Iy,Ixc);

%Deflection
[w1kN,qself,wInst] = calculate_deflection( Afu,Acu,rhof,rhoc,gammaQsls,...
    gammaGsls,nuxy,nuyx,B,L,Q1kN,qk,qdw,Dy,Dx,Dxy,DQy,DQx);
```

```
%Local Bending
[MRdlocal, MEd] = calculate_local_bending(x,gammaQuls,Qk,lc,kmod,fm,...
    gammaM,Ks,G23f,Eyf,nuxypf,nuyxpf);

%Shear stresses
[Tauxtopf,Tauxtopc,Tauytopc,Tauytopf,TauRdf,TauRdc,qdULS] = ...
    calculate_shear_stress(ls,x,B,L,h,alphaA,gammaQuls,gammaGuls,qk,...
    qself,qdw,lc,Dxy,Dx,Dy,DQx,DQy,nuxy,nuyx,Ix,Iy,gammaM,kmod,fvkf,fvkc,mcshear);

%Natural frequency
[f1] = calculate_eigenfrequency(qself,qdw,L,B,D,DQy,DQx);

%Unit impulse velocity
[v,vlimit] = calculate_unit_pulse_velocity(Dxc,Dxf,Dyc,Dyf,Afu,rhof,Acu,rhoc,L,B,f1);

%Local buckling
[P,Pcr] = calculate_local_buckling(x,qdULS,Q1kN,p,la,Excc);

%Constraints
c=[l1-x(1)/2;0-d1;0-j1;0-k1;5.77-h/max(x(2),x(3));h/min(x(2),x(3))-100;...
    wInst-min(B,L)/500;Tauxtopf-TauRdf;Tauytopf-TauRdf;...
    Tauxtopc-TauRdc;Tauytopc-TauRdc;w1kN-0.0015;8-f1;v-vlimit;...
    P-Pcr; x(4)-x(7); 2*x(4)-x(1);4*g1-lc;MEd-MRdlocal];
ceq=[2*d1-((x(1)-2*x(7)*(1-cos(x(5))))/sin(x(5)));...
    x(6)-(p-2*d1*cos(x(5))-2*x(7)*sin(x(5)));x(4)-tcmax;x(2)-tfmax;x(6)-0.03];
end
```

```
function [lc,ls,la,l1,h,g1,c1,d1,b1,p,theta,k1,e1,j1,a1] = calculate_geometry(x)
% Symmetric corrugation gives
ky=1;
kz=1;

h=x(1)+x(2)/2+x(3)/2+x(4);

% For all distances below, see figure 3.3 in Report
e1=x(7)*cos(x(5));
g1=x(7)*sin(x(5));
a1=(1-kz/2)*x(1)-x(7);
j1=a1+e1;
p=x(6)+2*g1+2*j1*(sin((pi/2)+x(5))/cos((pi/2)-x(5)));
b1=(1-ky/2)*p-(x(6)/2);
c1=(a1^2+b1^2)^0.5;
alpha1=atan(a1/b1);
beta1=asin(x(7)/c1);
theta=alpha1+beta1;
d1=(c1^2-x(7)^2)^0.5;
k1=b1-g1;

l1=(x(1)/2)-j1;                    % Height of radius (z-direction)
ls=x(6)+2*x(7)*theta+2*d1;         % Length of corrugation leg
la=2*d1;                           % Length of inclined corrugation
lc=2*p;                            % Length of cross-section
end
```

```
function [Acu,Afu,Ac,V,Ix,Iy,Ixf,Ixc,mcshear]=...
    calculate_crossconst(x,lc,ls,la,h,B,L,a1,d1)
%Area
Aftop=      x(2)*lc;
Afbot=      x(3)*lc;
```

```
AR=         x(7)*x(5)*x(4);
Af=         Aftop+Afbot;
Afu=        Af/lc;
Ac=         2*ls*x(4);
Acu=        Ac/lc;
Atot=       Af+Ac;
A=          Atot/lc;

%Volume
V=          A*B*L;

% Following equations used to calculate second moment of inertia
R1=         x(7)-x(4)/2;            %inner radius
R2=         x(7)+x(4)/2;            %outer radius
theta=      2*((90*pi/180)-x(5));   %angle
A1=         x(5)/2*R1^2;
A2=         x(5)/2*R2^2;
mca=        ((2/3*R2*sin(x(5))/x(5)*A2)-(2/3*R1*sin(x(5))/x(5)*A1))/...
            (A2-A1)+a1; %mass center arc

%Second moment of inertia
Iftopx=     (lc*x(2)^3)/12+lc*x(2)*(h/2)^2;
Ictopx=     (x(6)*x(4)^3)/12+x(6)*x(4)*(x(1)/2)^2;
Iincx2=     x(4)/sin(x(5))*((la-x(4)/tan(x(5)))*sin(x(5)))^3/12; %inclined part
Iincx1=     (x(4)/sin(x(5))*(x(4)/tan(x(5))*sin(x(5)))^3)/36+... %triangular part
            x(4)/sin(x(5))*(x(4)/tan(x(5))*sin(x(5)))/2*...
            ((la/2-x(4)/tan(x(5))+x(4)/sin(x(5))*cos(x(5))/2)*sin(x(5))...
            +(x(4)/tan(x(5))*sin(x(5)))/3)^2;

Iincx=      2*(Iincx1*2+Iincx2);
Icbotx=     Ictopx;
IcRtop1=    2*((pi/16*(R2^4-R1^4))-((theta-sin(theta))*(R2^4-R1^4)/16));
IcRtops=    2*((AR*(mca)^2)-AR*(((2/3*R2*sin(x(5))/x(5)*A2)-(2/3*R1*sin(x(5))/...
            x(5)*A1))/(A2-A1))^2);
IcRtop=     IcRtop1+IcRtops;
IcRbot=     IcRtop;
Ifbotx=     Iftopx;
Itotxf=     Ifbotx+Iftopx;
Itotxc=     Ictopx+Icbotx+Iincx+IcRtop+IcRbot;
Itotx=      Itotxf+Itotxc;

% I in y-direction (neglection core)
Iftopy=     (lc*x(2)^3)/12+lc*x(2)*(h/2)^2;
Ifboty=     Iftopy;
Itoty=      Iftopy+Ifboty;

% I per unit width, per meter
Ix=Itotx/lc;
Ixc=Itotxc/lc;
Ixf=Itotxf/lc;
Iy=Itoty/lc;

% Mass-center for calculation of shear, used later (top corrugation)
mcinc=d1*sin(x(5))/2;
mcfc=x(1)/2;
Afc=x(6)*x(4);
Ainc=d1*x(4);
```

```
mcshear=(mcinc*Ainc+mca*AR+mcfc*Afc/2)/(ls*x(4)/2);
end

function [Dxf,Dxc,Dyf,Dyc,D,Dx,Dy,DQy,DQx,Dxy,nuxy,nuyx,nuxypf,nuyxpf, Ks ] = ...
    calculate_Stiffness( x,h,Eyc,Exc,Eyf,Exf,nu12f,nu12c,Gxyf,Gxyc,...
    G23c,G23f,la,p,Acu,Afu,Ixf,Iy,Ixc)
%--------------------------------------------------------------------------
%   Axial stiffness: Ex, Ey
%   Horizontal shear stiffness: Gxy
%   Bending stiffness: Dx, Dy
%   Torsional stiffness: Dxy
%   Transverse shear stiffness perp. to the corrugation extrusion:DQx
%   Transverse shear stiffness para. to the corrugation extrusion:DQy
%   Poisson's ratio: nu, nuxy, nuyx, nuxp, nuyp
%--------------------------------------------------------------------------
ky=1;
kz=1;

% Libove & Hubka
% Bending stiffness to calculate poissons ratio(bending, nu)
Dxf=Exf*Ixf;
Dxc=Exc*Ixc;
Dyf=Eyf*Iy;
Dyc=Eyc*x(4)^3/12;

% Poisson's ratio  (Bending, nu)
nuxyf=nu12f;
nuyxf=nu12f*(Dyf/Dxf);
nuxyc=nu12c;
nuyxc=nu12c*(Dyc/Dxc);

nuxy=sqrt(nuxyf*nuxyc);
nuyx=sqrt(nuyxf*nuyxc);

% Bending stiffness
Dx=(Exc*Ixc)/(1-nuxyc*nuyxc)+(Exf*Ixf)/(1-nuxyf*nuyxf);
Dy=(Eyf*Iy) / (1-(nuxyf*nuyxf*(1-((Eyf*Iy)/Dx))));

% Poisson's ratio  (Stretching, nu')
nuxypf=nu12f;
nuyxpf=nu12f*(Eyf/Exf);
nuxypc=nu12c;
nuyxpc=nu12c*(Eyc/Exc);
nuxyp=sqrt(nuxypf*nuxypc);
nuyxp=sqrt(nuyxpf*nuyxpc);

EIyf=Eyf*x(2)^3/(12*(1-nuxypf*nuyxpf)); % For face in y-direction (for DQy)
EIyc=Eyc*x(4)^3/(12*(1-nuxypc*nuyxpc)); % For core in y-direction (for DQy)

% Axial stiffness (stretching, nu')
Ex=(Exc*Acu)/(1-nuxypc*nuyxpc)+(Exf*Afu)/(1-nuxypf*nuyxpf);
Ey=(Eyf*(x(2)+x(3)))/((1-nuxypf*nuyxpf)*(1-((Eyf*(x(2)+x(3))/Ex))));

EAyc=Eyc*x(4)/(1-nuxypc*nuyxpc);    % For core only (for DQy)

% Torsional stiffness
kc=0.5*(1+(x(3)-x(2))/2*h);         % 0.5 for symmetric case
GA=2*Gxyf*x(2)+(Gxyc*x(4)^2/Acu);
```

```
kGJ=((Gxyc*x(4)^2*kc/Acu)+Gxyf*x(3))/GA;
GJ=(Gxyf*x(2)*kGJ^2+(Gxyc*x(4)^2/Acu)*(kGJ-kc)^2+Gxyf*x(3)*(1-kGJ)^2)*h^2;

% Twisting
Dxy=2*GJ;                           % per unit width

% Transverse shear stiffness
GAyf=G23f*x(2);                     % For face only (for DQy)
GAyc=G23c*x(4);                     % For core only (for DQY)

% Horisontal shear stiffness
Gxy=GA;

% Transverse shear stiffness parallel to the corrugation
DQx=((Gxyc*x(4)^2)/Acu)*(h/p)^2;

% Transverse shear stiffness perpendicular to the corrugation
Ks=5/6;                             % Shear correction factor timochenko

% Following equations used to calculate DQy, see appendix B in Report
V1= x(6)+2*x(7)*x(5)+la;
V2= V1*p/2;
V3= V1*x(1)/2;
V4= 0.5*x(7)^3*(2*x(5)-sin(2*x(5)))+0.5*x(7)*x(5)*(p^2+(p-x(6))^2)-...
    2*x(7)^2*(1-cos(x(5)))*(p-x(6))+...
    1/12*la*(3*p^2+(la*cos(x(5)))^2)+1/3*((p^3+(1/8*(x(6))^3))-(p-1/2*(x(6)))^3);
V5= 0.5*x(7)*(2*x(5)-sin(2*x(5)))+la*sin(x(5))^2;
V6= 0.5*x(7)*(2*x(5)+sin(2*x(5)))+la*cos(x(5))^2 +x(6);
V7= x(7)*sin(x(5))^2+0.5*la*sin(2*x(5));
V8= x(7)^3*(1-cos(x(5)))^2+x(7)*(0.5*p*la-x(7)*x(1))*(1-cos(x(5)))-...
    x(7)^2*(p-(x(6)))*(x(5)-sin(x(5)))+1/12*la^2*(3*p+la*cos(x(5)))*...
    sin(x(5))+0.5*x(7)*x(1)*(2*p-x(6))*x(5)+1/8*x(1)*x(6)*(4*p-x(6));
V9=2*x(7)^3*(1.5*x(5)-2*sin(x(5))+0.25*sin(2*x(5)))-2*x(1)*x(7)^2*...
    (x(5)-sin(x(5)))+x(1)^2*x(7)*x(5)+1/12*(la)^3*sin(x(5))^2+...
    0.25*x(1)^2*((la)+2*x(6));

C1= (p^2/(3*EIyf)+1/(Ks*GAyf))*p;
C2= -1/EIyc*(0.5*(x(4)+x(2))*V1+V3)*p;
C3= -(1/EIyc*V4+1/EAyc*V5+1/(Ks*GAyc)*V6);
C4= (p^2/(3*EIyf)+1/EIyc*V2+1/(Ks*GAyf))*p;
C5= 1/EIyc*(0.5*(x(2)+x(4))*V2+V8)-(1/EAyc-1/(Ks*GAyc))*V7;
C6= (p^2/(3*EIyf)+1/(Ks*GAyf))*p;
C7= (1/3*p^2*(2/EIyf)+2/(Ks*GAyf)+(p*V1)/EIyc)*p;
C8= (p^2/(3*EIyf)-V2/EIyc+1/(Ks*GAyf))*p;
C9= p/EIyc*V2;
C10= 1/EIyc*(1/4*(x(2)+x(4))^2*V1+(x(2)+x(4))*V3+V9)+V6/EAyc+V5/(Ks*GAyc);

DQy= 1/ ( (2*C1*C5*C6+(C6-C1)*(C2*C3-C5*C9))/(C3*C7-C4*C8) * 1/h +...
    (C1*C3*C6/(C3*C7-C4*C8)) * 1/p+...
    (C10+(C5^2*C7-C2*C5*(C1-C4)-C2*(C2*C3-C5*C9))/(C3*C7-C4*C8))*p/h^2);

% Stiffness constants (used for general shell stiffness matrix)
D=zeros(6,6);
D(1,1)=Ex;
D(1,2)=Ey*nuxyp;
D(2,1)=Ex*nuyxp;
D(2,2)=Ey;
D(3,3)=Gxy;
```

```
D(4,4)=Dx;
D(4,5)=Dy*nuxy;
D(5,4)=Dx*nuyx;
D(5,5)=Dy;
D(6,6)=Dxy/2;
end
```

```
function [w1kN,qself,wInst] = calculate_deflection(Afu,Acu,rhof,rhoc,...
    gammaQsls,gammaGsls,nuxy,nuyx,B,L,Q1kN,qk,qdw,Dy,Dx,Dxy,DQy,DQx)
Y=B/2;                    % Where the maximum deflection is (middle)
X=L/2;                    % Where the maximum deflection is (middle)
dX=0.05;                  % Surface of the pointload in x-direction (small)
dY=0.05;                  % Surface of the pointload in y-direction (small)
r=30;                     % Number of iterations in the for-loop

% Loads
g=9.81;                                 % Gravity
Gssp=Afu*rhof+Acu*rhoc;                 % Self-weight per unit width [kg]
qself=Gssp*g;                           % Self-weight per unit width [kN]
qd=gammaQsls*qk+gammaGsls*(qself+qdw);  % Distributed load
qper=gammaGsls*(qself+qdw);             % Permanent actions

%Inital values for loop used below
w1kN=0;
wInst=0;
wPer=0;

% Deflection, see equations in Report
for m=1:r
    for n=1:r
        a=m*pi/L;   %alpha
        b=n*pi/B;   %beta

        qC=((16*qd)/(m*n*pi^2));
        qP=((16*qper)/(m*n*pi^2));
        Q1=4*Q1kN/(m*n*pi^2*dX*dY)*(cos(a*(L-dX)/2)-cos(a*(L+dX)/2))*...
            (cos(b*(B-dY)/2)-cos(b*(B+dY)/2));

        Wmn= (-Dx*Dxy*a^2*b^2*nuyx-Dxy*Dy*a^2*b^2*nuxy+Dx*Dxy*a^4+...
            +2*Dx*Dy*a^2*b^2-Dxy*DQx*a^2*nuxy*nuyx+Dxy*Dy*b^4+...
            -Dxy*DQy*b^2*nuxy*nuyx+2*Dx*DQy*a^2+Dxy*DQx*a^2+...
            +Dxy*DQy*b^2+2*DQx*Dy*b^2-2*DQx*DQy*nuxy*nuyx+...
            +2*DQx*DQy)...
            /...
            (-Dx*Dxy*DQx*a^4*b^2*nuyx+...
            -Dx*Dxy*DQy*a^2*b^4*nuyx-Dxy*DQx*Dy*a^4*b^2*nuxy+...
            -Dxy*Dy*DQy*a^2*b^4*nuxy+Dx*Dxy*DQx*a^6+...
            +Dx*Dxy*DQy*a^4*b^2+2*Dx*DQx*Dy*a^4*b^2+...
            +2*Dx*Dy*DQy*a^2*b^4+Dxy*DQx*Dy*a^2*b^4+...
            -4*Dxy*DQx*DQy*a^2*b^2*nuxy*nuyx+Dxy*Dy*DQy*b^6+...
            +2*Dx*DQx*DQy*a^2*b^2*nuyx+2*DQx*Dy*DQy*a^2*b^2*nuxy+...
            +2*Dx*DQx*DQy*a^4+4*Dxy*DQx*DQy*a^2*b^2+...
            +2*DQx*Dy*DQy*b^4);

        wInst=wInst+(Wmn*qC*sin(a*X)*sin(b*Y));
        wPer=wPer+(Wmn*qP*sin(a*X)*sin(b*Y));
        w1kN=w1kN+(Wmn*Q1*sin(a*X)*sin(b*Y));
```

```
    end
end

end
```

```
function [MRdlocal,MEd] = calculate_local_bending(x,gammaQuls,Qk,lc,...
    kmod,fm,gammaM,Ks,G23f,Eyf,nuxypf,nuyxpf)
%-------------------------------------------------------------------------
P=Qk*gammaQuls;                         %Point load
bw=4;                                   %Width of the beam model
GA=G23f*(x(4));
EI=Eyf*(x(4)^3)/(12*(1-nuxypf*nuyxpf));
n=Ks*GA*lc^2/(EI);                      %Shear reduction factor

% Load effect
MEd=(3/8)*(n/(5*n+6))*P*lc;

% Section modulus
W=(bw*x(2)^2)/6;

% Bending resistance
MRdlocal = W*kmod*fm/gammaM;
end
```

```
function [Tauxtopf,Tauxtopc,Tauytopc,Tauytopf,TauRdf,TauRdc,qdULS] = ...
    calculate_shear_stress(ls,x,B,L,h,alphaA,gammaQuls,gammaGuls,qk,...
    qself,qdw,lc,Dxy,Dx,Dy,DQx,DQy,nuxy,nuyx,Ix,Iy,gammaM,kmod,fvkf,fvkc,mcshear)
%-------------------------------------------------------------------------
xx=0;   yx=B/2;        % Where the highest shearforce in x-direction occur
xy=L/2; yy=0;          % Where the highest shearforce in y-direction occur
r=30;                  % Number of for-loop iterations

% Loads
qdULS=alphaA*gammaQuls*qk+gammaGuls*(qself+qdw);

%Inital values for loop used below
Tx=0;
Ty=0;

for m=1:2:r
    for n=1:2:r
        qmn=(16*qdULS)/(m*n*pi^2);

        Xmn=((1/2)*(m*pi/L)^5*((Dx*Dxy)/(1-nuxy*nuyx))+(m*pi/L)^3*(n*pi/B)^2*...
            ((Dx*Dy/(1-nuxy*nuyx))-((Dxy*(nuxy*Dy+nuyx*Dx))/(2*(1-nuxy*nuyx))))+...
            (1/2)*(m*pi/L)*(n*pi/B)^4*(Dy*Dxy)/(1-nuxy*nuyx)+DQy*(m*pi/L)*...
            ((m*pi/L)^2*Dx/(1-nuxy*nuyx)+(n*pi/B)^2*(Dxy+(nuyx*Dx)/(1-nuxy*nuyx))))/DQy;

        Ymn=((-(1/2)*(n*pi/B)^5*((Dy*Dxy)/(1-nuxy*nuyx))-(m*pi/L)^2*(n*pi/B)^3*...
            ((Dx*Dy/(1-nuxy*nuyx))-((Dxy*(nuxy*Dy+nuyx*Dx))/(2*(1-nuxy*nuyx))))-...
            (1/2)*(m*pi/L)^4*(n*pi/B)*(Dx*Dxy)/(1-nuxy*nuyx)-DQx*(n*pi/B)*...
            ((n*pi/B)^2*Dy/(1-nuxy*nuyx)+(m*pi/L)^2*(Dxy+(nuyx*Dy)/(1-nuxy*nuyx))))/DQx);

        Zmn=((m*pi/L)*Xmn)-((n*pi/B)*Ymn);

        Tx=Tx+(((Xmn*qmn)/Zmn)*cos(m*pi*xx/L)*sin(n*pi*xy/B));
        Ty=Ty+(((Ymn*qmn)/Zmn)*sin(m*pi*yx/L)*cos(n*pi*yy/B));
```

```
    end
end
% Shear force in the upper flange in x- and y-direction
nrfc=1/lc;

Stopxf=x(2)*(h/2);
btopxf=nrfc*x(6);

Stopyf=x(2)*(h/2);
btopyf=nrfc*lc;

Tauxtopf=(Tx*Stopxf)/(Ix*btopxf);
Tauytopf=abs((Ty*Stopyf)/(Iy*btopyf));

TauRdf=kmod*fvkf/gammaM;

% Shear force in the middle of the core in x- and y-direction
nrb=2/lc;

Stopxc=x(2)*(h/2)+(ls*x(4)*mcshear);
btopxc=nrb*x(4);

Stopyc=x(2)*(h/2)+(ls*x(4)*mcshear);
btopyc=1;

Tauxtopc=(Tx*Stopxc)/(Ix*btopxc);
Tauytopc=abs((Ty*Stopyc)/(Iy*btopyc));

TauRdc=kmod*fvkc/gammaM;
end
```

```
function [f1] = calculate_eigenfrequency(qself,qdw,L,B,D,DQy,DQx)
%--------------------------------------------------------------------------
g=9.82;
mfreq=(qself+qdw)/g;    % Mass per square meter
m33=mfreq;              % (Same notation as in Report)
K=5/6;                  % Shear correction factor

% Frequency modes
ms=1;
ns=1;
alphas=ms*pi/L;
betas=ns*pi/B;

% Definition of Q-functions
Qs=zeros(6,6);
Qs(1,1)=D(1,1);
Qs(1,2)=D(1,2);
Qs(2,2)=D(2,2);
Qs(4,4)=DQy;
Qs(5,5)=DQx;
Qs(6,6)=D(3,3);

% In-plane constants
As=zeros(6,6);
As(1,1)=Qs(1,1);
As(1,2)=Qs(1,2);
As(2,2)=Qs(2,2);
```

```
As(4,4)=K*Qs(4,4);
As(5,5)=K*Qs(5,5);
As(6,6)=Qs(6,6);

% Out-of-plane constants
Ds=zeros(6,6);
Ds(1,1)=D(4,4);
Ds(1,2)=D(4,5);
Ds(2,2)=D(5,5);
Ds(6,6)=D(6,6);

% s-functions
s=zeros(6,6);
s(1,1)=As(1,1)*alphas^2+As(6,6)*betas^2;
s(1,2)=As(1,2)+As(6,6)*betas*alphas;
s(2,2)=As(6,6)*alphas^2+As(2,2)*betas^2;
s(3,3)=K*(As(5,5)*alphas^2+As(4,4)*betas^2);
s(3,4)=K*As(5,5)*alphas;
s(3,5)=K*As(4,4)*betas;
s(4,4)=Ds(1,1)*alphas^2+Ds(6,6)*betas^2+K*As(5,5);
s(4,5)=(Ds(1,2)+Ds(6,6))*(alphas*betas);
s(5,5)=Ds(6,6)*alphas^2+Ds(2,2)*betas^2+K*As(4,4);
s(6,6)=s(4,4)*s(5,5)-s(4,5)^2;

% Simplified s-functions
sI=zeros(3,3);
sI(1,1)=s(1,1);
sI(1,2)=s(1,2);
sI(2,2)=s(2,2);
sI(3,3)=s(3,3)-(s(3,4)*s(5,5)-s(3,5)*s(4,5))*(s(3,4)/s(6,6))-...
    (s(3,5)*s(4,4)-s(3,4)*s(4,5))*(s(3,5)/s(6,6));

% Frequency
f1=1/(2*pi)*(sqrt(1/m33))*sqrt(sI(3,3));
end
```

```
function [v,vlimit] = calculate_unit_pulse_velocity(Dxc,Dxf,Dyc,Dyf,Afu...
    ,rhof,Acu,rhoc,L,B,f1)
EIl=Dxc+Dxf;                %Stiffness in x-direction
EIb=Dyc+Dyf;                %Stiffness in y-direction
m2=Afu*1*rhof+Acu*1*rhoc;   %Mass per m2
n40=(((40/f1)^2-1)*((B/L)^4)*(EIl/EIb))^0.25;
v=(4*(0.4+0.6*n40))  /  (m2*B*L+200);
vlimit=100^(f1*0.01-1);
end
```

```
function [P,Pcr] = calculate_local_buckling(x,qdULS,Q1kN,p,la,Excc)
% Critical buckling length of fictive buckling strip, see Report
Lcr=2*x(6)+la+2*x(7)*x(5);

% angle of the fictive buckling strip, see Report
theta=atan(x(1)/(p+x(6)));

% Second moment of inertia of buckling strip, per unit width
Ib=x(4)^3/12;

% Cross section area, per unit width
Acr=1*x(4);
```

```
% loads
Pd=qdULS*p/sin(theta);      % uniformly distributed load, per unit width
Pp=Q1kN/sin(theta);         % point load
P=max(Pd,Pp);

% critical load
Pcr=Excc*Ib*pi^2/Lcr^2;     % critical buckling force, Pcr
end
```

```
function plot_corr(x,lc,d1)
%Top and bot flange
plot([0 lc],[0 0],'r')
hold on
plot([0 lc],[x(3) x(3)],'r')
plot([0 lc],[x(1)+x(3)+x(4) x(1)+x(3)+x(4)],'r')
plot([0 lc],[x(1)+x(2)+x(3)+x(4) x(1)+x(2)+x(3)+x(4)],'r')
axis equal

%Half fc
plot([0 x(6)/2],[x(3) x(3)],'b')
plot([0 x(6)/2],[x(3)+x(4) x(3)+x(4)],'b')

%1st arc
xc=x(6)/2;
yc=x(3)+x(4)/2+x(7);
t=linspace(- 2*pi*90/360+x(5),-90/360*2*pi);
r1 = x(7);
r2 = x(7)+ x(4);
r3 = x(7)+ x(4)/2;
xCir1=r1*cos(t)+xc;
yCir1=r1*sin(t)+yc+x(4)/2;
xCir2=r2*cos(t)+xc;
yCir2=r2*sin(t)+yc+x(4)/2;
plot(xCir1,yCir1,'b')
plot(xCir2,yCir2,'b')

%Inclined part
xh1=xCir1(1)+cos(x(5))*2*d1;
yh1=yCir1(1)+sin(x(5))*2*d1;
plot([xCir1(1) xh1],[yCir1(1) yh1],'b')
xh2=xCir2(1)+cos(x(5))*2*d1;
yh2=yCir2(1)+sin(x(5))*2*d1;
plot([xCir2(1) xh2],[yCir2(1) yh2],'b')

%2nd arc
xc=lc/2-x(6)/2;
yc=x(3)+x(4)/2+x(1)-x(7);
t=linspace(90/360*2*pi, 2*pi*90/360+x(5));
r1 = x(7);
r2 = x(7)- x(4);
xCir1=r1*cos(t)+xc;
yCir1=r1*sin(t)+yc+x(4)/2;
xCir2=r2*cos(t)+xc;
yCir2=r2*sin(t)+yc+x(4)/2;
plot(xCir1,yCir1,'b')
plot(xCir2,yCir2,'b')

%One fc
```

```
plot([lc/2-x(6)/2 lc/2+x(6)/2],[x(1)+x(3) x(1)+x(3)],'b')
plot([lc/2-x(6)/2 lc/2+x(6)/2],[x(1)+x(3)+x(4) x(1)+x(3)+x(4)],'b')

%3rd arc
xc=lc/2+x(6)/2;
yc=x(3)+x(4)/2+x(1)-x(7);
t=linspace(2*pi*90/360-x(5),2*pi*90/360);
r1 = x(7);
r2 = x(7)- x(4);
xCir1=r1*cos(t)+xc;
yCir1=r1*sin(t)+yc+x(4)/2;
xCir2=r2*cos(t)+xc;
yCir2=r2*sin(t)+yc+x(4)/2;
plot(xCir1,yCir1,'b')
plot(xCir2,yCir2,'b')

%tilted part
xh1=xCir1(1)+cos(x(5))*2*d1;
yh1=yCir1(1)-sin(x(5))*2*d1;
plot([xCir1(1) xh1],[yCir1(1) yh1],'b')
xh2=xCir2(1)+cos(x(5))*2*d1;
yh2=yCir2(1)-sin(x(5))*2*d1;
plot([xCir2(1) xh2],[yCir2(1) yh2],'b')

%4th arc
xc=lc-x(6)/2;
yc=x(3)+x(4)/2+x(7);
t=linspace(-2*pi*90/360-x(5),-90/360*2*pi);
r1 = x(7);
r2 = x(7)+ x(4);
xCir1=r1*cos(t)+xc;
yCir1=r1*sin(t)+yc+x(4)/2;
xCir2=r2*cos(t)+xc;
yCir2=r2*sin(t)+yc+x(4)/2;
plot(xCir1,yCir1,'b')
plot(xCir2,yCir2,'b')

%Half fc
plot([lc-x(6)/2 lc],[x(3) x(3)],'b')
plot([lc-x(6)/2 lc],[x(3)+x(4) x(3)+x(4)],'b')
end
```

```
function [ L,B,nu12f,nu12c,rhoc,rhof,Exc,Eyc,Exf,Eyf,Gxyc,Gxyf,G23c,G23f...
    ,fm,fvkc,fvkf,gammaM,gammaGsls,gammaQsls,gammaGuls,gammaQuls,qk,Qk,...
    qdw,Q1kN,kmod,alphaA,Excc] = Indata(FaceMat,FaceAngle,FaceThickness,...
    CoreMat,CoreAngle,CoreThickness,B,L)
% Material Properties
[Exf,Eyf,Exc,Eyc,Excc,Gxyf,Gxyc,G23f,G23c,fvkf,fvkc,fm]=...
    Material_Properties(FaceMat,FaceAngle,FaceThickness,CoreMat,CoreAngle,CoreThickness);
% Poisson's ratio
[nu12f,nu12c]=poissons(FaceMat,FaceAngle,CoreMat,CoreAngle,Exf,Eyf,Exc,Eyc);
% Density
[rhoc,rhof]=density(FaceMat,FaceThickness,CoreMat);
%--------------------------------------------------------------------------
% Partial factors
gammaM   =1.2;
gammaGsls=1;
gammaQsls=1;
```

```
gammaGuls=1.35;
gammaQuls=1.5;
% Variable loads
qk=2e3;                     % Imposed load on floors [N/m^2]
Qk=2e3;                     % Point load for local effects (imposed) [N]
qdw=50*9.81;          % Added dead weight [ceilinf, flooring etc.) [N/m^2]
Q1kN=1e3;                   % Point load (for dyunamic requirement) [N]
kmod=0.8;                   % Load-duration: Medium
alphaA=min(1,0.5+10/(L*B)); % Area reduction factor (in ULS)
end
```

```
function [Exf,Eyf,Exc,Eyc,Excc,Gxyf,Gxyc,G23f,G23c,fvkf,fvkc,fm]=...
    Material_Properties(FaceMat,FaceAngle,FaceThickness,CoreMat,...
    CoreAngle,CoreThickness)
%%%%%%%%%%%-Face-%%%%%%%%%%%%%%%%%%%%%%
if strcmp(FaceMat, 'C')
    if FaceThickness==6.5
        if FaceAngle==0
            Exf=9.462e9; Eyf=3.538e9; fm=29.1e6;
            Gxyf=0.53e9; G13f=0.066e9; G23f=0.041e9;
            fr0kf=2.05e6; fr90kf=1.14e6; fvkf=fr0kf;
        elseif FaceAngle==90
            Exf=3.538e9; Eyf=9.462e9; fm=16.6e6;
            Gxyf=0.53e9; G13f=0.041e9; G23f=0.066e9;
            fr0kf=2.05e6; fr90kf=1.14e6; fvkf=fr90kf;
        end
    elseif FaceThickness==9
        if FaceAngle==0
            Exf=8.465e9; Eyf=4.535e9; fm=26.0e6;
            Gxyf=0.53e9; G13f=0.069e9; G23f=0.052e9;
            fr0kf=1.72e6; fr90kf=1.51e6; fvkf=fr0kf;
        elseif FaceAngle==90
            Exf=4.535e9; Eyf=8.465e9; fm=18.3e6;
            Gxyf=0.53e9; G23f=0.052e9; G13f=0.069e9;
            fr0kf=1.72e6; fr90kf=1.51e6; fvkf=fr90kf;
        end
    elseif FaceThickness==12
        if FaceAngle==0
            Exf=7.963e9; Eyf=5.037e9; fm=24.5e6;
            Gxyf=0.53e9; G13f=0.069e9; G23f=0.057e9;
            fr0kf=1.78e6; fr90kf=1.42e6; fvkf=fr0kf;
        elseif FaceAngle==90
            Exf=5.037e9; Eyf=7.963e9; fm=19.0e6;
            Gxyf=0.53e9; G13f=0.057e9; G23f=0.069e9;
            fr0kf=1.78e6; fr90kf=1.42e6; fvkf=fr90kf;
        end
    elseif FaceThickness==15
        if FaceAngle==0
            Exf=7.663e9; Eyf=5.337e9; fm=23.6e6;
            Gxyf=0.53e9; G13f=0.069e9; G23f=0.059e9;
            fr0kf=1.68e6; fr90kf=1.53e6; fvkf=fr0kf;
        elseif FaceAngle==90
            Exf=5.337e9; Eyf=7.663e9; fm=19.3e6;
            Gxyf=0.53e9; G13f=0.059e9; G23f=0.069e9;
            fr0kf=1.68e6; fr90kf=1.53e6; fvkf=fr90kf;
        end
    elseif FaceThickness==18
        if FaceAngle==0
```

```
            Exf=7.464e9; Eyf=5.536e9; fm=23.0e6;
            Gxyf=0.53e9; G13f=0.069e9; G23f=0.061e9;
            fr0kf=1.71e6; fr90kf=1.50e6; fvkf=fr0kf;
        elseif FaceAngle==90
            Exf=5.536e9; Eyf=7.464e9; fm=19.5e6;
            Gxyf=0.53e9; G13f=0.061e9; G23f=0.069e9;
            fr0kf=1.71e6; fr90kf=1.50e6; fvkf=fr90kf;
        end
    elseif FaceThickness==21
        if FaceAngle==0
            Exf=7.323e9; Eyf=5.677e9; fm=22.5e6;
            Gxyf=0.53e9; G13f=0.069e9; G23f=0.062e9;
            fr0kf=1.66e6; fr90kf=1.55e6; fvkf=fr0kf;
        elseif FaceAngle==90
            Exf=5.677e9; Eyf=7.323e9; fm=19.6e6;
            Gxyf=0.53e9; G13f=0.062e9; G23f=0.069e9;
            fr0kf=1.66e6; fr90kf=1.55e6; fvkf=fr90kf;
        end
    elseif FaceThickness==24
        if FaceAngle==0
            Exf=7.218e9; Eyf=5.782e9; fm=22.2e6;
            Gxyf=0.53e9; G13f=0.069e9; G23f=0.063e9;
            fr0kf=1.68e6; fr90kf=1.53e6; fvkf=fr0kf;
        elseif FaceAngle==90
            Exf=5.782e9; Eyf=7.218e9; fm=19.7e6;
            Gxyf=0.53e9; G13f=0.063e9; G23f=0.069e9;
            fr0kf=1.68e6; fr90kf=1.53e6; fvkf=fr90kf;
        end
    elseif FaceThickness==27
        if FaceAngle==0
            Exf=7.137e9; Eyf=5.863e9; fm=22.0e6;
            Gxyf=0.53e9; G13f=0.068e9; G23f=0.063e9;
            fr0kf=1.65e6; fr90kf=1.56e6; fvkf=fr0kf;
        elseif FaceAngle==90
            Exf=5.863e9; Eyf=7.137e9; fm=19.7e6;
            Gxyf=0.53e9; G13f=0.063e9; G23f=0.068e9;
            fr0kf=1.65e6; fr90kf=1.56e6; fvkf=fr90kf;
        end
    elseif FaceThickness==30
        if FaceAngle==0
            Exf=7.072e9; Eyf=5.928e9; fm=21.8e6;
            Gxyf=0.53e9; G13f=0.068e9; G23f=0.064e9;
            fr0kf=1.66e6; fr90kf=1.54e6; fvkf=fr0kf;
        elseif FaceAngle==90
            Exf=5.928e9; Eyf=7.072e9; fm=19.8e6;
            Gxyf=0.53e9; G13f=0.064e9; G23f=0.068e9;
            fr0kf=1.66e6; fr90kf=1.54e6; fvkf=fr90kf;
        end
    end
elseif strcmp(FaceMat, 'B')
    if FaceThickness==6.5
        if FaceAngle==0
            Exf=12.737e9; Eyf=4.763e9; fm=50.9e6;
            Gxyf=0.62e9; G13f=0.169e9; G23f=0.123e9;
            fr0kf=3.20e6; fr90kf=1.78e6; fvkf=fr0kf;
        elseif FaceAngle==90
            Exf=4.763e9; Eyf=12.737e9; fm=29.0e6;
            Gxyf=0.62e9; G13f=0.123e9; G23f=0.169e9;
```

```
            fr0kf=3.20e6; fr90kf=1.78e6; fvkf=fr90kf;
        end
    elseif FaceThickness==9
        if FaceAngle==0
            Exf=11.395e9; Eyf=6.105e9; fm=45.6e6;
            Gxyf=0.62e9; G13f=0.206e9; G23f=0.155e9;
            fr0kf=2.68e6; fr90kf=2.35e6; fvkf=fr0kf;
        elseif FaceAngle==90
            Exf=6.105e9; Eyf=11.395e9; fm=32.1e6;
            Gxyf=0.62e9; G13f=0.155e9; G23f=0.206e9;
            fr0kf=2.68e6; fr90kf=2.35e6; fvkf=fr90kf;
        end
    elseif FaceThickness==12
        if FaceAngle==0
            Exf=10.719e9; Eyf=6.781e9; fm=42.9e6;
            Gxyf=0.62e9; G13f=0.207e9; G23f=0.170e9;
            fr0kf=2.78e6; fr90kf=2.22e6; fvkf=fr0kf;
        elseif FaceAngle==90
            Exf=6.781e9; Eyf=10.719e9; fm=33.2e6;
            Gxyf=0.62e9; G13f=0.170e9; G23f=0.207e9;
            fr0kf=2.78e6; fr90kf=2.22e6; fvkf=fr90kf;
        end
    elseif FaceThickness==15
        if FaceAngle==0
            Exf=10.316e9; Eyf=7.184e9; fm=41.3e6;
            Gxyf=0.62e9; G13f=0.207e9; G23f=0.178e9;
            fr0kf=2.62e6; fr90kf=2.39e6; fvkf=fr0kf;
        elseif FaceAngle==90
            Exf=7.184e9; Eyf=10.316e9; fm=33.8e6;
            Gxyf=0.62e9; G13f=0.178e9; G23f=0.207e9;
            fr0kf=2.62e6; fr90kf=2.39e6; fvkf=fr90kf;
        end
    elseif FaceThickness==18
        if FaceAngle==0
            Exf=10.048e9; Eyf=7.452e9; fm=40.2e6;
            Gxyf=0.62e9; G13f=0.206e9; G23f=0.183e9;
            fr0kf=2.67e6; fr90kf=2.34e6; fvkf=fr0kf;
        elseif FaceAngle==90
            Exf=7.452e9; Eyf=10.048e9; fm=34.1e6;
            Gxyf=0.62e9; G13f=0.183e9; G23f=0.206e9;
            fr0kf=2.67e6; fr90kf=2.34e6; fvkf=fr90kf;
        end
    elseif FaceThickness==21
        if FaceAngle==0
            Exf=9.858e9; Eyf=7.642e9; fm=39.4e6;
            Gxyf=0.62e9; G13f=0.206e9; G23f=0.186e9;
            fr0kf=2.59e6; fr90kf=2.41e6; fvkf=fr0kf;
        elseif FaceAngle==90
            Exf=7.642e9; Eyf=9.858e9; fm=34.3e6;
            Gxyf=0.62e9; G13f=0.186e9; G23f=0.206e9;
            fr0kf=2.59e6; fr90kf=2.41e6; fvkf=fr90kf;
        end
    elseif FaceThickness==24
        if FaceAngle==0
            Exf=9.717e9; Eyf=7.783e9; fm=38.9e6;
            Gxyf=0.62e9; G13f=0.206e9; G23f=0.189e9;
            fr0kf=2.62e6; fr90kf=2.39e6; fvkf=fr0kf;
        elseif FaceAngle==90
```

```
            Exf=7.783e9; Eyf=9.717e9; fm=34.4e6;
            Gxyf=0.62e9; G13f=0.189e9; G23f=0.206e9;
            fr0kf=2.62e6; fr90kf=2.39e6; fvkf=fr90kf;
        end
    elseif FaceThickness==27
        if FaceAngle==0
            Exf=9.607e9; Eyf=7.893e9; fm=38.4e6;
            Gxyf=0.62e9; G13f=0.205e9; G23f=0.190e9;
            fr0kf=2.57e6; fr90kf=2.43e6; fvkf=fr0kf;
        elseif FaceAngle==90
            Exf=7.893e9; Eyf=9.607e9; fm=34.5e6;
            Gxyf=0.62e9; G13f=0.190e9; G23f=0.205e9;
            fr0kf=2.57e6; fr90kf=2.43e6; fvkf=fr90kf;
        end
    elseif FaceThickness==30
        if FaceAngle==0
            Exf=9.519e9; Eyf=7.981e9; fm=38.1e6;
            Gxyf=0.62e9; G13f=0.205e9; G23f=0.192e9;
            fr0kf=2.59e6; fr90kf=2.41e6; fvkf=fr0kf;
        elseif FaceAngle==90
            Exf=7.981e9; Eyf=9.519e9; fm=34.6e6;
            Gxyf=0.62e9; G13f=0.192e9; G23f=0.205e9;
            fr0kf=2.59e6; fr90kf=2.41e6; fvkf=fr90kf;
        end
    elseif FaceThickness==35
        if FaceAngle==0
            Exf=9.389e9; Eyf=8.111e9; fm=37.6e6;
            Gxyf=0.62e9; G13f=0.204e9; G23f=0.193e9;
            fr0kf=2.57e6; fr90kf=2.43e6; fvkf=fr0kf;
        elseif FaceAngle==90
            Exf=8.111e9; Eyf=9.389e9; fm=34.7e6;
            Gxyf=0.62e9; G13f=0.193e9; G23f=0.204e9;
            fr0kf=2.57e6; fr90kf=2.43e6; fvkf=fr90kf;
        end
    elseif FaceThickness==40
        if FaceAngle==0
            Exf=9.296e9; Eyf=8.204e9; fm=37.2e6;
            Gxyf=0.62e9; G13f=0.204e9; G23f=0.195e9;
            fr0kf=2.56e6; fr90kf=2.44e6; fvkf=fr0kf;
        elseif FaceAngle==90
            Exf=8.204e9; Eyf=9.296e9; fm=34.7e6;
            Gxyf=0.62e9; G13f=0.195e9; G23f=0.204e9;
            fr0kf=2.56e6; fr90kf=2.44e6; fvkf=fr90kf;
        end
    elseif FaceThickness==45
        if FaceAngle==0
            Exf=9.259e9; Eyf=8.241e9; fm=37.0e6;
            Gxyf=0.62e9; G13f=0.203e9; G23f=0.195e9;
            fr0kf=2.55e6; fr90kf=2.46e6; fvkf=fr0kf;
        elseif FaceAngle==90
            Exf=8.241e9; Eyf=9.259e9; fm=34.7e6;
            Gxyf=0.62e9; G13f=0.195e9; G23f=0.203e9;
            fr0kf=2.55e6; fr90kf=2.46e6; fvkf=fr90kf;
        end
    elseif FaceThickness==50
        if FaceAngle==0
            Exf=9.198e9; Eyf=8.302e9; fm=36.8e6;
            Gxyf=0.62e9; G13f=0.203e9; G23f=0.196e9;
```

```
            fr0kf=2.54e6; fr90kf=2.46e6; fvkf=fr0kf;
        elseif FaceAngle==90
            Exf=8.302e9; Eyf=9.198e9; fm=34.8e6;
            Gxyf=0.62e9; G13f=0.196e9; G23f=0.203e9;
            fr0kf=2.54e6; fr90kf=2.46e6; fvkf=fr90kf;
        end
    end
elseif strcmp(FaceMat, 'P')
    if FaceThickness==6
        Exf=3.2e9; Eyf=3.2e9; fm=14.2e6; fvkf=1.8e6;
        Gxyf=0.86e9; G13f=0.86e9; G23f=0.86e9;
    elseif FaceThickness==13
        Exf=2.9e9; Eyf=2.9e9; fm=12.5e6; fvkf=1.6e6;
        Gxyf=0.83e9; G13f=0.83e9; G23f=0.83e9;
    elseif FaceThickness==20
        Exf=2.7e9; Eyf=2.7e9; fm=10.8e6; fvkf=1.4e6;
        Gxyf=0.77e9; G13f=0.77e9; G23f=0.77e9;
    elseif FaceThickness==25
        Exf=2.4e9; Eyf=2.4e9; fm=9.2e6; fvkf=1.2e6;
        Gxyf=0.68e9; G13f=0.68e9; G23f=0.68e9;
    elseif FaceThickness==32
        Exf=2.1e9; Eyf=2.1e9; fm=7.5e6; fvkf=1.1e6;
        Gxyf=0.60e9; G13f=0.60e9; G23f=0.60e9;
    elseif FaceThickness==40
        Exf=1.8e9; Eyf=1.8e9; fm=5.8e6; fvkf=1.0e6;
        Gxyf=0.55e9; G13f=0.55e9; G23f=0.55e9;
    end
elseif strcmp(FaceMat, 'K')
    if FaceThickness==21
        if FaceAngle==0
            Exf=10e9; Eyf=2.4e9; fm=19e6; fvkf=4.5e6;
            Gxyf=0.6e9; G13f=0.6e9; G23f=0.6e9;
        elseif FaceAngle==90
            Exf=2.4e9; Eyf=10e9; fm=9e6; fvkf=4.5e6;
            Gxyf=0.6e9; G13f=0.6e9; G23f=0.6e9;
        end
    elseif FaceThickness==27
        if FaceAngle==0
            Exf=10.5e9; Eyf=2.4e9; fm=26e6; fvkf=4.5e6;
            Gxyf=0.6e9; G13f=0.6e9; G23f=0.6e9;
        elseif FaceAngle==90
            Exf=2.4e9; Eyf=10.5e9; fm=9e6; fvkf=4.5e6;
            Gxyf=0.6e9; G13f=0.6e9; G23f=0.6e9;
        end
    end
elseif strcmp(FaceMat, 'M')
    if FaceThickness==10
        Exf=1.042e9; Eyf=1.042e9; fm=18e6; fvkf=3.3e6;
        Gxyf=0.83e9; G13f=0.83e9; G23f=0.83e9;
    elseif FaceThickness==18
        Exf=2.415e9; Eyf=2.412e9; fm=18e6; fvkf=3.3e6;
        Gxyf=0.965e9; G13f=0.965e9; G23f=0.965e9;
    elseif FaceThickness==20
        Exf=5.56e9; Eyf=5.56e9; fm=18e6;
        Gxyf=2.059e9; G13f=2.059e9; G23f=2.059e9;
        fvkf=3.3e6;
    elseif FaceThickness==50
        Exf=4.2e9; Eyf=4.2e9; fm=18e6; fvkf=3.3e6;
```

```
        Gxyf=1.615e9; G13f=1.615e9; G23f=1.615e9;
    end
end

%%%%%%%%%%%%%%%-Core-%%%%%%%%%%%%%%%%
if strcmp(CoreMat, 'C')
    if CoreThickness==6.5
        if CoreAngle==0
            Exc=9.462e9; Eyc=3.538e9; Eycc=5.688e9;
            Gxyc=0.53e9; G13c=0.066e9; G23c=0.041e9;
            fr0kc=2.05e6; fr90kc=1.14e6; fvkc=fr0kc;
        elseif CoreAngle==90
            Exc=3.538e9; Eyc=9.462e9; Eycc=7.313e9;
            Gxyc=0.53e9; G13c=0.041e9; G23c=0.066e9;
            fr0kc=2.05e6; fr90kc=1.14e6; fvkc=fr90kc;
        end
    elseif CoreThickness==9
        if CoreAngle==0
            Exc=8.465e9; Eyc=4.535e9; Eycc=5.935e9;
            Gxyc=0.53e9; G13c=0.069e9; G23c=0.052e9;
            fr0kc=1.72e6; fr90kc=1.51e6; fvkc=fr0kc;
        elseif CoreAngle==90
            Exc=4.535e9; Eyc=8.465e9; Eycc=7.065e9;
            Gxyc=0.53e9; G23c=0.052e9; G13c=0.069e9;
            fr0kc=1.72e6; fr90kc=1.51e6; fvkc=fr90kc;
        end
    elseif CoreThickness==12
        if CoreAngle==0
            Exc=7.963e9; Eyc=5.037e9; Eycc=6.067e9;
            Gxyc=0.53e9; G13c=0.069e9; G23c=0.057e9;
            fr0kc=1.78e6; fr90kc=1.42e6; fvkc=fr0kc;
        elseif CoreAngle==90
            Exc=5.037e9; Eyc=7.963e9; Eycc=6.933e9;
            Gxyc=0.53e9; G13c=0.057e9; G23c=0.069e9;
            fr0kc=1.78e6; fr90kc=1.42e6; fvkc=fr90kc;
        end
    elseif CoreThickness==15
        if CoreAngle==0
            Exc=7.663e9; Eyc=5.337e9; Eycc=6.149e9;
            Gxyc=0.53e9; G13c=0.069e9; G23c=0.059e9;
            fr0kc=1.68e6; fr90kc=1.53e6; fvkc=fr0kc;
        elseif CoreAngle==90
            Exc=5.337e9; Eyc=7.663e9; Eycc=6.851e9;
            Gxyc=0.53e9; G13c=0.059e9; G23c=0.069e9;
            fr0kc=1.68e6; fr90kc=1.53e6; fvkc=fr90kc;
        end
    elseif CoreThickness==18
        if CoreAngle==0
            Exc=7.464e9; Eyc=5.536e9; Eycc=6.205e9;
            Gxyc=0.53e9; G13c=0.069e9; G23c=0.061e9;
            fr0kc=1.71e6; fr90kc=1.50e6; fvkc=fr0kc;
        elseif CoreAngle==90
            Exc=5.536e9; Eyc=7.464e9; Eycc=6.795e9;
            Gxyc=0.53e9; G13c=0.061e9; G23c=0.069e9;
            fr0kc=1.71e6; fr90kc=1.50e6; fvkc=fr90kc;
        end
    elseif CoreThickness==21
        if CoreAngle==0
```

```
            Exc=7.323e9; Eyc=5.677e9; Eycc=6.245e9;
            Gxyc=0.53e9; G13c=0.069e9; G23c=0.062e9;
            fr0kc=1.66e6; fr90kc=1.55e6; fvkc=fr0kc;
        elseif CoreAngle==90
            Exc=5.677e9; Eyc=7.323e9; Eycc=6.755e9;
            Gxyc=0.53e9; G13c=0.062e9; G23c=0.069e9;
            fr0kc=1.66e6; fr90kc=1.55e6; fvkc=fr90kc;
        end
    elseif CoreThickness==24
        if CoreAngle==0
            Exc=7.218e9; Eyc=5.782e9; Eycc=6.276e9;
            Gxyc=0.53e9; G13c=0.069e9; G23c=0.063e9;
            fr0kc=1.68e6; fr90kc=1.53e6; fvkc=fr0kc;
        elseif CoreAngle==90
            Exc=5.782e9; Eyc=7.218e9; Eycc=6.724e9;
            Gxyc=0.53e9; G13c=0.063e9; G23c=0.069e9;
            fr0kc=1.68e6; fr90kc=1.53e6; fvkc=fr90kc;
        end
    elseif CoreThickness==27
        if CoreAngle==0
            Exc=7.137e9; Eyc=5.863e9; Eycc=6.300e9;
            Gxyc=0.53e9; G13c=0.068e9; G23c=0.063e9;
            fr0kc=1.65e6; fr90kc=1.56e6; fvkc=fr0kc;
        elseif CoreAngle==90
            Exc=5.863e9; Eyc=7.137e9; Eycc=6.700e9;
            Gxyc=0.53e9; G13c=0.063e9; G23c=0.068e9;
            fr0kc=1.65e6; fr90kc=1.56e6; fvkc=fr90kc;
        end
    elseif CoreThickness==30
        if CoreAngle==0
            Exc=7.072e9; Eyc=5.928e9; Eycc=6.319e9;
            Gxyc=0.53e9; G13c=0.068e9; G23c=0.064e9;
            fr0kc=1.66e6; fr90kc=1.54e6; fvkc=fr0kc;
        elseif CoreAngle==90
            Exc=5.928e9; Eyc=7.072e9; Eycc=6.681e9;
            Gxyc=0.53e9; G13c=0.064e9; G23c=0.068e9;
            fr0kc=1.66e6; fr90kc=1.54e6; fvkc=fr90kc;
        end
    end
elseif strcmp(CoreMat, 'B')
    if CoreThickness==6.5
        if CoreAngle==0
            Exc=12.737e9; Eyc=4.763e9; Eycc=7.656e9;
            Gxyc=0.62e9; G13c=0.169e9; G23c=0.123e9;
            fr0kc=3.20e6; fr90kc=1.78e6; fvkc=fr0kc;
        elseif CoreAngle==90
            Exc=4.763e9; Eyc=12.737e9; Eycc=9.844e9;
            Gxyc=0.62e9; G13c=0.123e9; G23c=0.169e9;
            fr0kc=3.20e6; fr90kc=1.78e6; fvkc=fr90kc;
        end
    elseif CoreThickness==9
        if CoreAngle==0
            Exc=11.395e9; Eyc=6.105e9; Eycc=7.989e9;
            Gxyc=0.62e9; G13c=0.206e9; G23c=0.155e9;
            fr0kc=2.68e6; fr90kc=2.35e6; fvkc=fr0kc;
        elseif CoreAngle==90
            Exc=6.105e9; Eyc=11.395e9; Eycc=9.511e9;
            Gxyc=0.62e9; G13c=0.155e9; G23c=0.206e9;
```

```
            fr0kc=2.68e6; fr90kc=2.35e6; fvkc=fr90kc;
        end
    elseif CoreThickness==12
        if CoreAngle==0
            Exc=10.719e9; Eyc=6.781e9; Eycc=8.167e9;
            Gxyc=0.62e9; G13c=0.207e9; G23c=0.170e9;
            fr0kc=2.78e6; fr90kc=2.22e6; fvkc=fr0kc;
        elseif CoreAngle==90
            Exc=6.781e9; Eyc=10.719e9; Eycc=9.333e9;
            Gxyc=0.62e9; G13c=0.170e9; G23c=0.207e9;
            fr0kc=2.78e6; fr90kc=2.22e6; fvkc=fr90kc;
        end
    elseif CoreThickness==15
        if CoreAngle==0
            Exc=10.316e9; Eyc=7.184e9; Eycc=8.277e9;
            Gxyc=0.62e9; G13c=0.207e9; G23c=0.178e9;
            fr0kc=2.62e6; fr90kc=2.39e6; fvkc=fr0kc;
        elseif CoreAngle==90
            Exc=7.184e9; Eyc=10.316e9; Eycc=9.223e9;
            Gxyc=0.62e9; G13c=0.178e9; G23c=0.207e9;
            fr0kc=2.62e6; fr90kc=2.39e6; fvkc=fr90kc;
        end
    elseif CoreThickness==18
        if CoreAngle==0
            Exc=10.048e9; Eyc=7.452e9; Eycc=8.352e9;
            Gxyc=0.62e9; G13c=0.206e9; G23c=0.183e9;
            fr0kc=2.67e6; fr90kc=2.34e6; fvkc=fr0kc;
        elseif CoreAngle==90
            Exc=7.452e9; Eyc=10.048e9; Eycc=9.148e9;
            Gxyc=0.62e9; G13c=0.183e9; G23c=0.206e9;
            fr0kc=2.67e6; fr90kc=2.34e6; fvkc=fr90kc;
        end
    elseif CoreThickness==21
        if CoreAngle==0
            Exc=9.858e9; Eyc=7.642e9; Eycc=8.407e9;
            Gxyc=0.62e9; G13c=0.206e9; G23c=0.186e9;
            fr0kc=2.59e6; fr90kc=2.41e6; fvkc=fr0kc;
        elseif CoreAngle==90
            Exc=7.642e9; Eyc=9.858e9; Eycc=9.093e9;
            Gxyc=0.62e9; G13c=0.186e9; G23c=0.206e9;
            fr0kc=2.59e6; fr90kc=2.41e6; fvkc=fr90kc;
        end
    elseif CoreThickness==24
        if CoreAngle==0
            Exc=9.717e9; Eyc=7.783e9; Eycc=8.448e9;
            Gxyc=0.62e9; G13c=0.206e9; G23c=0.189e9;
            fr0kc=2.62e6; fr90kc=2.39e6; fvkc=fr0kc;
        elseif CoreAngle==90
            Exc=7.783e9; Eyc=9.717e9; Eycc=9.052e9;
            Gxyc=0.62e9; G13c=0.189e9; G23c=0.206e9;
            fr0kc=2.62e6; fr90kc=2.39e6; fvkc=fr90kc;
        end
    elseif CoreThickness==27
        if CoreAngle==0
            Exc=9.607e9; Eyc=7.893e9; Eycc=8.481e9;
            Gxyc=0.62e9; G13c=0.205e9; G23c=0.190e9;
            fr0kc=2.57e6; fr90kc=2.43e6; fvkc=fr0kc;
        elseif CoreAngle==90
```

```
            Exc=7.893e9; Eyc=9.607e9; Eycc=9.019e9;
            Gxyc=0.62e9; G13c=0.190e9; G23c=0.205e9;
            fr0kc=2.57e6; fr90kc=2.43e6; fvkc=fr90kc;
        end
    elseif CoreThickness==30
        if CoreAngle==0
            Exc=9.519e9; Eyc=7.981e9; Eycc=8.507e9;
            Gxyc=0.62e9; G13c=0.205e9; G23c=0.192e9;
            fr0kc=2.59e6; fr90kc=2.41e6; fvkc=fr0kc;
        elseif CoreAngle==90
            Exc=7.981e9; Eyc=9.519e9; Eycc=8.993e9;
            Gxyc=0.62e9; G13c=0.192e9; G23c=0.205e9;
            fr0kc=2.59e6; fr90kc=2.41e6; fvkc=fr90kc;
        end
    elseif CoreThickness==35
        if CoreAngle==0
            Exc=9.389e9; Eyc=8.111e9; Eycc=8.547e9;
            Gxyc=0.62e9; G13c=0.204e9; G23c=0.193e9;
            fr0kc=2.57e6; fr90kc=2.43e6; fvkc=fr0kc;
        elseif CoreAngle==90
            Exc=8.111e9; Eyc=9.389e9; Eycc=8.953e9;
            Gxyc=0.62e9; G13c=0.193e9; G23c=0.204e9;
            fr0kc=2.57e6; fr90kc=2.43e6; fvkc=fr90kc;
        end
    elseif CoreThickness==40
        if CoreAngle==0
            Exc=9.296e9; Eyc=8.204e9; Eycc=8.575e9;
            Gxyc=0.62e9; G13c=0.204e9; G23c=0.195e9;
            fr0kc=2.56e6; fr90kc=2.44e6; fvkc=fr0kc;
        elseif CoreAngle==90
            Exc=8.204e9; Eyc=9.296e9; Eycc=8.925e9;
            Gxyc=0.62e9; G13c=0.195e9; G23c=0.204e9;
            fr0kc=2.56e6; fr90kc=2.44e6; fvkc=fr90kc;
        end
    elseif CoreThickness==45
        if CoreAngle==0
            Exc=9.259e9; Eyc=8.241e9; Eycc=8.586e9;
            Gxyc=0.62e9; G13c=0.203e9; G23c=0.195e9;
            fr0kc=2.55e6; fr90kc=2.46e6; fvkc=fr0kc;
        elseif CoreAngle==90
            Exc=8.241e9; Eyc=9.259e9; Eycc=8.914e9;
            Gxyc=0.62e9; G13c=0.195e9; G23c=0.203e9;
            fr0kc=2.55e6; fr90kc=2.46e6; fvkc=fr90kc;
        end
    elseif CoreThickness==50
        if CoreAngle==0
            Exc=9.198e9; Eyc=8.302e9; Eycc=8.605e9;
            Gxyc=0.62e9; G13c=0.203e9; G23c=0.196e9;
            fr0kc=2.54e6; fr90kc=2.46e6; fvkc=fr0kc;
        elseif CoreAngle==90
            Exc=8.302e9; Eyc=9.198e9; Eycc=8.895e9;
            Gxyc=0.62e9; G13c=0.196e9; G23c=0.203e9;
            fr0kc=2.54e6; fr90kc=2.46e6; fvkc=fr90kc;
        end
    elseif strcmp(CoreMat, 'P')
        if CoreThickness==6
            Exc=3.2e9; Eyc=3.2e9; Eycc=1.8e9;
            Gxyc=0.86e9; G13c=0.86e9; G23c=0.86e9;
```

```
            fvkc=1.8e6;
        elseif CoreThickness==13
            Exc=2.9e9; Eyc=2.9e9; Eycc=1.7e9;
            Gxyc=0.83e9; G13c=0.83e9; G23c=0.83e9;
            fvkc=1.6e6;
        elseif CoreThickness==20
            Exc=2.7e9; Eyc=2.7e9; Eycc=1.6e9;
            Gxyc=0.77e9; G13c=0.77e9; G23c=0.77e9;
            fvkc=1.4e6;
        elseif CoreThickness==25
            Exc=2.4e9; Eyc=2.4e9; Eycc=1.4e9;
            Gxyc=0.68e9; G13c=0.68e9; G23c=0.68e9;
            fvkc=1.2e6;
        elseif CoreThickness==32
            Exc=2.1e9; Eyc=2.1e9; Eycc=1.2e9;
            Gxyc=0.60e9; G13c=0.60e9; G23c=0.60e9;
            fvkc=1.1e6;
        elseif CoreThickness==40
            Exc=1.8e9; Eyc=1.8e9; Eycc=1.1e9;
            Gxyc=0.55e9; G13c=0.55e9; G23c=0.55e9;
            fvkc=1.0e6;
        end
    elseif strcmp(CoreMat, 'K')
        if CoreThickness==21
            if CoreAngle==0
                Exc=10e9; Eyc=2.4e9; Eycc=9e9; fvkc=4.5e6;
                Gxyc=0.6e9; G13c=0.6e9; G23c=0.6e9;
            elseif CoreAngle==90
                Exc=2.4e9; Eyc=10e9; Eycc=19e9; fvkc=4.5e6;
                Gxyc=0.6e9; G13c=0.6e9; G23c=0.6e9;
            end
        elseif CoreThickness==27
            if CoreAngle==0
                Exc=10.5e9; Eyc=2.4e9; Eycc=9e9; fvkc=4.5e6;
                Gxyc=0.6e9; G13c=0.6e9; G23c=0.6e9;
            elseif CoreAngle==90
                Exc=2.4e9; Eyc=10.5e9; Eycc=26e9; fvkc=4.5e6;
                Gxyc=0.6e9; G13c=0.6e9; G23c=0.6e9;
            end
        end
    end
end
Excc=Eycc;
end
```

```
function [nu12f,nu12c]=poissons(FaceMat,FaceAngle,CoreMat,CoreAngle,Exf,Eyf,Exc,Eyc)
if strcmp(FaceMat, 'C')
    nu12f=0.5;
    nu13f=0.05;
    if FaceAngle==90
        nu12f=nu12f*Exf/Eyf;
        nu13f=0.01;
    end
elseif strcmp(FaceMat, 'P')
    nu12f=0.2;
    nu13f=0.2;
    if FaceAngle==90
        nu12f=nu12f*Exf/Eyf;
```

```
        nu13f=0.2;
    end
elseif strcmp(FaceMat, 'B')
    nu12f=0.5;
    nu13f=0.05;
    if FaceAngle==90
        nu12f=nu12f*Exf/Eyf;
        nu13f=0.01;
    end
elseif strcmp(FaceMat, 'K')
    nu12f=0.02;
    nu13f=0.02;
    if FaceAngle==90
        nu12f=nu12f*Exf/Eyf;
        nu13f=0.02;
    end
elseif strcmp(FaceMat, 'M')
    nu12f=0.35;
    nu13f=0.35;
    if FaceAngle==90
        nu12f=nu12f*Exf/Eyf;
        nu13f=0.35;
    end
end

if strcmp(CoreMat, 'C')
    nu12c=0.5;
    nu13c=0.05;
    if CoreAngle==90
        nu12c=nu12c*Exc/Eyc;
        nu13c=0.01;
    end
elseif strcmp(CoreMat, 'P')
    nu12c=0.2;
    nu13c=0.2;
    if CoreAngle==90
        nu12c=nu12c*Exc/Eyc;
        nu13c=0.2;
    end
elseif strcmp(CoreMat, 'B')
    nu12c=0.5;
    nu13c=0.05;
    if CoreAngle==90
        nu12c=nu12c*Exc/Eyc;
        nu13c=0.01;
    end
elseif strcmp(CoreMat, 'K')
    nu12c=0.02;
    nu13c=0.02;
    if CoreAngle==90
        nu12c=nu12c*Exc/Eyc;
        nu13c=0.02;
    end
end
end

function [rhoc,rhof]=density(FaceMat,FaceThickness,CoreMat)
if strcmp(FaceMat, 'B')
```

```
    rhof=630;
elseif strcmp(FaceMat, 'C')
    rhof=410;
elseif strcmp(FaceMat, 'P')
    if FaceThickness==6
        rhof=650;
    elseif FaceThickness==13
        rhof=600;
    elseif FaceThickness==20
        rhof=550;
    elseif FaceThickness==25
        rhof=550;
    elseif FaceThickness==32
        rhof=500;
    elseif FaceThickness==40
        rhof=500;
    end
elseif strcmp(FaceMat, 'K')
    rhof=480;
elseif strcmp(FaceMat, 'M')
    rhof=1000;
end
if strcmp(CoreMat, 'C')
    rhoc=410;
elseif strcmp(CoreMat, 'B')
    rhoc=630;
end
end
```

Published with MATLAB® R2017a

C Abaqus

To verify the analytic solution and to make ULS controls Abaqus/CAE 6.13-3. Four different models were made for each optimal case, one for the deflection from uniformly distributed load, one for the fundamental frequency, one for the deflection from 1 kN point load and one for the buckling analyses. These were models initially in both solid and shell elements. This appendix will show the steps for first solid element and then shell elements with the material combination C/C/C.

C.1 Solid elements

Part module: The part were made as *3D solid extrusion elements* for all the three parts, two faces and one corrugated core. The corrugated core were imported as a sketch from AutoCAD.

Property module: The material properties for each part were created with the material manager by using the *Density - Uniform* and *Elastic material - Engineering constants* as input, see Figure C.1. Every part is then added with a *Solid, Homogeneous* section type.

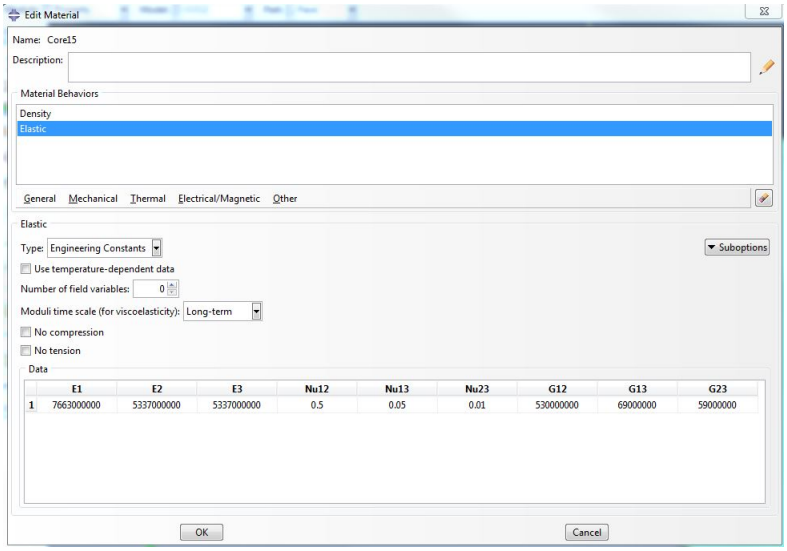

Figure C.1: Material properties input for the material C/C/C with a thickness of 15 mm

The grain orientation of each part is defined by the steps *Property - Assign material orientation*. For the face this is made by using a *Datum CSYS* and creating a coordinate system in the grain orientation, see Figure C.2. For the corrugated core the grain orientation is more complex and is made by using a so called *Discrete* orientation and defining a normal axis (the surface of the core) and a primary axis (center line of corrugation).

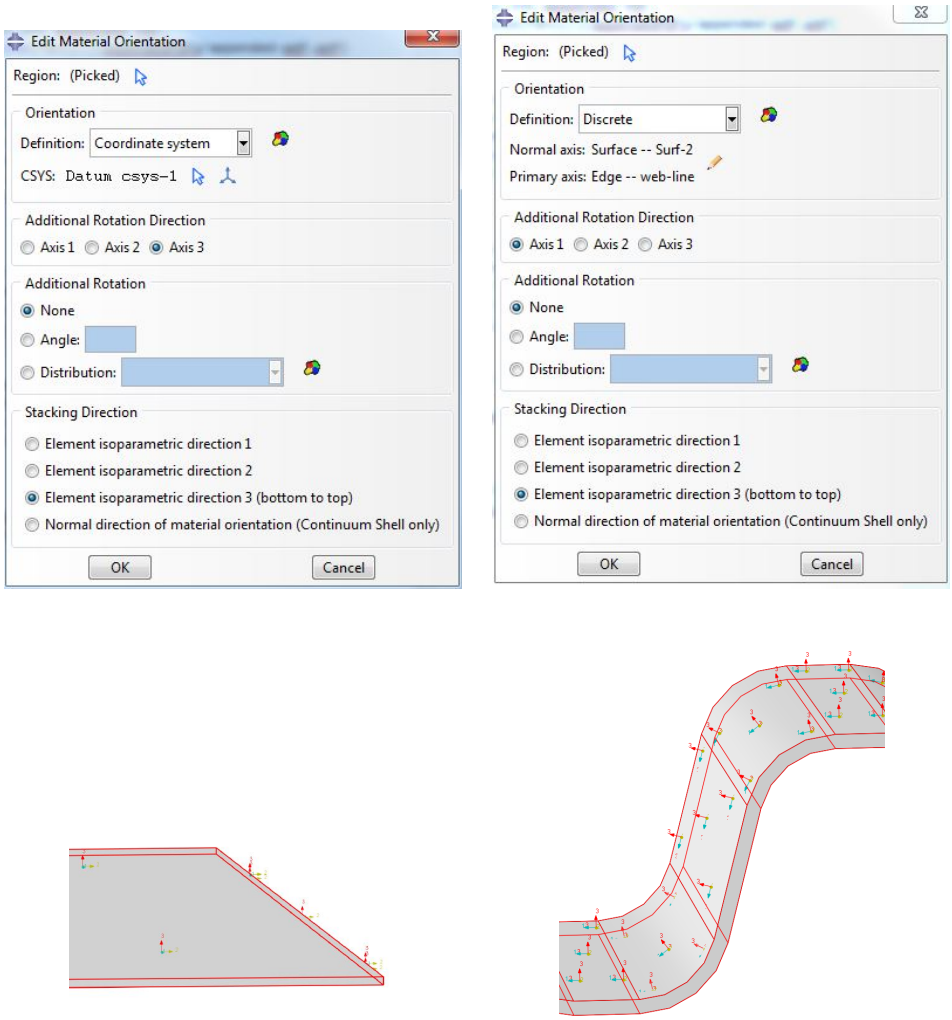

Figure C.2: Modeling of grain orientation of a floor with the orientation (∥-⊥-∥). To the left the face and to the right the corrugated core.

Assembly module: The parts are being assembled in the interaction point of the core and the face. For solid elements there is a "real thickness" and therefor easy to assembly

Step module: The steps are different depending on what analysis that is modeled.

- *Static, General* - used for the deflection caused by uniformly distributed load, deflection caused by 1 kN point load and the stresses.
- *Frequency, linear perturbation* - used for the fundamental frequency
- *Buckle, linear perturbation* - used for the buckling analyses

Interaction module: In this module the adhesive is modeled. This is made by *Create constraints - Tie - Surface* and then choosing the face as master surface and the interaction surface f_c as slave surface, see

Figure C.3. This constraints means that no relative motion between the two constrained parts will exist.

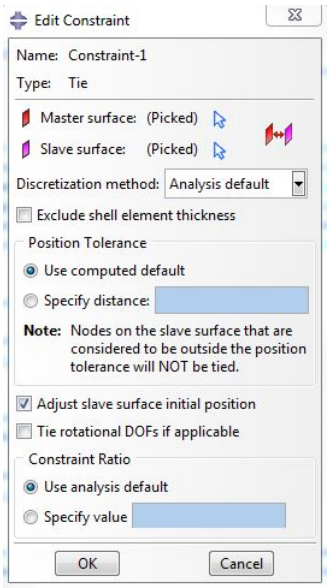

Figure C.3: Modeling the adhesive at the interaction point with a Tie - Constraint

Load module: The loads are created as pressure and gravity load by *Create load - Pressure and/or Gravity* loads that act on the surface are:

- *Preassure*: Imposed load 2 kN/m^2 and Installations 50 kg/m^2 - added for the deflection caused by uniformly distributed load, stresses and the buckling analyses.
- *Preassure*: Imposed load acting on a surface of 50x50 mm with a magnitude of 400 kN/m^2 - added for the deflection caused by 1 kN point load.
- *Gravity*: Self-weight with a magnitude of 9.81 m/s^2 - added for the deflection caused by uniformly distributed load, deflection caused by 1 kN point load, stresses and the buckling analyses.

For the fundamental frequency the installation load of 50 kg/m^2 is converted to a density and added to the density in the *Property module* for each part. This is calculated as a volume-ratio of the parts to distribute the load to the different parts. This is made because as a default in Abaqus you can not add any load when calculating the fundamental frequency and by doing this all the permanent load can be added when doing this analysis.

The floor is modeled as hard simply supported along all four edges. This is modeled by *Create Boundary Condition - Displacement/Rotation* and for giving it a zero vertical displacement and also a zero horizontal displacement parallel to the edge. For the edge with the corrugation the surfaces of the corrugation and the mid lines of the faces are chosen as regions for the boundary conditions. For the other edge, the one parallel to the corrugation extrusion, only the mid line of the faces is chosen as regions for the boundary condition.

Mesh: A convergence study is made and is never converging for the solid elements. Therefore the mesh i chosen to have the same size as for the shell elements, see Section C.2 and Figure C.4

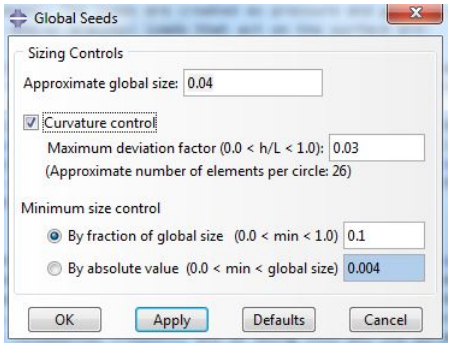

Figure C.4: Mesh size for the solid elements

C.2 Shell elements

Part module: The part were made as *3D Shell extrusion elements* for all the three parts, two faces and one corrugated core. The corrugated core were imported as a sketch from AutoCAD.

Property module: The material properties for each part were created with the material manager by using the *Density - Uniform* and *Elastic material - Lamina* as input, see Figure C.5. Every part is then added with a *Shell, Homogeneous* section type.

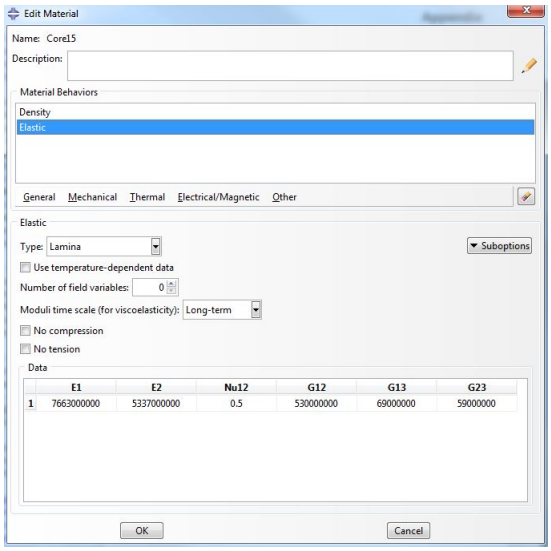

Figure C.5: Material properties input for the material C/C/C with a thickness of 15 mm

The grain orientation of each part is defined with the same method used for the faces for the solid elements, for both the faces and the core in shell elements.

Assembly module: The parts are being assembled in the interaction point of the core and the face. The shell elements are assembled with a distance between the core and the faces, this distance is half of the face thickness and half of the core thickness.

Step module: Same as for solid elements, see Section C.1.

Interaction module: Same as for solid elements, see Section C.1.

Load module: Same as for solid elements, see Section C.1. The regions picked for the boundary condition is for shell elements the corrugated line and the line of edge line of the faces.

Mesh: A convergence study is made and the results are converging with a approximate global size of 0.04 and a curvature control with maximum deviation factor of 0.03.

D Graphs for the selection process

In the selection process, when going from 320 cases to 20 cases, following graphs are used. In Section 7.2 the selection process is further explained. The graphs used in the selection process are organized in this Appendix after this order:

- Total height of all material combinations.
- All optimized variables, including the total height, for birch plywood as core material. First for the 4x6 floor and the for the 6x4 floor.
- All optimized variables, including the total height, for conifer plywood as core material. First for the 4x6 floor and the for the 6x4 floor.

The optimized variables on the y-axis are:

h_{tot}	Total height of the floor, [mm]
α_c	Inclination angle, [°]
V	Total volume of the floor, [m^3]
p	Half corrugation length, [mm]
t_f	Thickness of the face, [mm]
h_c	Height of the corrugation, [mm]
R_c	Curvature of the corrugation, [mm]
f_c	Length of the interaction surface, [mm]

Total height all material combinations

(B/B/B), 4x6 floor

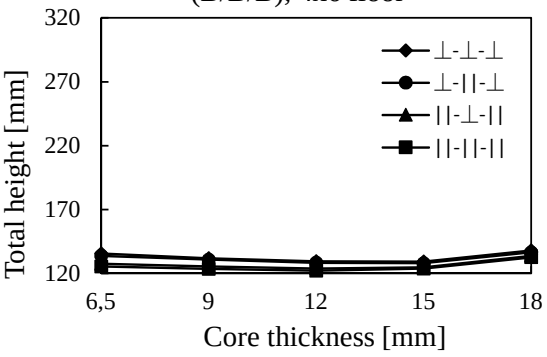

(B/B/B), 6x4 floor

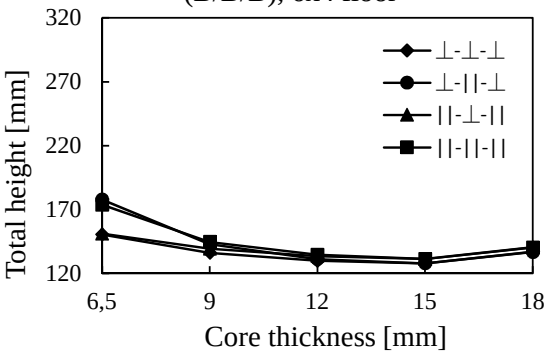

(C/B/C), 4x6 floor

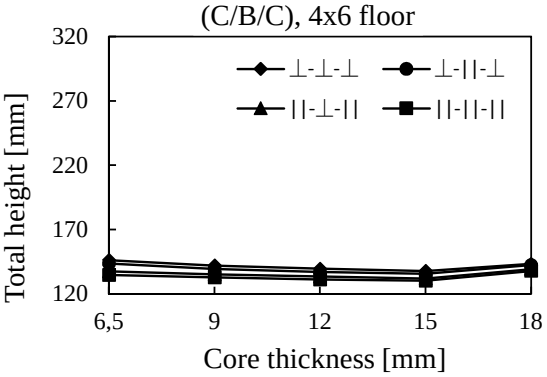

(C/B/C), 6x4 floor

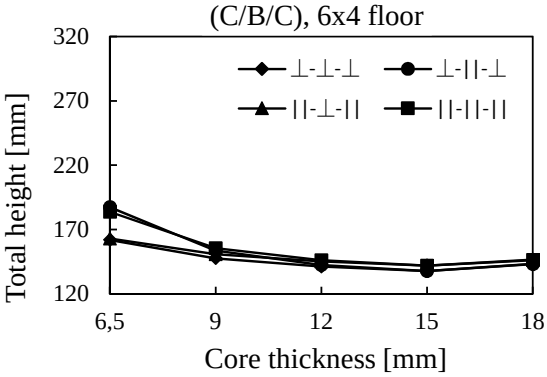

(K/B/K), 4x6 floor

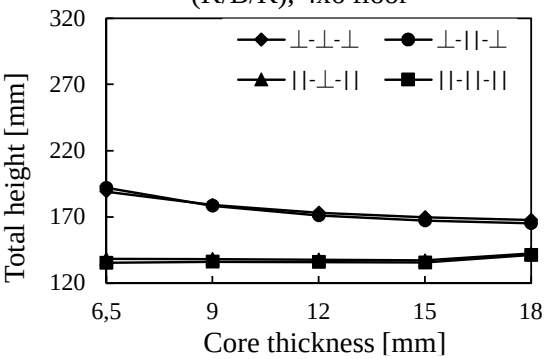

(K/B/K), 6x4 floor

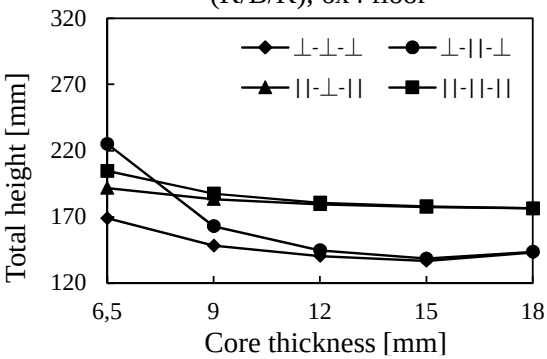

(M/B/M), 4x6 floor

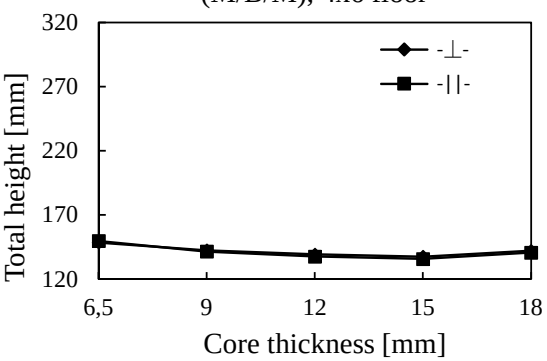

(M/B/M), 6x4 floor

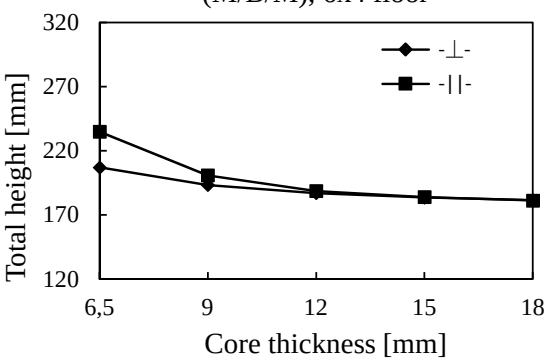

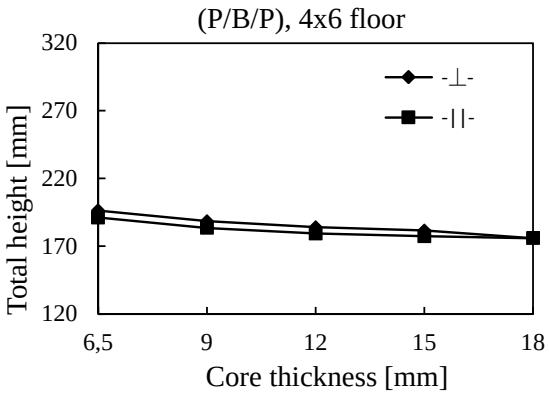
(P/B/P), 4x6 floor
Total height [mm]
320
270
220
170
120
6,5
9
12
15
18
Core thickness [mm]
-⊥-
-||-

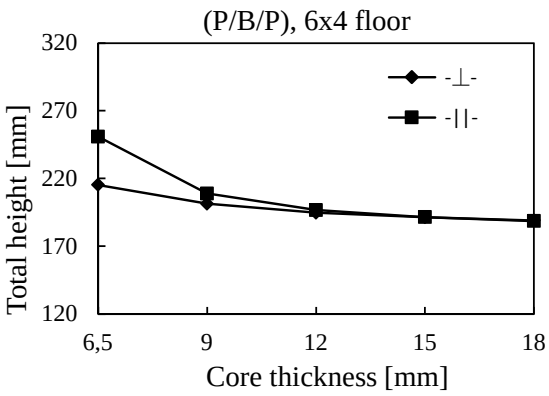
(P/B/P), 6x4 floor
Total height [mm]
320
270
220
170
120
6,5
9
12
15
18
Core thickness [mm]
-⊥-
-||-

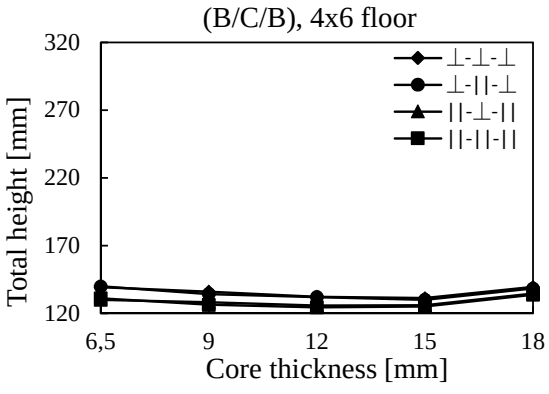
(B/C/B), 4x6 floor
Total height [mm]
320
270
220
170
120
6,5
9
12
15
18
Core thickness [mm]
⊥-⊥-⊥
⊥-||-⊥
||-⊥-||
||-||-||

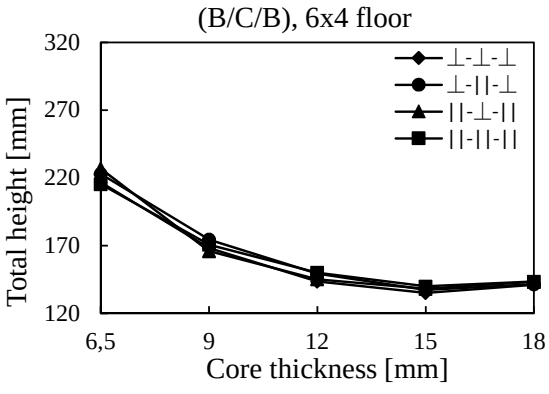
(B/C/B), 6x4 floor
Total height [mm]
320
270
220
170
120
6,5
9
12
15
18
Core thickness [mm]
⊥-⊥-⊥
⊥-||-⊥
||-⊥-||
||-||-||

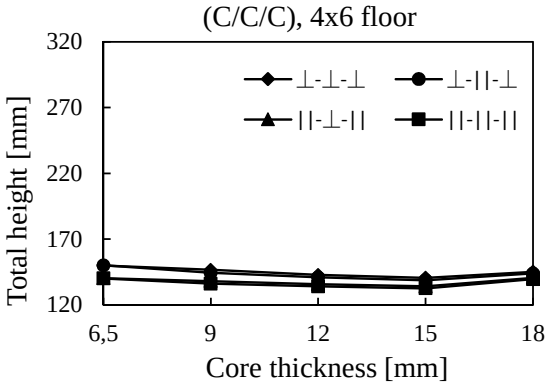
(C/C/C), 4x6 floor
Total height [mm]
320
270
220
170
120
6,5
9
12
15
18
Core thickness [mm]
⊥-⊥-⊥
⊥-||-⊥
||-⊥-||
||-||-||

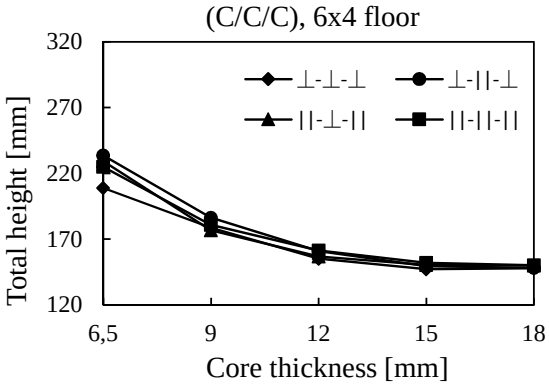
(C/C/C), 6x4 floor
Total height [mm]
320
270
220
170
120
6,5
9
12
15
18
Core thickness [mm]
⊥-⊥-⊥
⊥-||-⊥
||-⊥-||
||-||-||

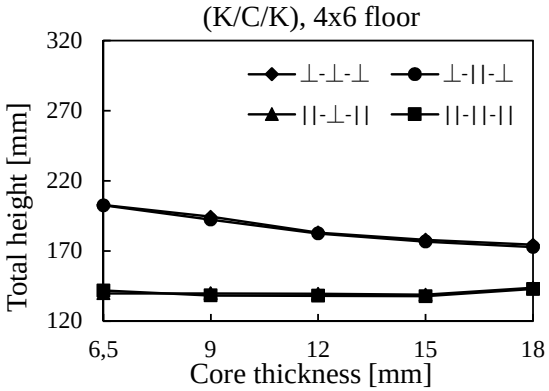
(K/C/K), 4x6 floor
Total height [mm]
320
270
220
170
120
6,5
9
12
15
18
Core thickness [mm]
⊥-⊥-⊥
⊥-||-⊥
||-⊥-||
||-||-||

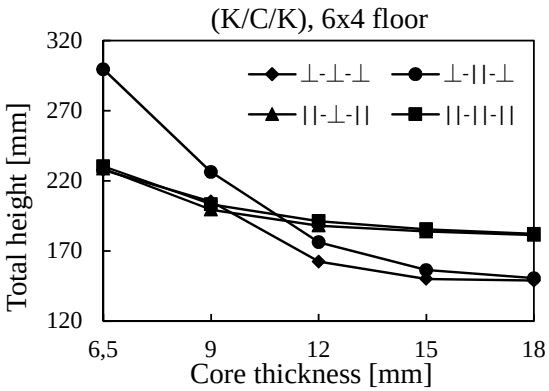
(K/C/K), 6x4 floor
Total height [mm]
320
270
220
170
120
6,5
9
12
15
18
Core thickness [mm]
⊥-⊥-⊥
⊥-||-⊥
||-⊥-||
||-||-||

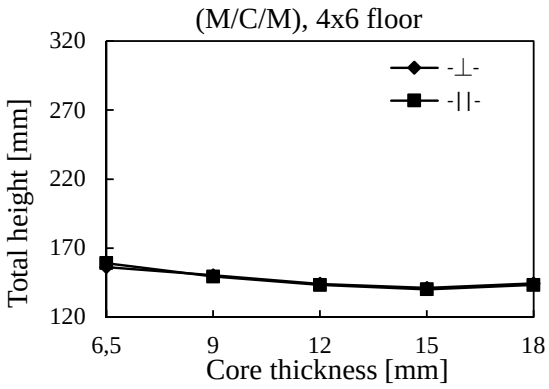
(M/C/M), 4x6 floor
Total height [mm]
320
270
220
170
120
6,5
9
12
15
18
Core thickness [mm]
-⊥-
-||-

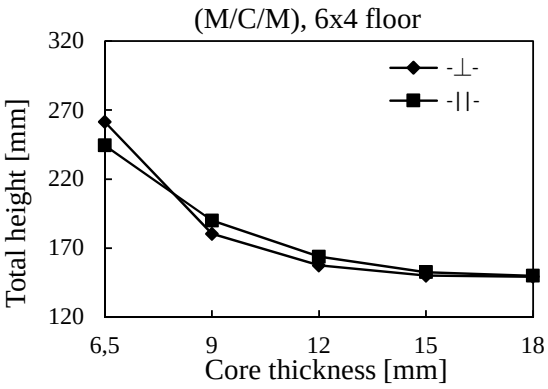
(M/C/M), 6x4 floor
Total height [mm]
320
270
220
170
120
6,5
9
12
15
18
Core thickness [mm]
-⊥-
-||-

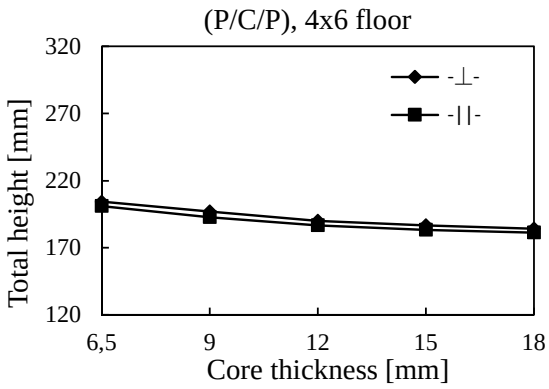
(P/C/P), 4x6 floor
Total height [mm]
320
270
220
170
120
6,5
9
12
15
18
Core thickness [mm]
-⊥-
-||-

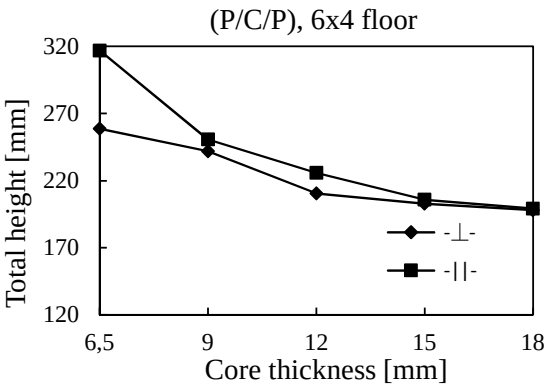
(P/C/P), 6x4 floor
Total height [mm]
320
270
220
170
120
6,5
9
12
15
18
Core thickness [mm]
-⊥-
-||-

4x6 Floor

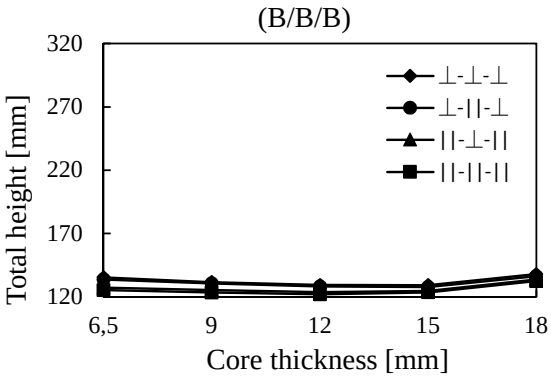
(B/B/B)
Total height [mm]
320
270
220
170
120
⊥-⊥-⊥
⊥-||-⊥
||-⊥-||
||-||-||
6,5
9
12
15
18
Core thickness [mm]

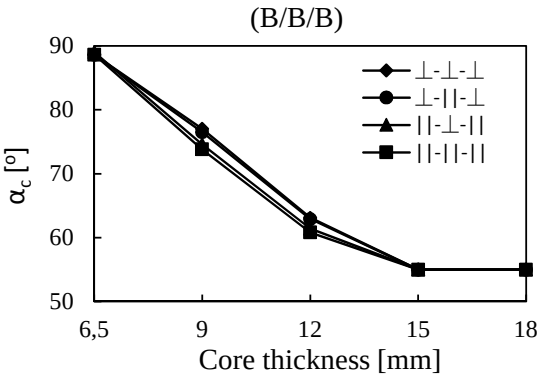
(B/B/B)
α_c [°]
90
80
70
60
50
⊥-⊥-⊥
⊥-||-⊥
||-⊥-||
||-||-||
6,5
9
12
15
18
Core thickness [mm]

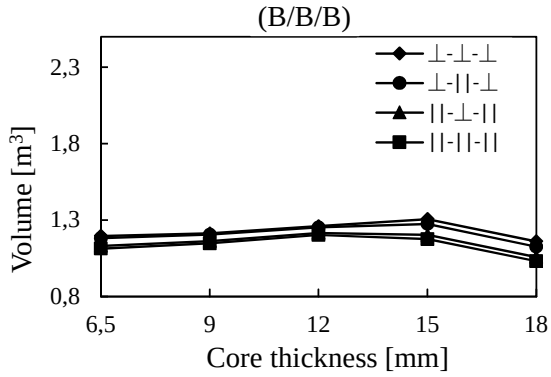
(B/B/B)
Volume [m³]
2,3
1,8
1,3
0,8
⊥-⊥-⊥
⊥-||-⊥
||-⊥-||
||-||-||
6,5
9
12
15
18
Core thickness [mm]

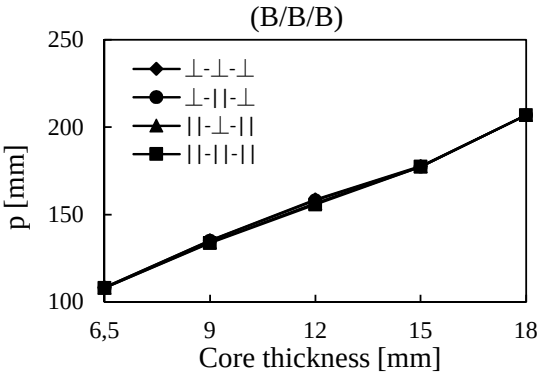
(B/B/B)
p [mm]
250
200
150
100
⊥-⊥-⊥
⊥-||-⊥
||-⊥-||
||-||-||
6,5
9
12
15
18
Core thickness [mm]

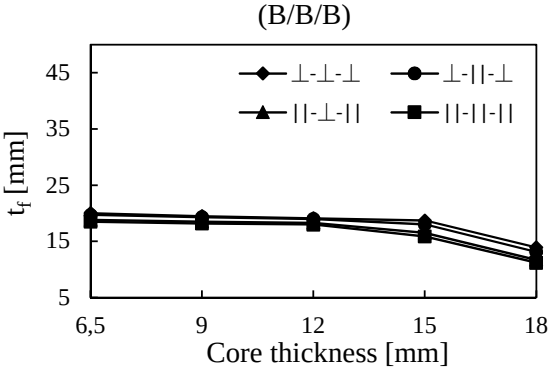
(B/B/B)
t_f [mm]
45
35
25
15
5
⊥-⊥-⊥
⊥-||-⊥
||-⊥-||
||-||-||
6,5
9
12
15
18
Core thickness [mm]

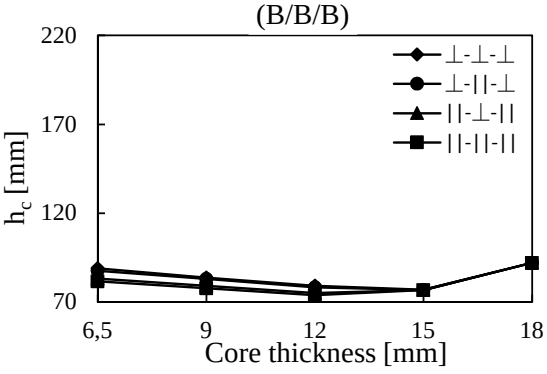
(B/B/B)
h_c [mm]
220
170
120
70
⊥-⊥-⊥
⊥-||-⊥
||-⊥-||
||-||-||
6,5
9
12
15
18
Core thickness [mm]

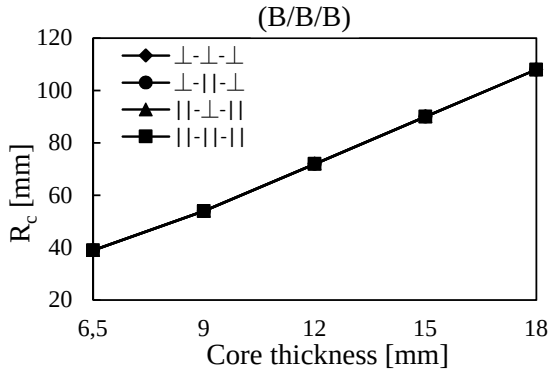
(B/B/B)
R_c [mm]
120
100
80
60
40
20
⊥-⊥-⊥
⊥-||-⊥
||-⊥-||
||-||-||
6,5
9
12
15
18
Core thickness [mm]

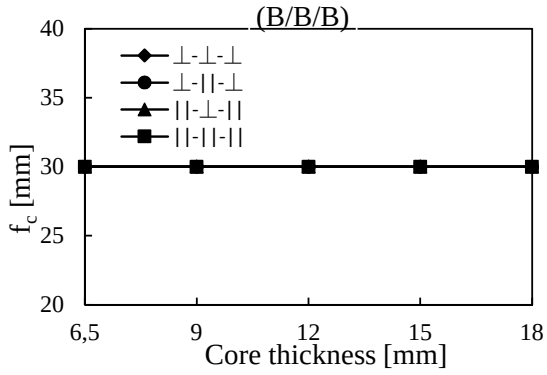
(B/B/B)
f_c [mm]
40
35
30
25
20
⊥-⊥-⊥
⊥-||-⊥
||-⊥-||
||-||-||
6,5
9
12
15
18
Core thickness [mm]

6x4 Floor

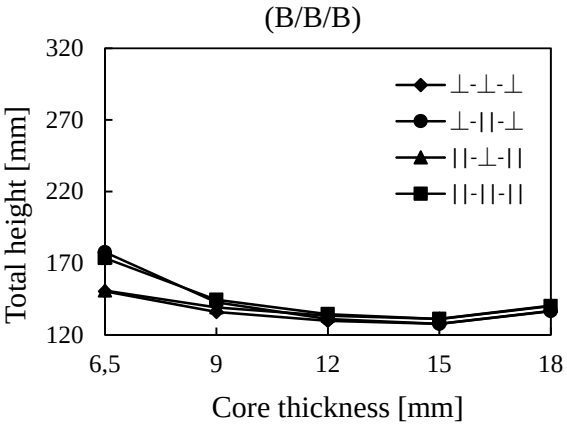
(B/B/B)
Total height [mm]
320
270
220
170
120
6,5
9
12
15
18
Core thickness [mm]
⊥-⊥-⊥
⊥-||-⊥
||-⊥-||
||-||-||

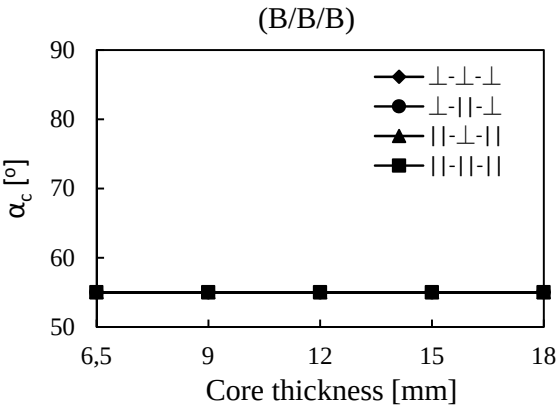
(B/B/B)
α_c [º]
90
80
70
60
50
6,5
9
12
15
18
Core thickness [mm]
⊥-⊥-⊥
⊥-||-⊥
||-⊥-||
||-||-||

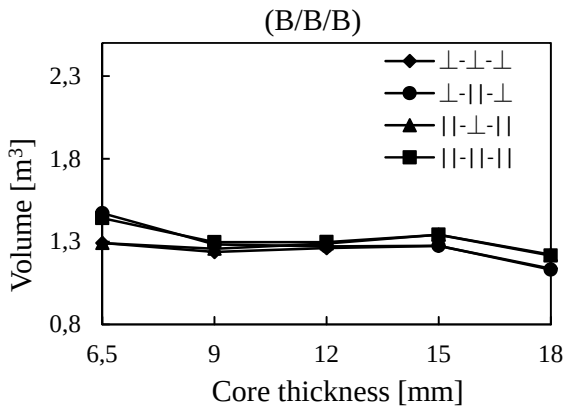
(B/B/B)
Volume [m^3]
2,3
1,8
1,3
0,8
6,5
9
12
15
18
Core thickness [mm]
⊥-⊥-⊥
⊥-||-⊥
||-⊥-||
||-||-||

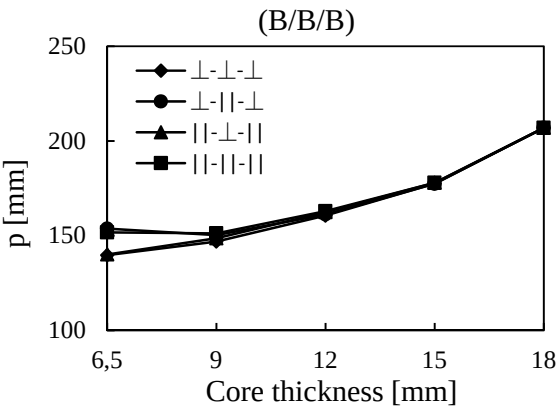
(B/B/B)
p [mm]
250
200
150
100
6,5
9
12
15
18
Core thickness [mm]
⊥-⊥-⊥
⊥-||-⊥
||-⊥-||
||-||-||

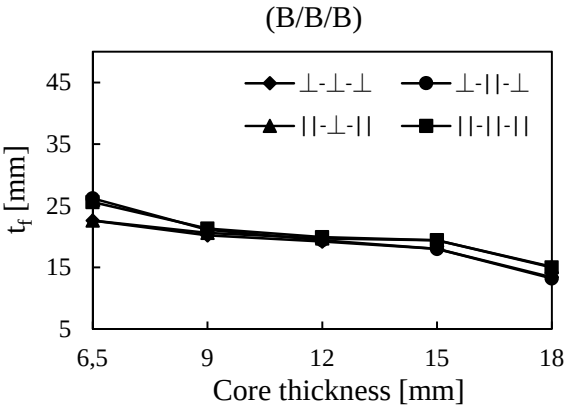
(B/B/B)
t_f [mm]
45
35
25
15
5
6,5
9
12
15
18
Core thickness [mm]
⊥-⊥-⊥
⊥-||-⊥
||-⊥-||
||-||-||

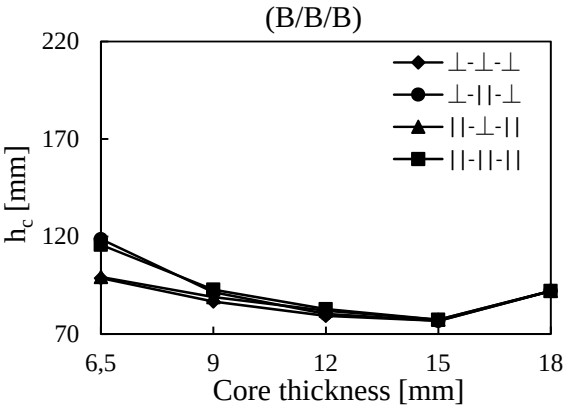
(B/B/B)
h_c [mm]
220
170
120
70
6,5
9
12
15
18
Core thickness [mm]
⊥-⊥-⊥
⊥-||-⊥
||-⊥-||
||-||-||

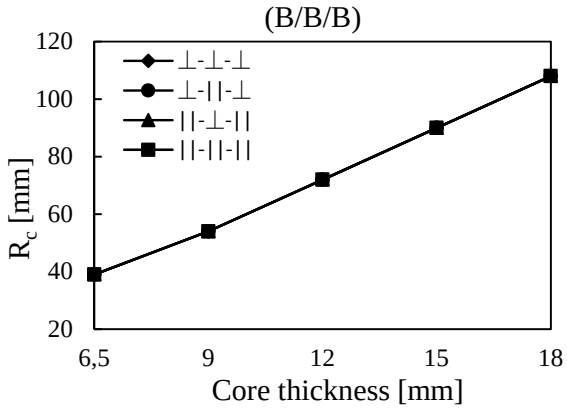
(B/B/B)
R_c [mm]
120
100
80
60
40
20
6,5
9
12
15
18
Core thickness [mm]
⊥-⊥-⊥
⊥-||-⊥
||-⊥-||
||-||-||

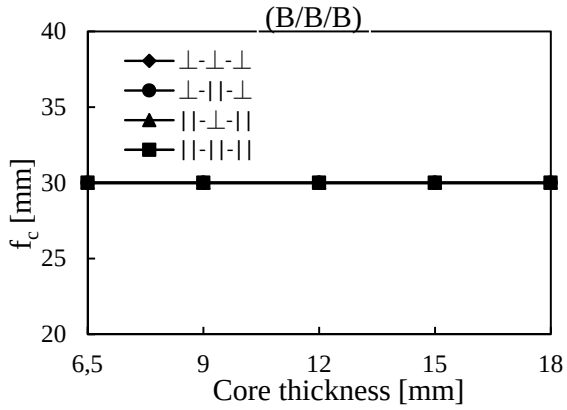
(B/B/B)
f_c [mm]
40
35
30
25
20
6,5
9
12
15
18
Core thickness [mm]
⊥-⊥-⊥
⊥-||-⊥
||-⊥-||
||-||-||

4x6 Floor

(C/B/C)

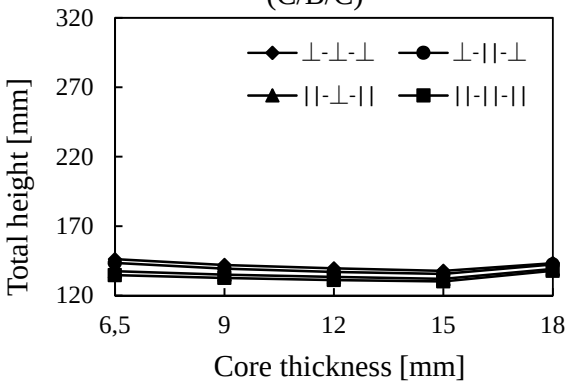

(C/B/C)

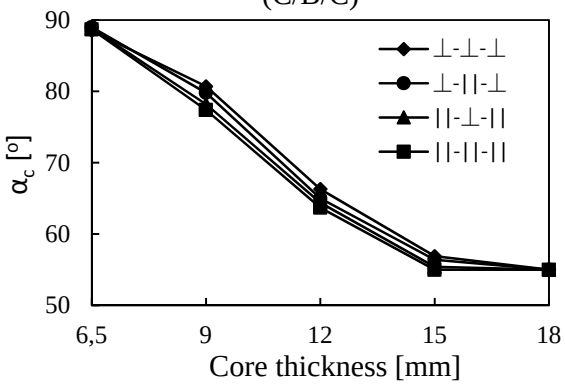

(C/B/C)

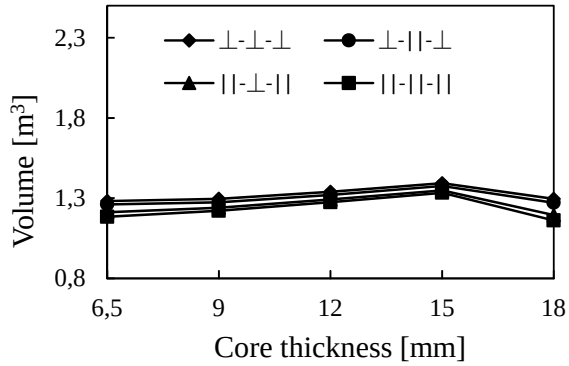

(C/B/C)

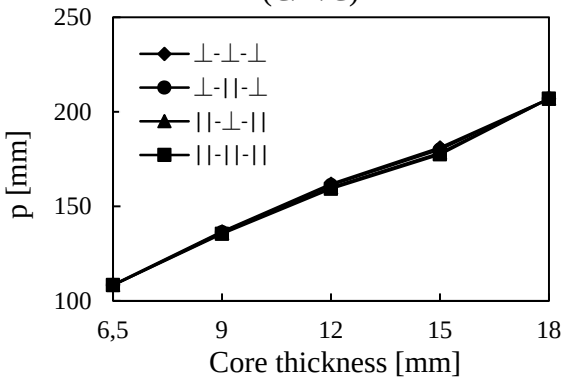

(C/B/C)

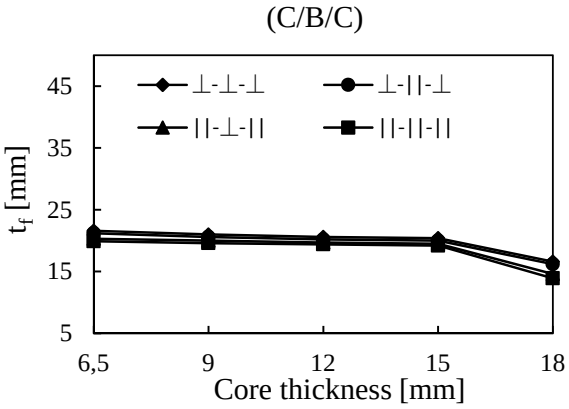

(C/B/C)

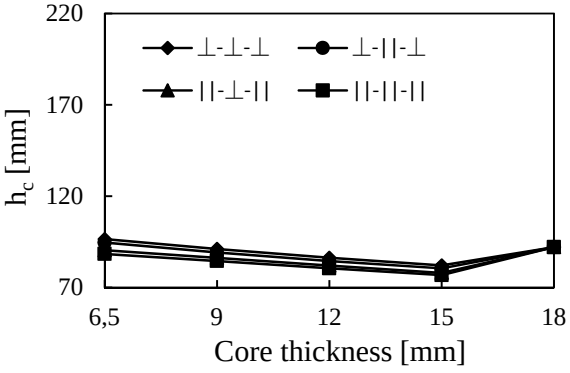

(C/B/C)

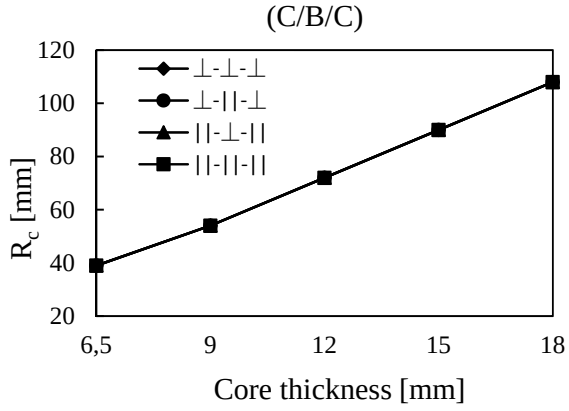

(C/B/C)

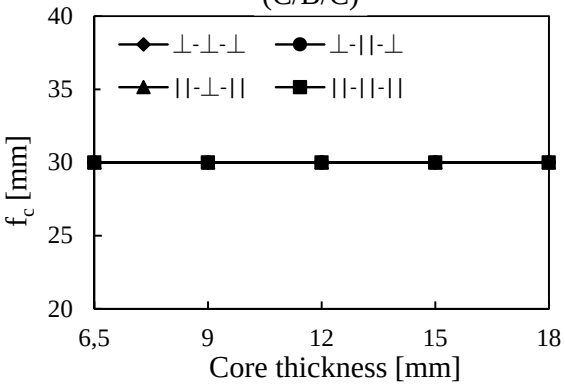

6x4 Floor

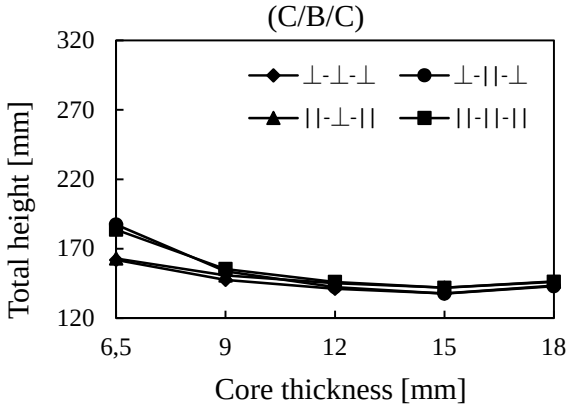
(C/B/C)
Total height [mm]
320
270
220
170
120
6,5
9
12
15
18
Core thickness [mm]
⊥-⊥-⊥
⊥-||-⊥
||-⊥-||
||-||-||

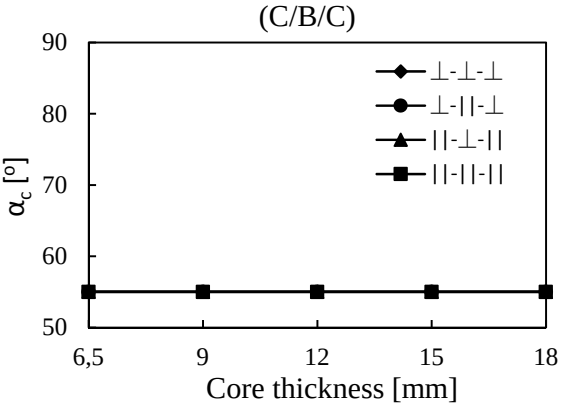
(C/B/C)
α_c [°]
90
80
70
60
50
6,5
9
12
15
18
Core thickness [mm]
⊥-⊥-⊥
⊥-||-⊥
||-⊥-||
||-||-||

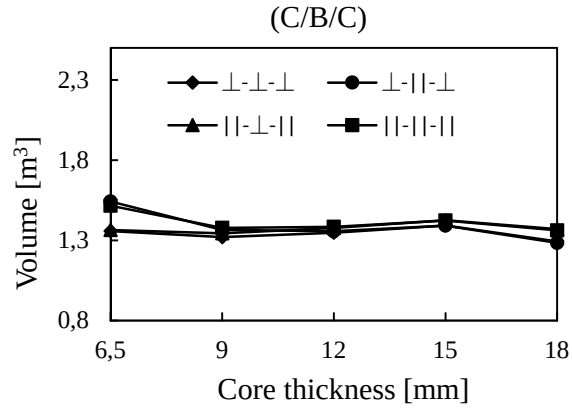
(C/B/C)
Volume [m³]
2,3
1,8
1,3
0,8
6,5
9
12
15
18
Core thickness [mm]
⊥-⊥-⊥
⊥-||-⊥
||-⊥-||
||-||-||

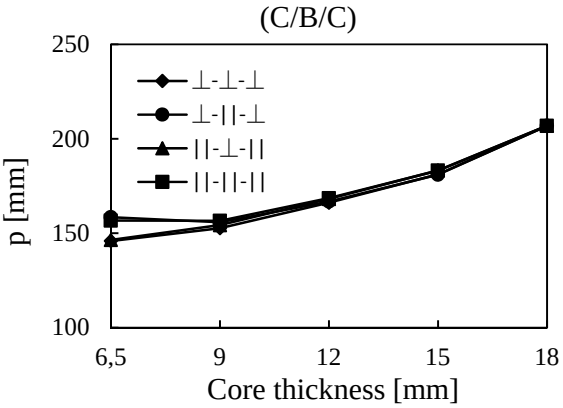
(C/B/C)
p [mm]
250
200
150
100
6,5
9
12
15
18
Core thickness [mm]
⊥-⊥-⊥
⊥-||-⊥
||-⊥-||
||-||-||

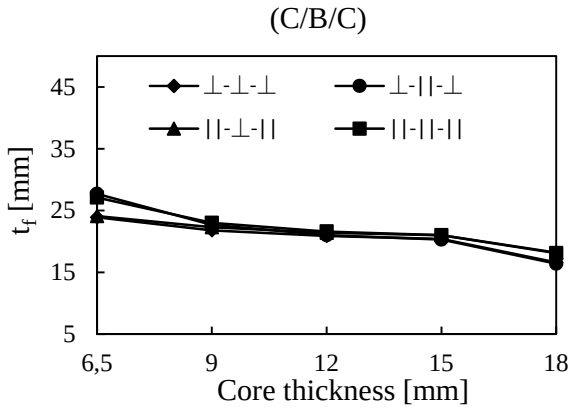
(C/B/C)
t_f [mm]
45
35
25
15
5
6,5
9
12
15
18
Core thickness [mm]
⊥-⊥-⊥
⊥-||-⊥
||-⊥-||
||-||-||

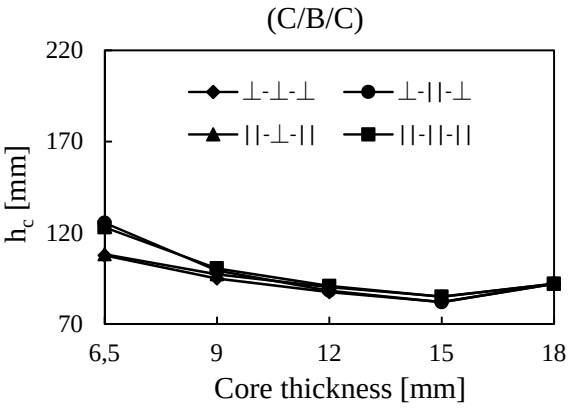
(C/B/C)
h_c [mm]
220
170
120
70
6,5
9
12
15
18
Core thickness [mm]
⊥-⊥-⊥
⊥-||-⊥
||-⊥-||
||-||-||

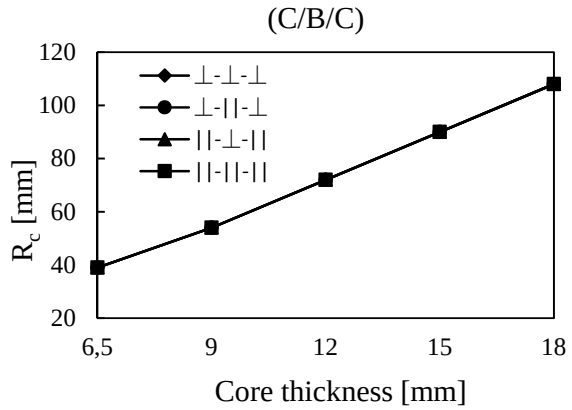
(C/B/C)
R_c [mm]
120
100
80
60
40
20
6,5
9
12
15
18
Core thickness [mm]
⊥-⊥-⊥
⊥-||-⊥
||-⊥-||
||-||-||

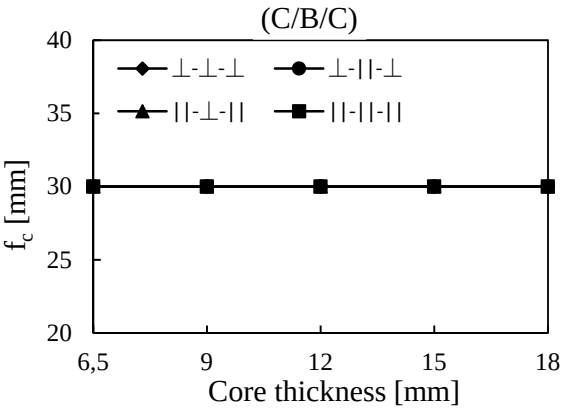
(C/B/C)
f_c [mm]
40
35
30
25
20
6,5
9
12
15
18
Core thickness [mm]
⊥-⊥-⊥
⊥-||-⊥
||-⊥-||
||-||-||

4x6 Floor

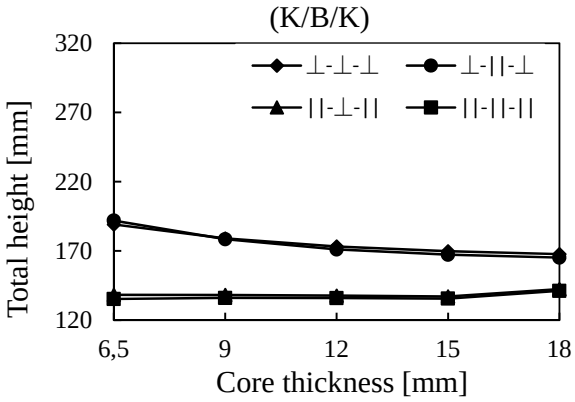
(K/B/K)
Total height [mm]
320
270
220
170
120
⊥-⊥-⊥
⊥-||-⊥
||-⊥-||
||-||-||
6,5
9
12
15
18
Core thickness [mm]

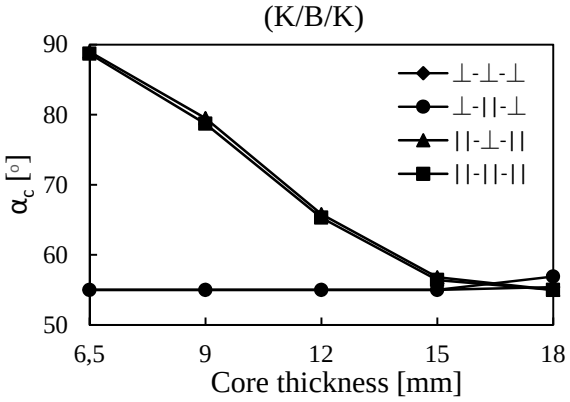
(K/B/K)
α_c [°]
90
80
70
60
50
⊥-⊥-⊥
⊥-||-⊥
||-⊥-||
||-||-||
6,5
9
12
15
18
Core thickness [mm]

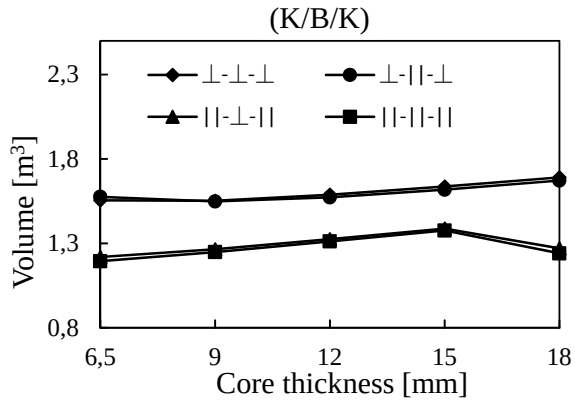
(K/B/K)
Volume [m³]
2,3
1,8
1,3
0,8
⊥-⊥-⊥
⊥-||-⊥
||-⊥-||
||-||-||
6,5
9
12
15
18
Core thickness [mm]

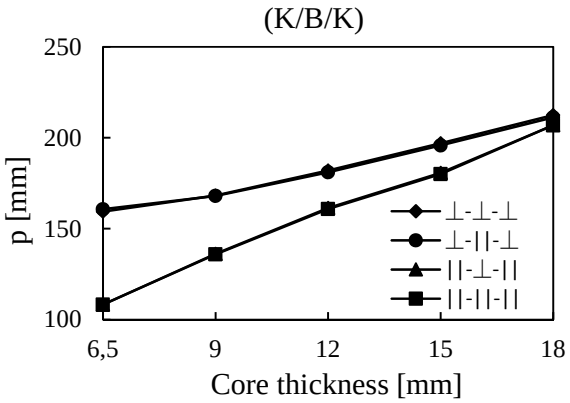
(K/B/K)
p [mm]
250
200
150
100
⊥-⊥-⊥
⊥-||-⊥
||-⊥-||
||-||-||
6,5
9
12
15
18
Core thickness [mm]

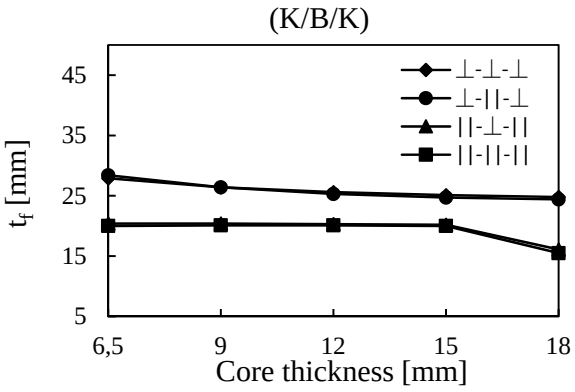
(K/B/K)
t_f [mm]
45
35
25
15
5
⊥-⊥-⊥
⊥-||-⊥
||-⊥-||
||-||-||
6,5
9
12
15
18
Core thickness [mm]

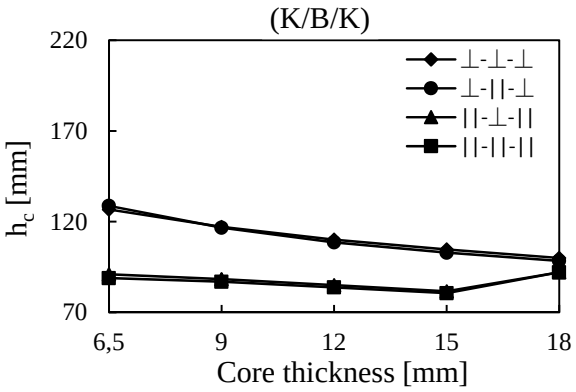
(K/B/K)
h_c [mm]
220
170
120
70
⊥-⊥-⊥
⊥-||-⊥
||-⊥-||
||-||-||
6,5
9
12
15
18
Core thickness [mm]

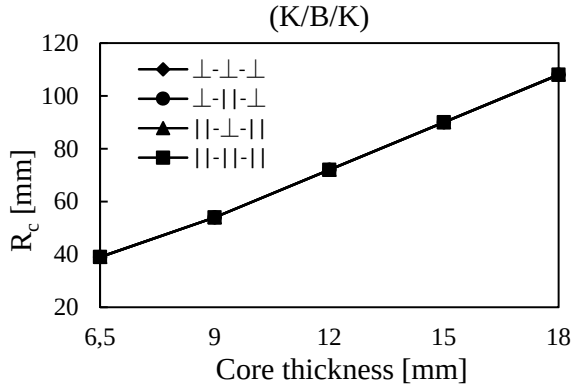
(K/B/K)
R_c [mm]
120
100
80
60
40
20
⊥-⊥-⊥
⊥-||-⊥
||-⊥-||
||-||-||
6,5
9
12
15
18
Core thickness [mm]

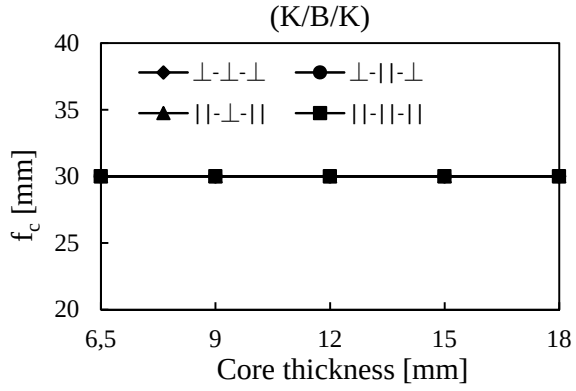
(K/B/K)
f_c [mm]
40
35
30
25
20
⊥-⊥-⊥
⊥-||-⊥
||-⊥-||
||-||-||
6,5
9
12
15
18
Core thickness [mm]

6x4 Floor

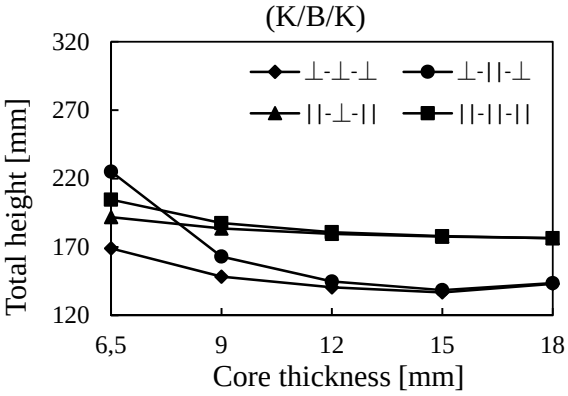
(K/B/K)
Total height [mm]
320
270
220
170
120
⊥-⊥-⊥
⊥-||-⊥
||-⊥-||
||-||-||
6,5
9
12
15
18
Core thickness [mm]

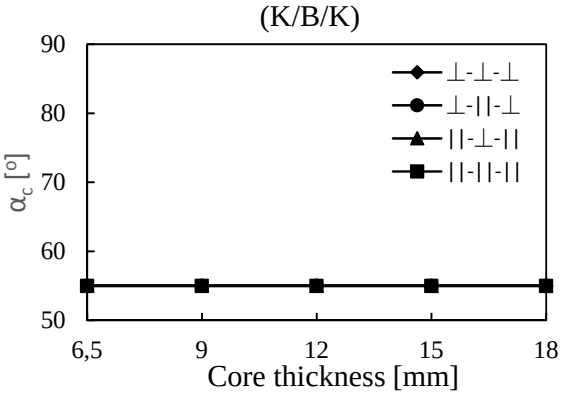
(K/B/K)
α_c [°]
90
80
70
60
50
⊥-⊥-⊥
⊥-||-⊥
||-⊥-||
||-||-||
6,5
9
12
15
18
Core thickness [mm]

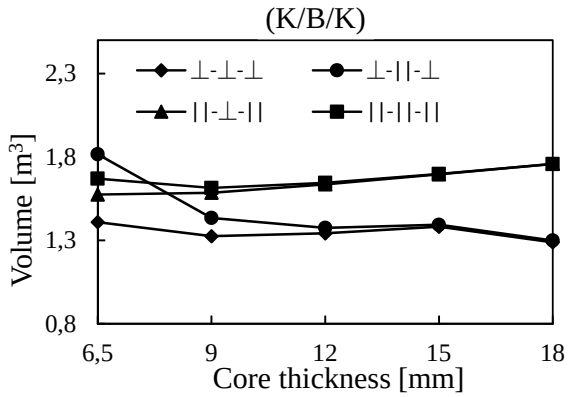
(K/B/K)
Volume [m³]
2,3
1,8
1,3
0,8
⊥-⊥-⊥
⊥-||-⊥
||-⊥-||
||-||-||
6,5
9
12
15
18
Core thickness [mm]

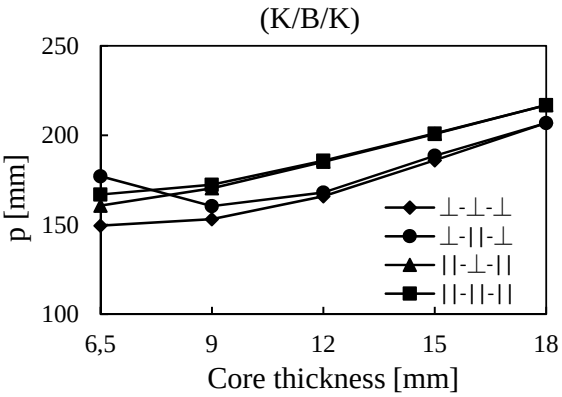
(K/B/K)
p [mm]
250
200
150
100
⊥-⊥-⊥
⊥-||-⊥
||-⊥-||
||-||-||
6,5
9
12
15
18
Core thickness [mm]

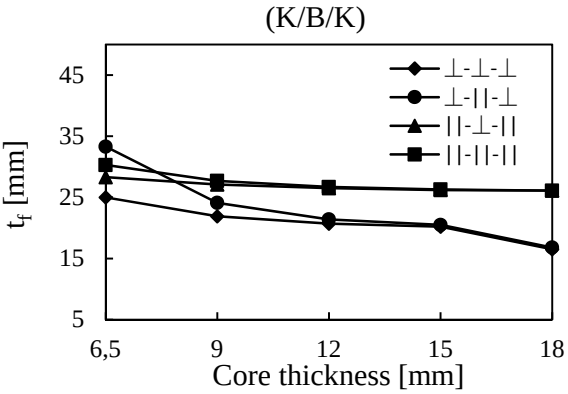
(K/B/K)
t_f [mm]
45
35
25
15
5
⊥-⊥-⊥
⊥-||-⊥
||-⊥-||
||-||-||
6,5
9
12
15
18
Core thickness [mm]

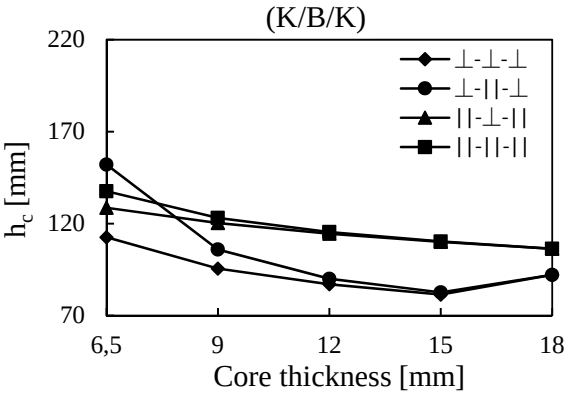
(K/B/K)
h_c [mm]
220
170
120
70
⊥-⊥-⊥
⊥-||-⊥
||-⊥-||
||-||-||
6,5
9
12
15
18
Core thickness [mm]

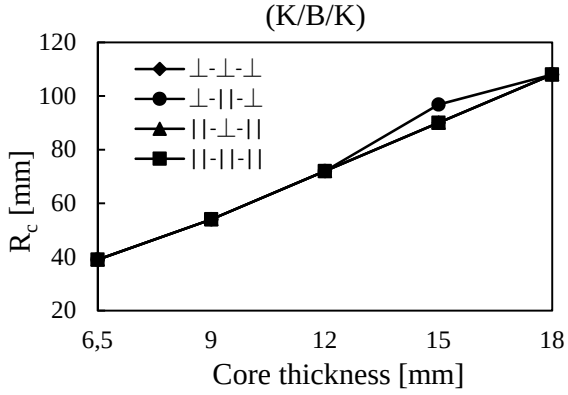
(K/B/K)
R_c [mm]
120
100
80
60
40
20
⊥-⊥-⊥
⊥-||-⊥
||-⊥-||
||-||-||
6,5
9
12
15
18
Core thickness [mm]

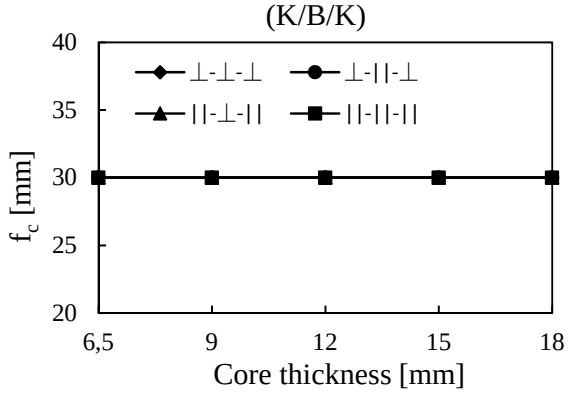
(K/B/K)
f_c [mm]
40
35
30
25
20
⊥-⊥-⊥
⊥-||-⊥
||-⊥-||
||-||-||
6,5
9
12
15
18
Core thickness [mm]

4x6 Floor

(M/B/M)

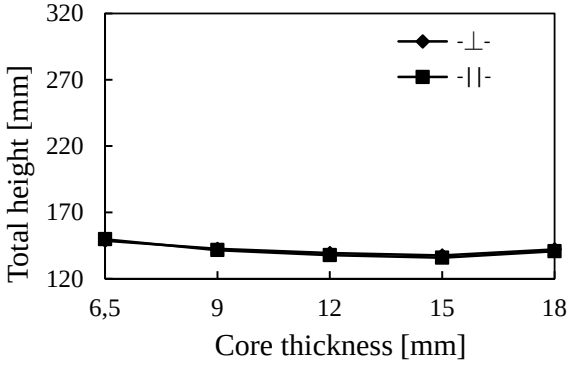

(M/B/M)

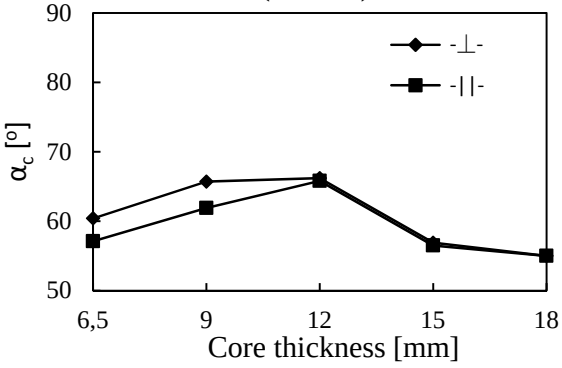

(M/B/M)

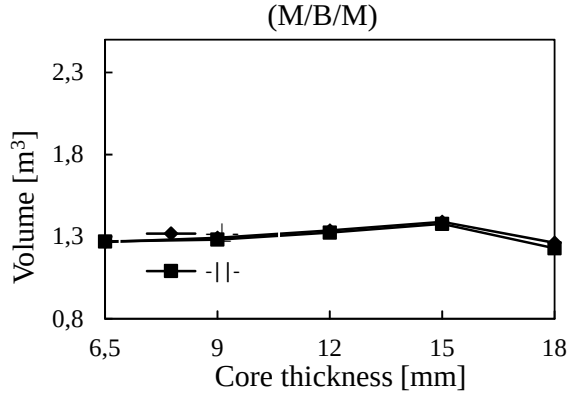

(M/B/M)

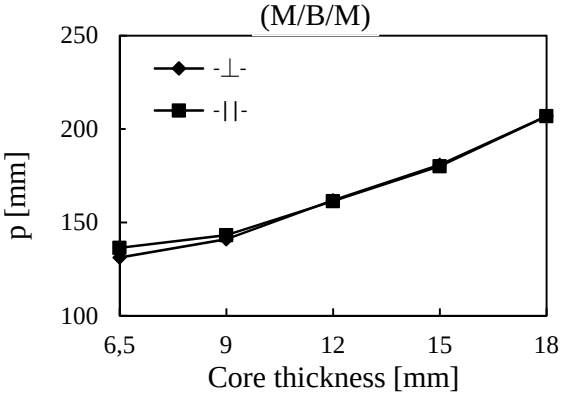

(M/B/M)

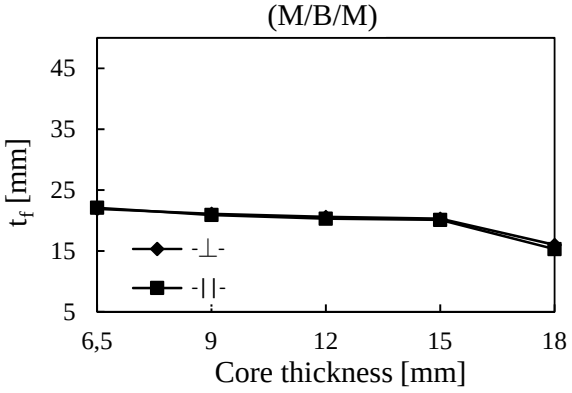

(M/B/M)

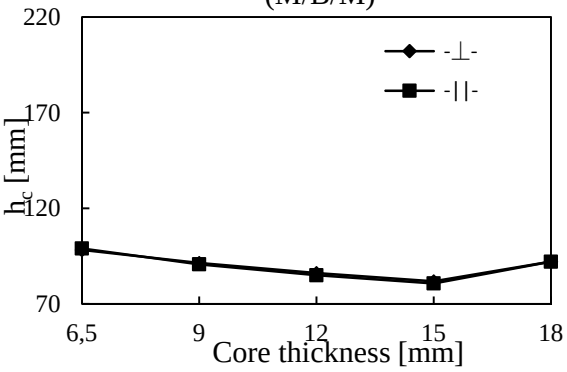

(M/B/M)

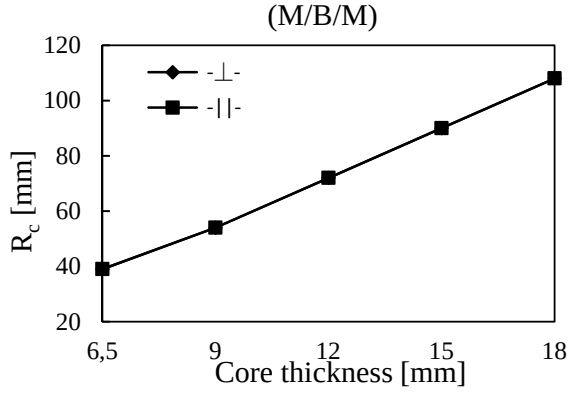

(M/B/M)

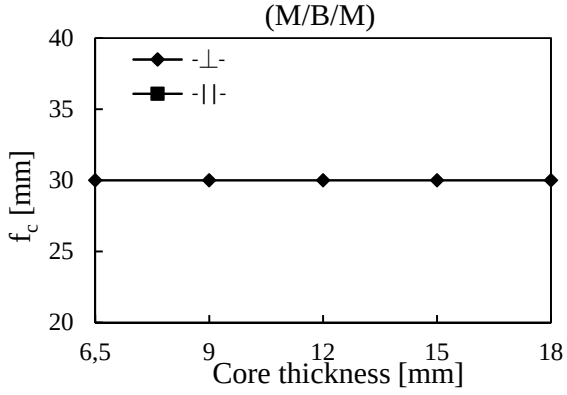

6x4 Floor

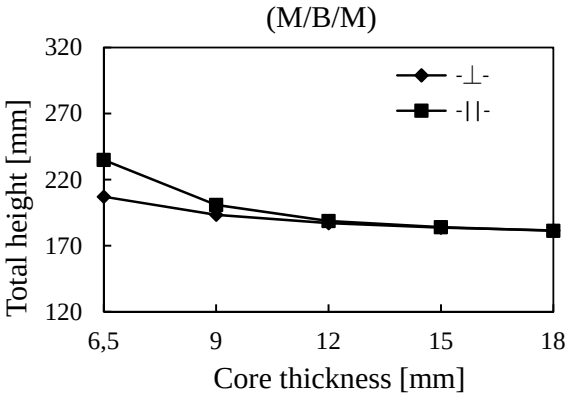
(M/B/M)
Total height [mm]
320
270
220
170
120
-⊥-
-||-
6,5
9
12
15
18
Core thickness [mm]

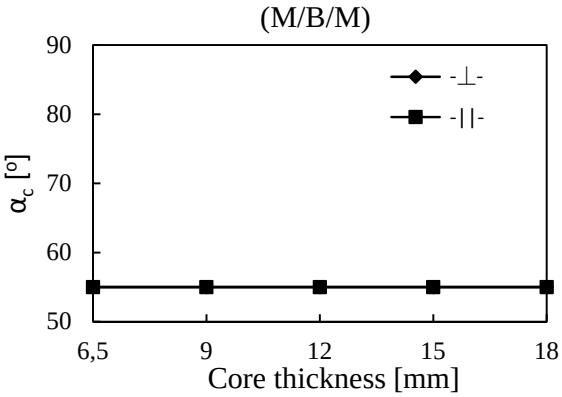
(M/B/M)
α_c [º]
90
80
70
60
50
-⊥-
-||-
6,5
9
12
15
18
Core thickness [mm]

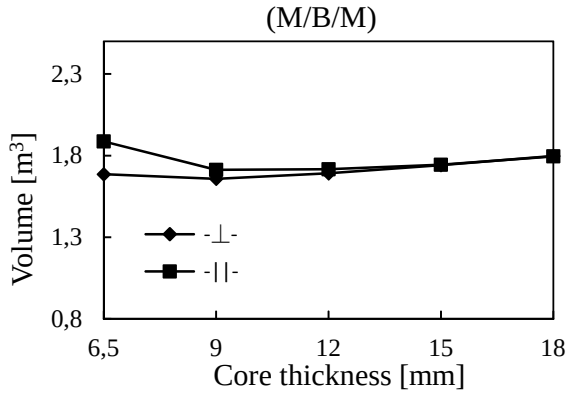
(M/B/M)
Volume [m^3]
2,3
1,8
1,3
0,8
-⊥-
-||-
6,5
9
12
15
18
Core thickness [mm]

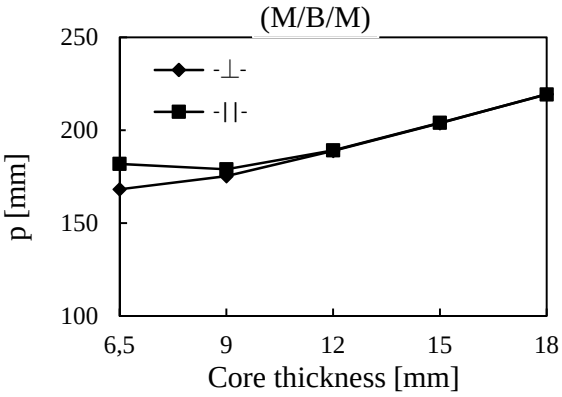
(M/B/M)
p [mm]
250
200
150
100
-⊥-
-||-
6,5
9
12
15
18
Core thickness [mm]

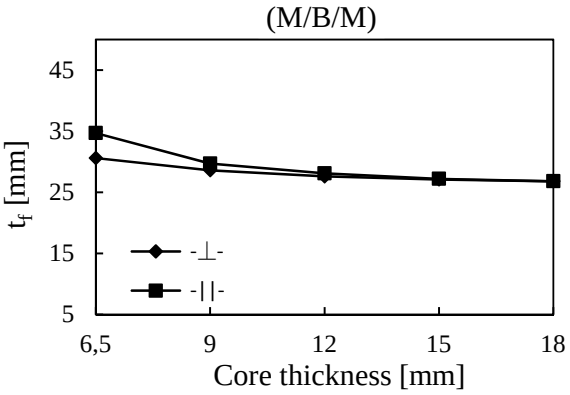
(M/B/M)
t_f [mm]
45
35
25
15
5
-⊥-
-||-
6,5
9
12
15
18
Core thickness [mm]

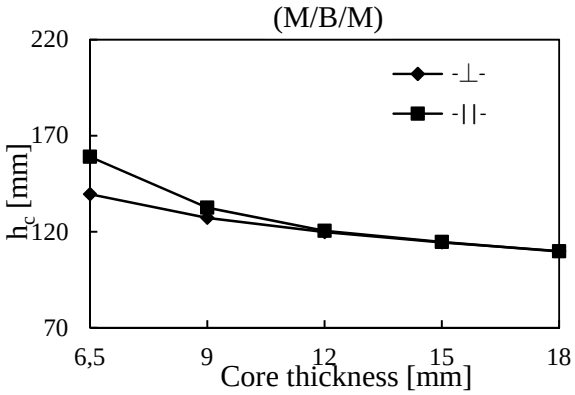
(M/B/M)
h_c [mm]
220
170
120
70
-⊥-
-||-
6,5
9
12
15
18
Core thickness [mm]

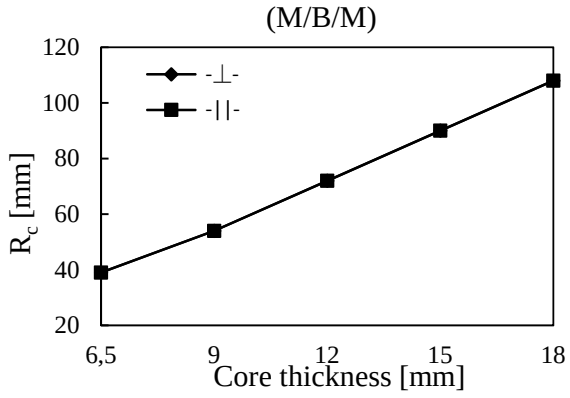
(M/B/M)
R_c [mm]
120
100
80
60
40
20
-⊥-
-||-
6,5
9
12
15
18
Core thickness [mm]

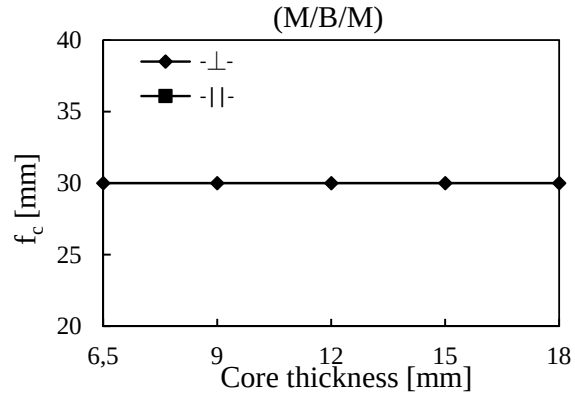
(M/B/M)
f_c [mm]
40
35
30
25
20
-⊥-
-||-
6,5
9
12
15
18
Core thickness [mm]

4x6 Floor

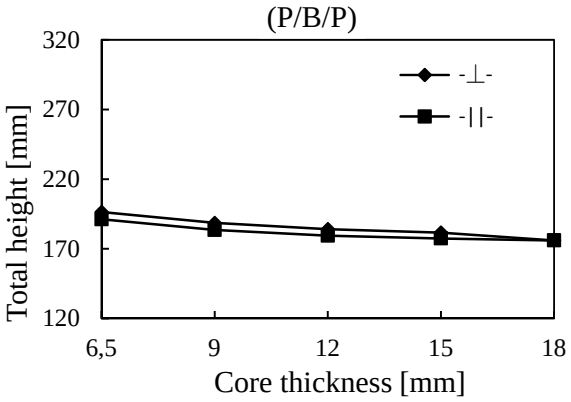
(P/B/P)
Total height [mm]
320
270
220
170
120
-⊥-
-||-
6,5
9
12
15
18
Core thickness [mm]

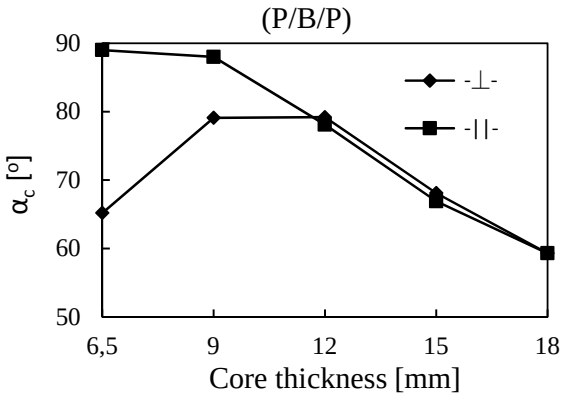
(P/B/P)
α_c [º]
90
80
70
60
50
-⊥-
-||-
6,5
9
12
15
18
Core thickness [mm]

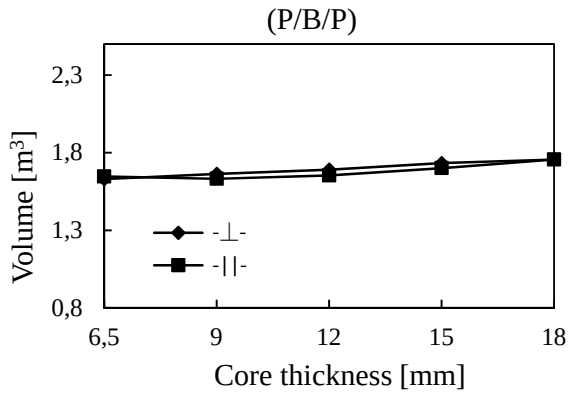
(P/B/P)
Volume [m³]
2,3
1,8
1,3
0,8
-⊥-
-||-
6,5
9
12
15
18
Core thickness [mm]

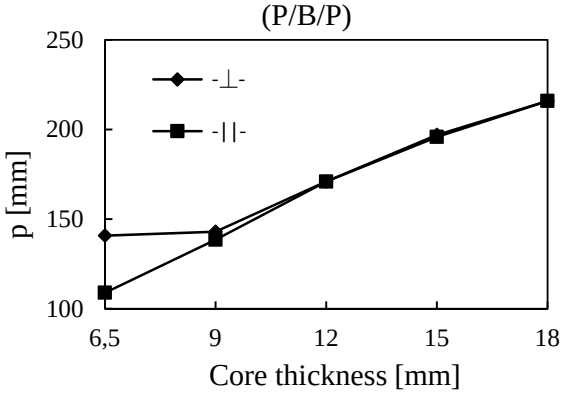
(P/B/P)
p [mm]
250
200
150
100
-⊥-
-||-
6,5
9
12
15
18
Core thickness [mm]

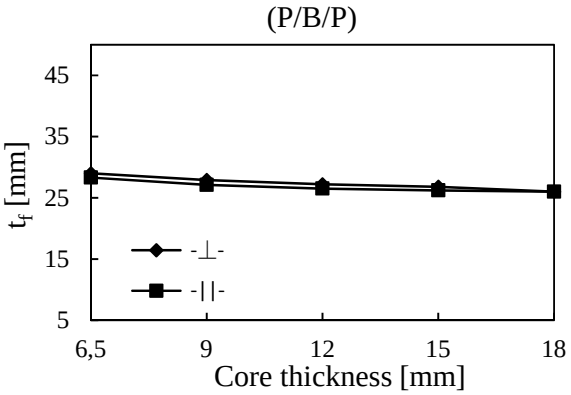
(P/B/P)
t_f [mm]
45
35
25
15
5
-⊥-
-||-
6,5
9
12
15
18
Core thickness [mm]

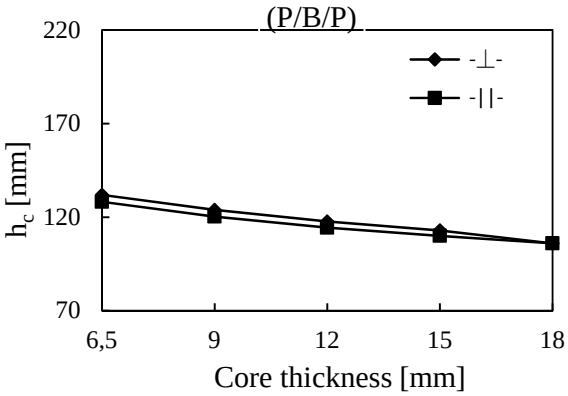
(P/B/P)
h_c [mm]
220
170
120
70
-⊥-
-||-
6,5
9
12
15
18
Core thickness [mm]

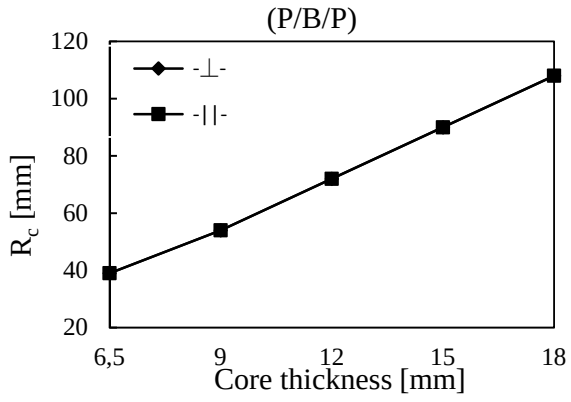
(P/B/P)
R_c [mm]
120
100
80
60
40
20
-⊥-
-||-
6,5
9
12
15
18
Core thickness [mm]

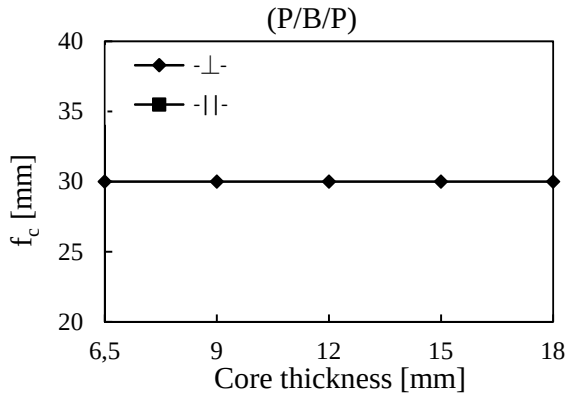
(P/B/P)
f_c [mm]
40
35
30
25
20
-⊥-
-||-
6,5
9
12
15
18
Core thickness [mm]

6x4 Floor

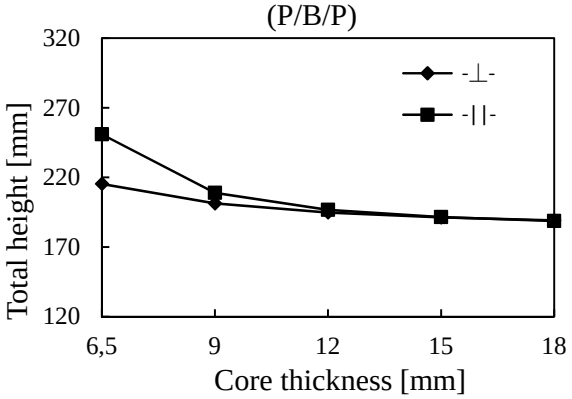
(P/B/P)
Total height [mm]
320
270
220
170
120
-⊥-
-||-
6,5
9
12
15
18
Core thickness [mm]

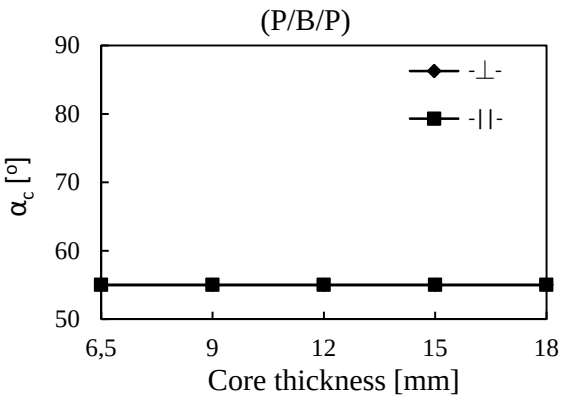
(P/B/P)
α_c [°]
90
80
70
60
50
-⊥-
-||-
6,5
9
12
15
18
Core thickness [mm]

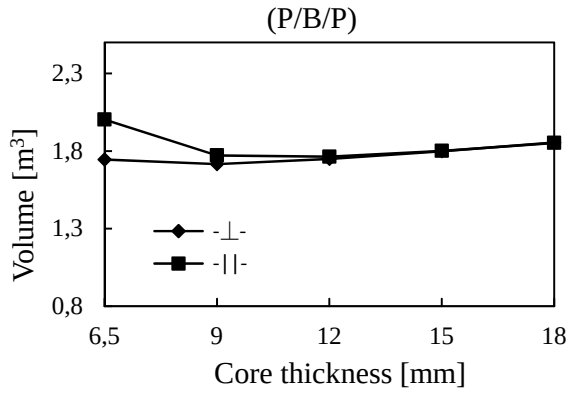
(P/B/P)
Volume [m³]
2,3
1,8
1,3
0,8
-⊥-
-||-
6,5
9
12
15
18
Core thickness [mm]

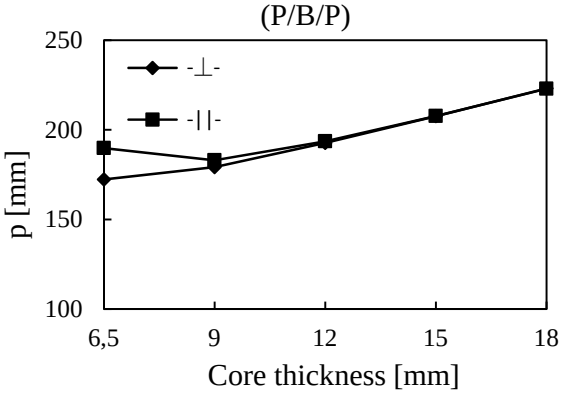
(P/B/P)
p [mm]
250
200
150
100
-⊥-
-||-
6,5
9
12
15
18
Core thickness [mm]

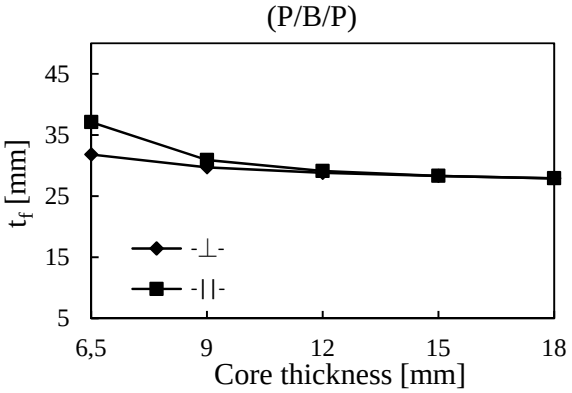
(P/B/P)
t_f [mm]
45
35
25
15
5
-⊥-
-||-
6,5
9
12
15
18
Core thickness [mm]

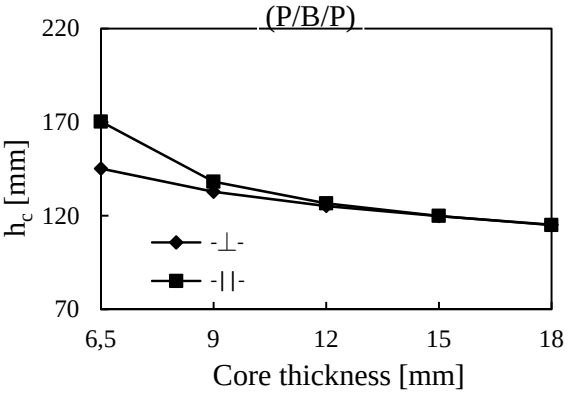
(P/B/P)
h_c [mm]
220
170
120
70
-⊥-
-||-
6,5
9
12
15
18
Core thickness [mm]

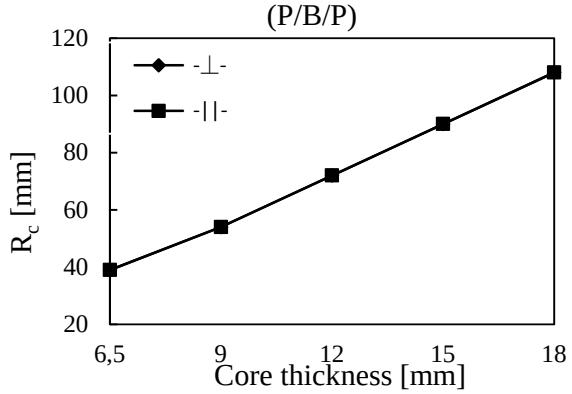
(P/B/P)
R_c [mm]
120
100
80
60
40
20
-⊥-
-||-
6,5
9
12
15
18
Core thickness [mm]

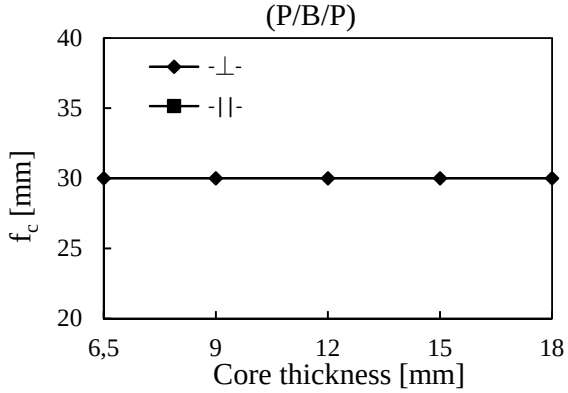
(P/B/P)
f_c [mm]
40
35
30
25
20
-⊥-
-||-
6,5
9
12
15
18
Core thickness [mm]

4x6 Floor

(B/C/B)

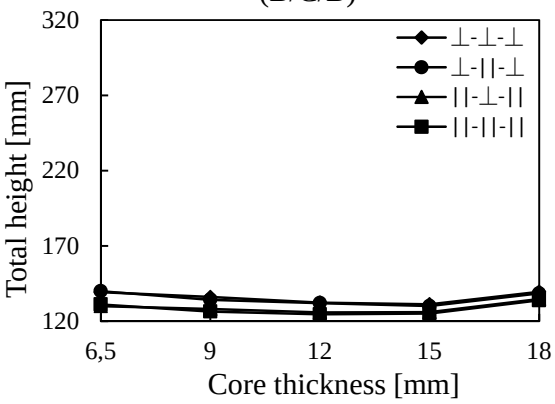

(B/C/B)

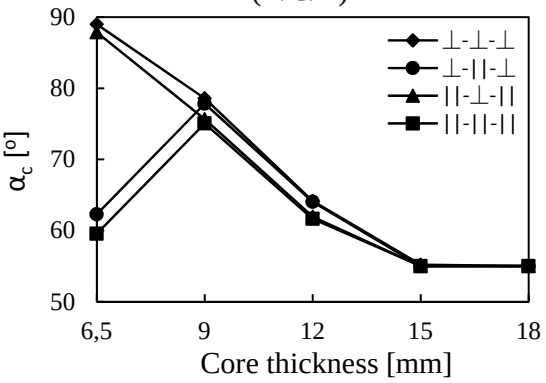

(B/C/B)

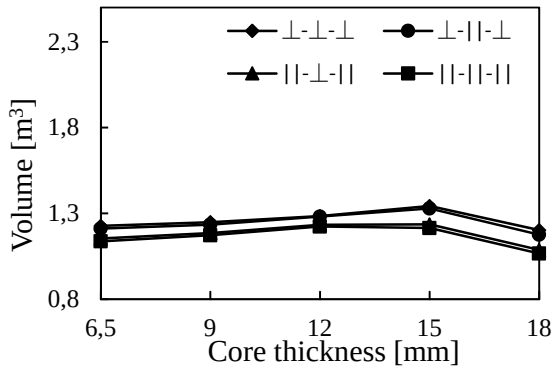

(B/C/B)

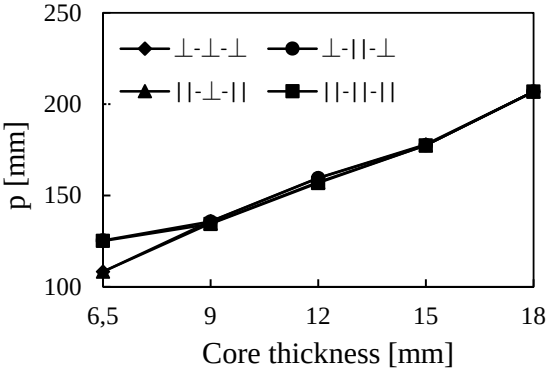

(B/C/B)

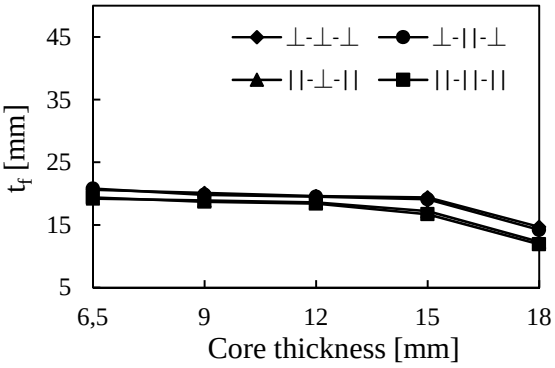

(B/C/B)

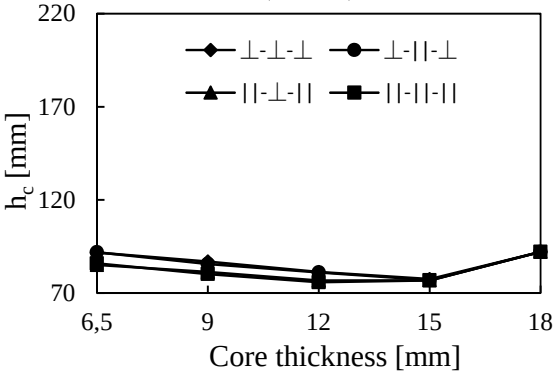

(B/C/B)

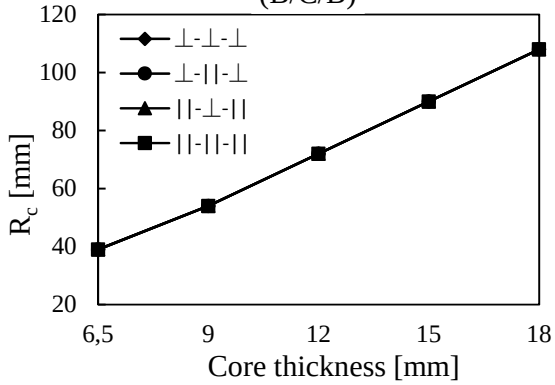

(B/C/B)

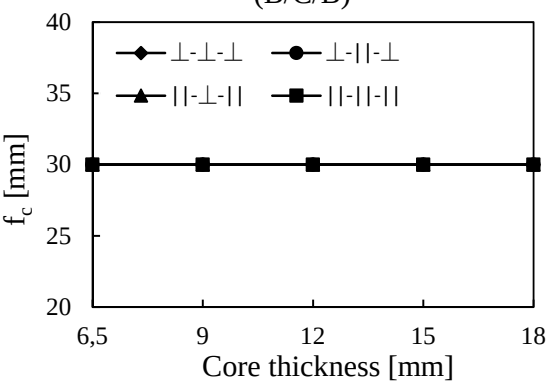

6x4 Floor

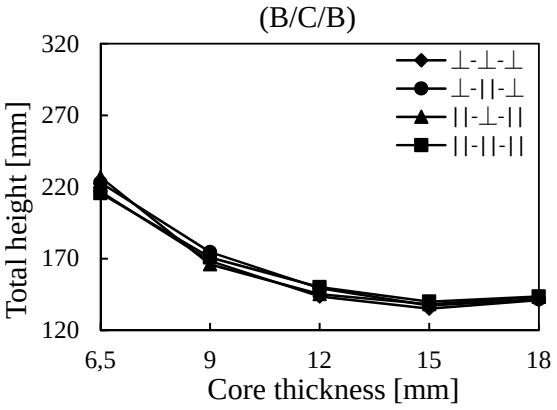
(B/C/B)
Total height [mm]
320
270
220
170
120
6,5
9
12
15
18
Core thickness [mm]
⊥-⊥-⊥
⊥-||-⊥
||-⊥-||
||-||-||

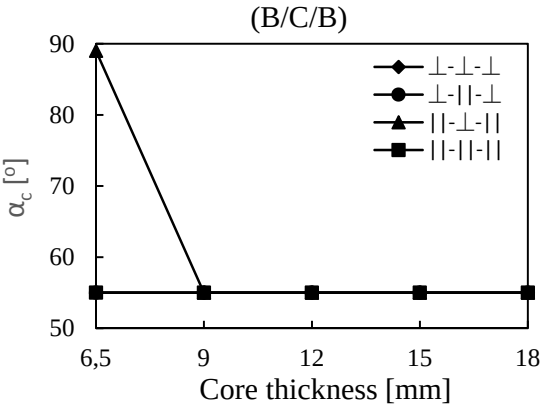
(B/C/B)
α_c [°]
90
80
70
60
50
6,5
9
12
15
18
Core thickness [mm]
⊥-⊥-⊥
⊥-||-⊥
||-⊥-||
||-||-||

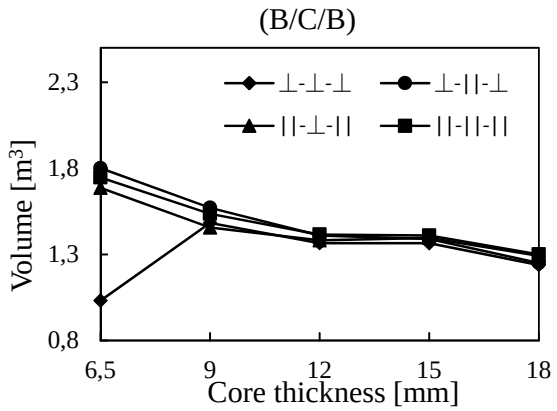
(B/C/B)
Volume [m^3]
2,3
1,8
1,3
0,8
6,5
9
12
15
18
Core thickness [mm]
⊥-⊥-⊥
⊥-||-⊥
||-⊥-||
||-||-||

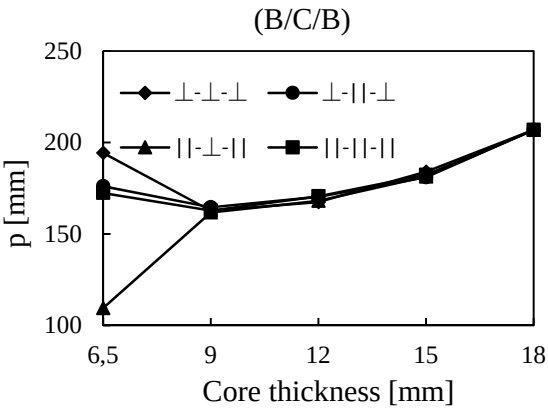
(B/C/B)
p [mm]
250
200
150
100
6,5
9
12
15
18
Core thickness [mm]
⊥-⊥-⊥
⊥-||-⊥
||-⊥-||
||-||-||

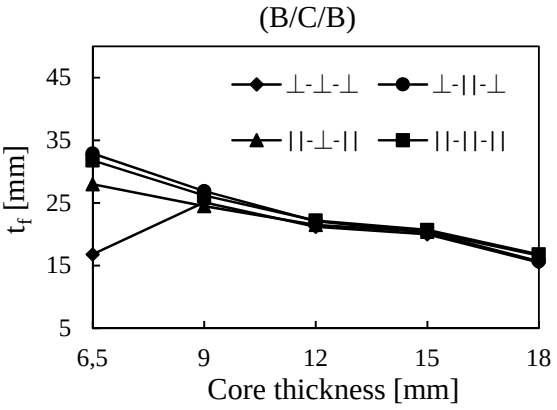
(B/C/B)
t_f [mm]
45
35
25
15
5
6,5
9
12
15
18
Core thickness [mm]
⊥-⊥-⊥
⊥-||-⊥
||-⊥-||
||-||-||

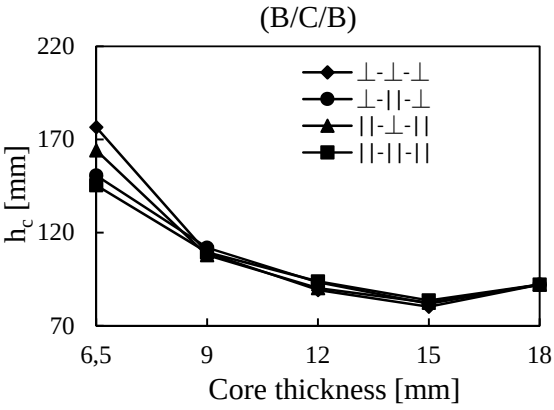
(B/C/B)
h_c [mm]
220
170
120
70
6,5
9
12
15
18
Core thickness [mm]
⊥-⊥-⊥
⊥-||-⊥
||-⊥-||
||-||-||

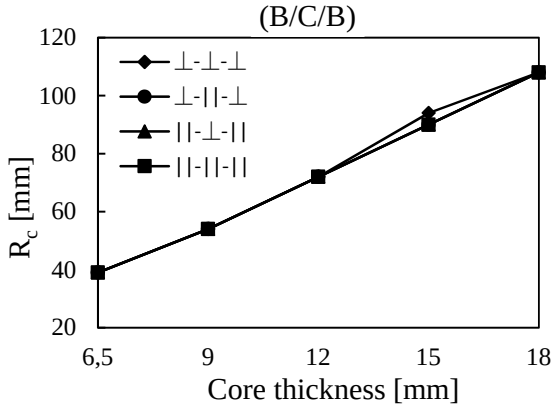
(B/C/B)
R_c [mm]
120
100
80
60
40
20
6,5
9
12
15
18
Core thickness [mm]
⊥-⊥-⊥
⊥-||-⊥
||-⊥-||
||-||-||

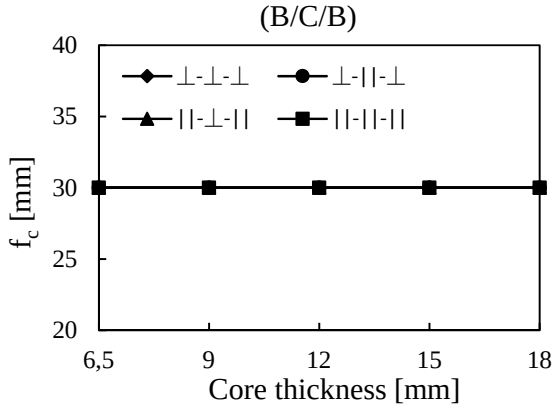
(B/C/B)
f_c [mm]
40
35
30
25
20
6,5
9
12
15
18
Core thickness [mm]
⊥-⊥-⊥
⊥-||-⊥
||-⊥-||
||-||-||

4x6 Floor

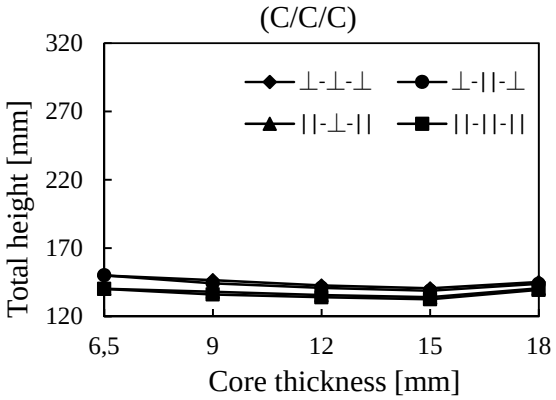
(C/C/C)
Total height [mm]
320
270
220
170
120
⊥-⊥-⊥
⊥-||-⊥
||-⊥-||
||-||-||
6,5
9
12
15
18
Core thickness [mm]

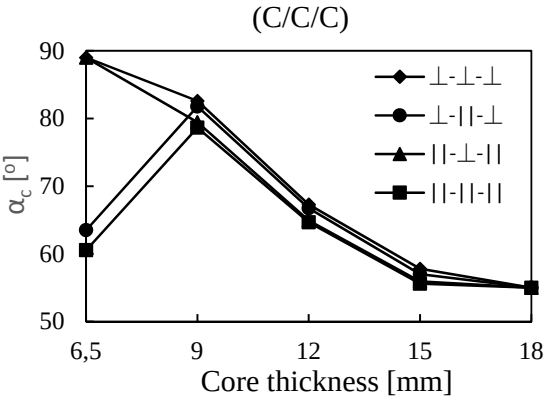
(C/C/C)
α_c [º]
90
80
70
60
50
⊥-⊥-⊥
⊥-||-⊥
||-⊥-||
||-||-||
6,5
9
12
15
18
Core thickness [mm]

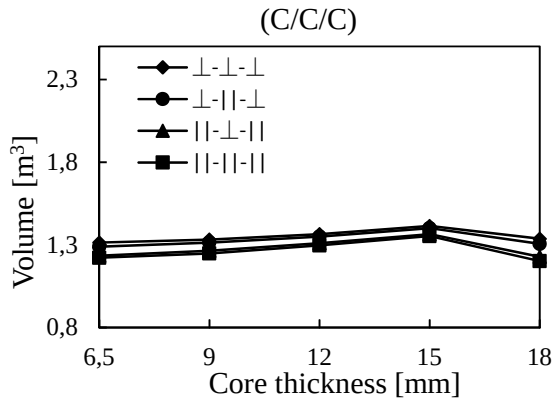
(C/C/C)
Volume [m³]
2,3
1,8
1,3
0,8
⊥-⊥-⊥
⊥-||-⊥
||-⊥-||
||-||-||
6,5
9
12
15
18
Core thickness [mm]

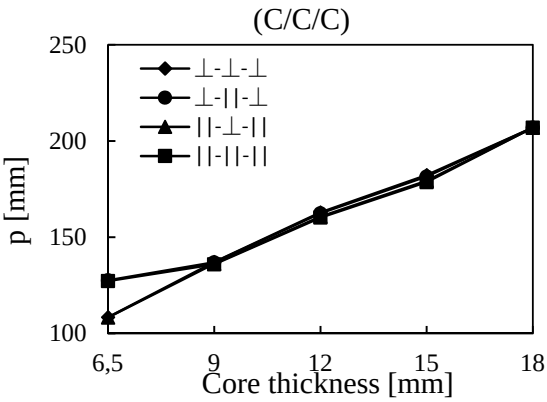
(C/C/C)
p [mm]
250
200
150
100
⊥-⊥-⊥
⊥-||-⊥
||-⊥-||
||-||-||
6,5
9
12
15
18
Core thickness [mm]

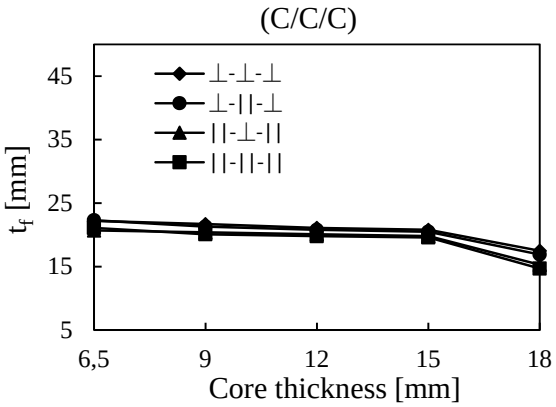
(C/C/C)
t_f [mm]
45
35
25
15
5
⊥-⊥-⊥
⊥-||-⊥
||-⊥-||
||-||-||
6,5
9
12
15
18
Core thickness [mm]

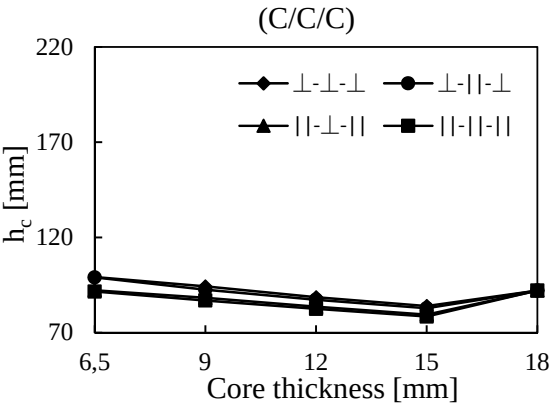
(C/C/C)
h_c [mm]
220
170
120
70
⊥-⊥-⊥
⊥-||-⊥
||-⊥-||
||-||-||
6,5
9
12
15
18
Core thickness [mm]

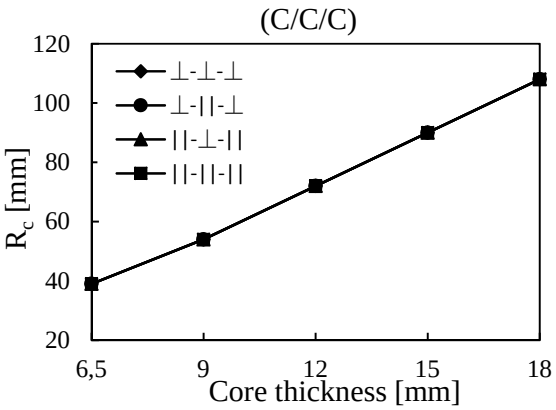
(C/C/C)
R_c [mm]
120
100
80
60
40
20
⊥-⊥-⊥
⊥-||-⊥
||-⊥-||
||-||-||
6,5
9
12
15
18
Core thickness [mm]

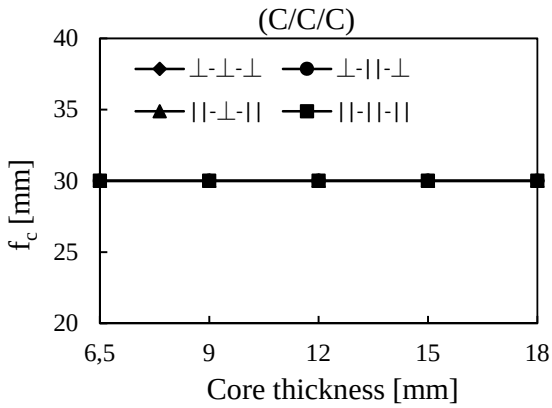
(C/C/C)
f_c [mm]
40
35
30
25
20
⊥-⊥-⊥
⊥-||-⊥
||-⊥-||
||-||-||
6,5
9
12
15
18
Core thickness [mm]

6x4 Floor

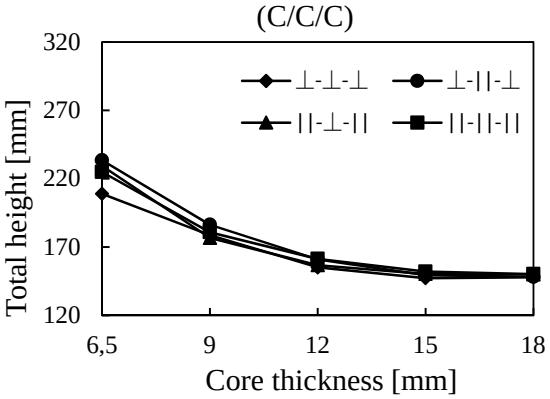
(C/C/C)
Total height [mm]
320
270
220
170
120
6,5
9
12
15
18
Core thickness [mm]
⊥-⊥-⊥
⊥-||-⊥
||-⊥-||
||-||-||

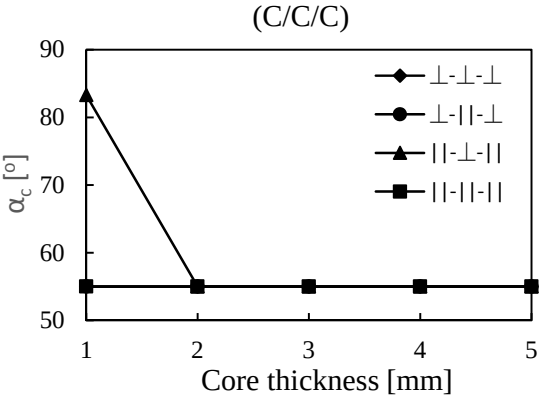
(C/C/C)
α_c [°]
90
80
70
60
50
1
2
3
4
5
Core thickness [mm]
⊥-⊥-⊥
⊥-||-⊥
||-⊥-||
||-||-||

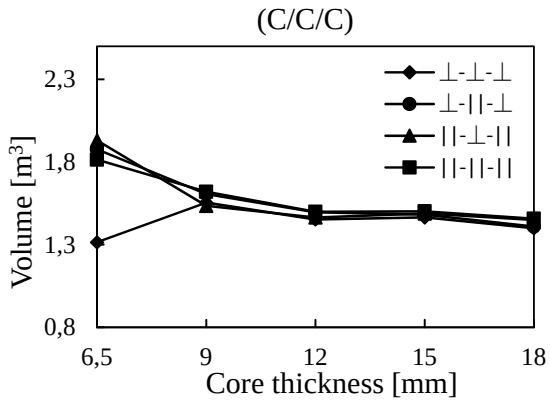
(C/C/C)
Volume [m^3]
2,3
1,8
1,3
0,8
6,5
9
12
15
18
Core thickness [mm]
⊥-⊥-⊥
⊥-||-⊥
||-⊥-||
||-||-||

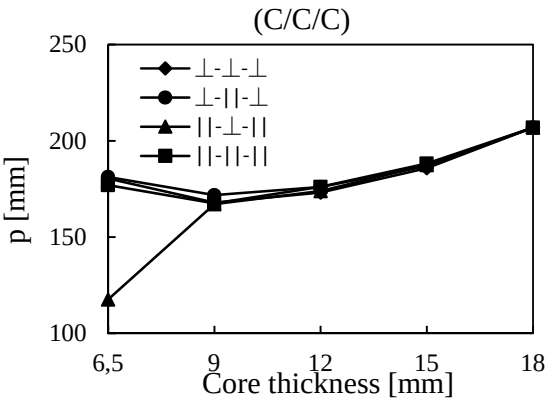
(C/C/C)
p [mm]
250
200
150
100
6,5
9
12
15
18
Core thickness [mm]
⊥-⊥-⊥
⊥-||-⊥
||-⊥-||
||-||-||

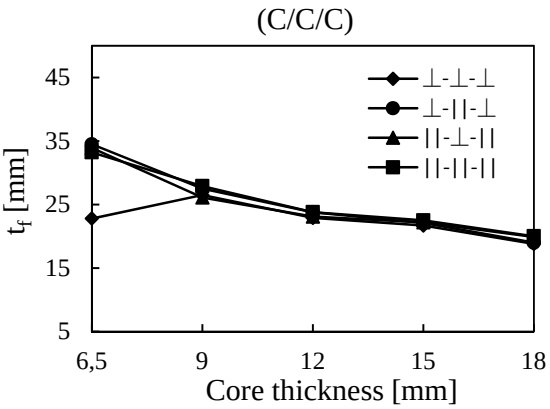
(C/C/C)
t_f [mm]
45
35
25
15
5
6,5
9
12
15
18
Core thickness [mm]
⊥-⊥-⊥
⊥-||-⊥
||-⊥-||
||-||-||

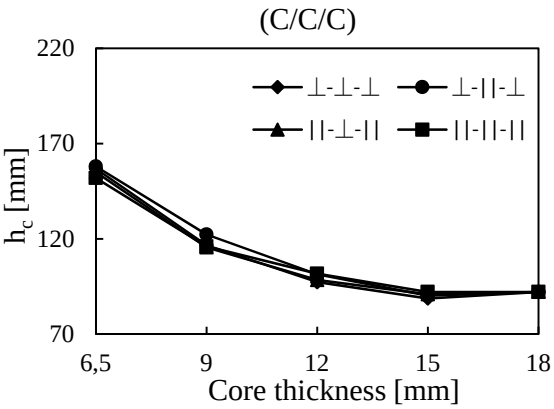
(C/C/C)
h_c [mm]
220
170
120
70
6,5
9
12
15
18
Core thickness [mm]
⊥-⊥-⊥
⊥-||-⊥
||-⊥-||
||-||-||

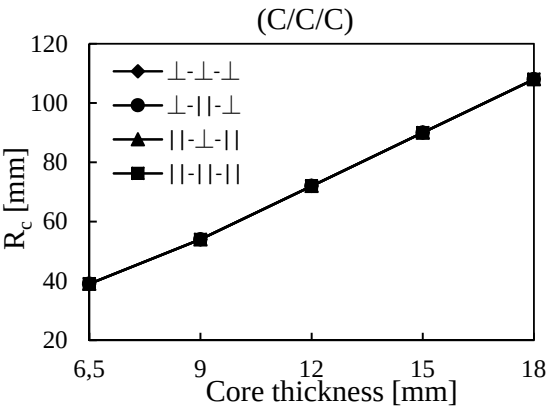
(C/C/C)
R_c [mm]
120
100
80
60
40
20
6,5
9
12
15
18
Core thickness [mm]
⊥-⊥-⊥
⊥-||-⊥
||-⊥-||
||-||-||

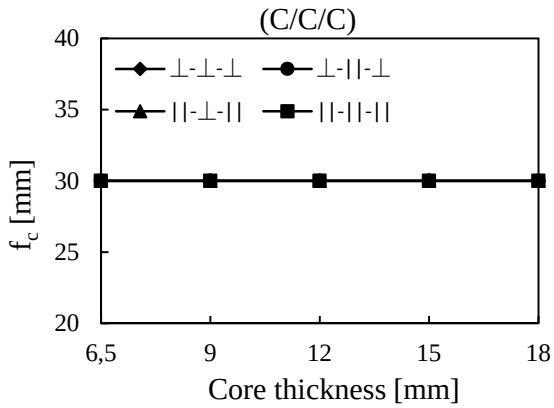
(C/C/C)
f_c [mm]
40
35
30
25
20
6,5
9
12
15
18
Core thickness [mm]
⊥-⊥-⊥
⊥-||-⊥
||-⊥-||
||-||-||

4x6 Floor

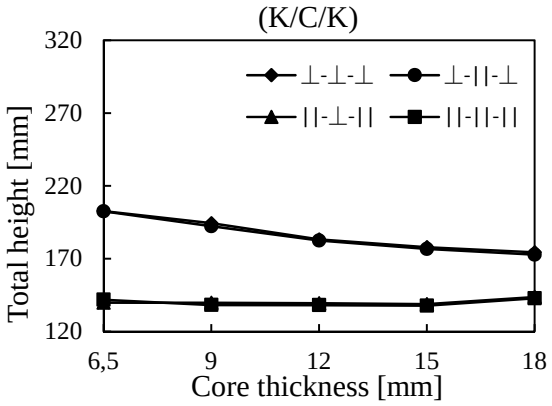
(K/C/K)
Total height [mm]
320
270
220
170
120
6,5
9
12
15
18
Core thickness [mm]
⊥-⊥-⊥
⊥-||-⊥
||-⊥-||
||-||-||

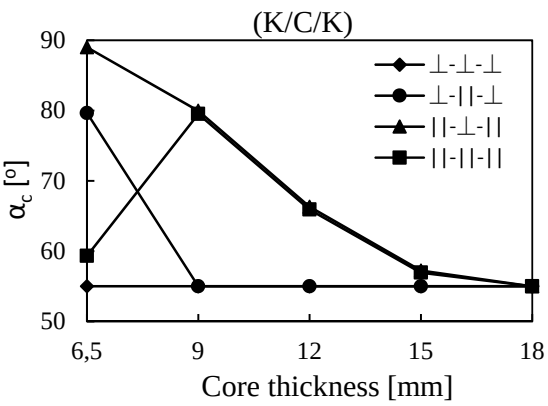
(K/C/K)
α_c [º]
90
80
70
60
50
6,5
9
12
15
18
Core thickness [mm]
⊥-⊥-⊥
⊥-||-⊥
||-⊥-||
||-||-||

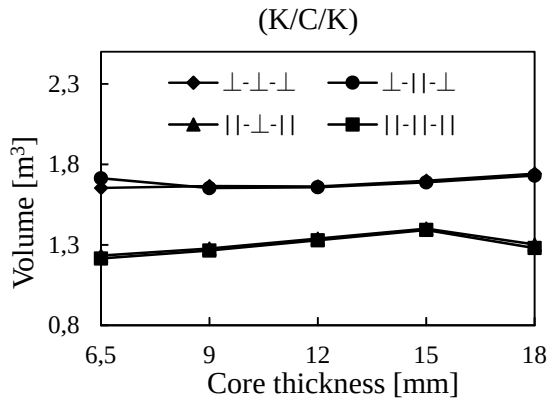
(K/C/K)
Volume [m³]
2,3
1,8
1,3
0,8
6,5
9
12
15
18
Core thickness [mm]
⊥-⊥-⊥
⊥-||-⊥
||-⊥-||
||-||-||

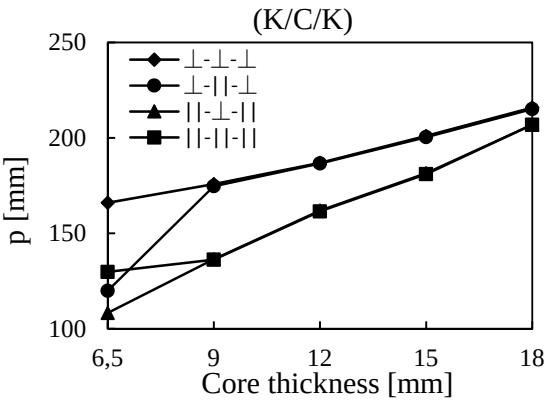
(K/C/K)
p [mm]
250
200
150
100
6,5
9
12
15
18
Core thickness [mm]
⊥-⊥-⊥
⊥-||-⊥
||-⊥-||
||-||-||

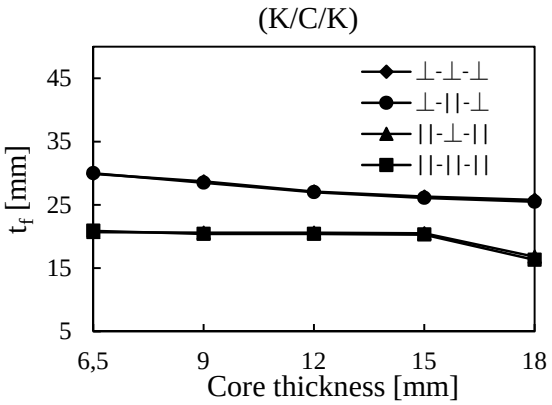
(K/C/K)
t_f [mm]
45
35
25
15
5
6,5
9
12
15
18
Core thickness [mm]
⊥-⊥-⊥
⊥-||-⊥
||-⊥-||
||-||-||

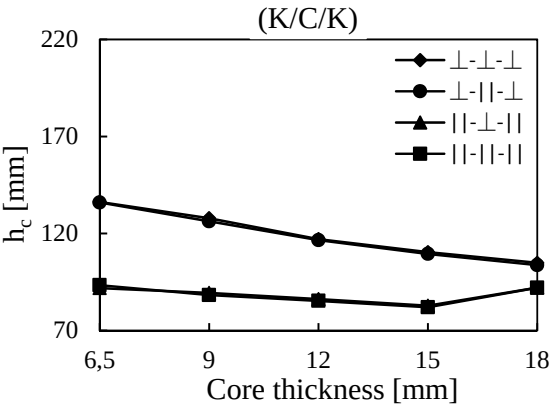
(K/C/K)
h_c [mm]
220
170
120
70
6,5
9
12
15
18
Core thickness [mm]
⊥-⊥-⊥
⊥-||-⊥
||-⊥-||
||-||-||

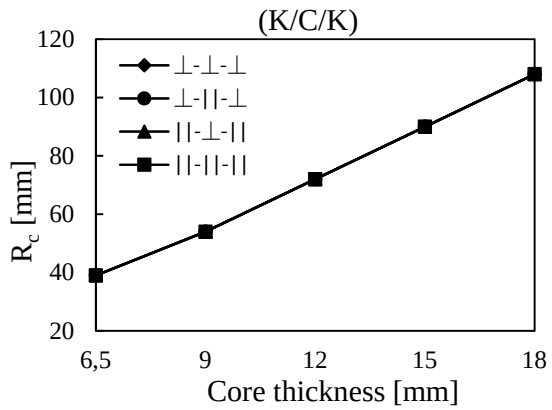
(K/C/K)
R_c [mm]
120
100
80
60
40
20
6,5
9
12
15
18
Core thickness [mm]
⊥-⊥-⊥
⊥-||-⊥
||-⊥-||
||-||-||

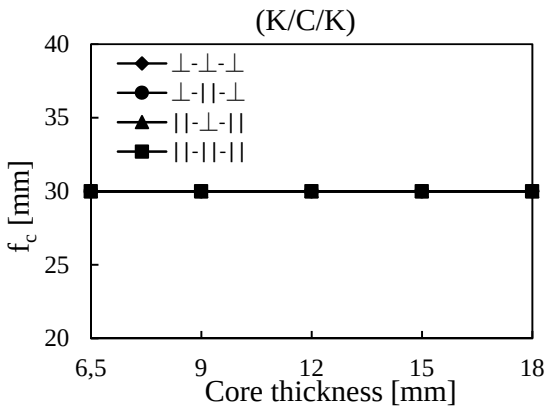
(K/C/K)
f_c [mm]
40
35
30
25
20
6,5
9
12
15
18
Core thickness [mm]
⊥-⊥-⊥
⊥-||-⊥
||-⊥-||
||-||-||

6x4 Floor

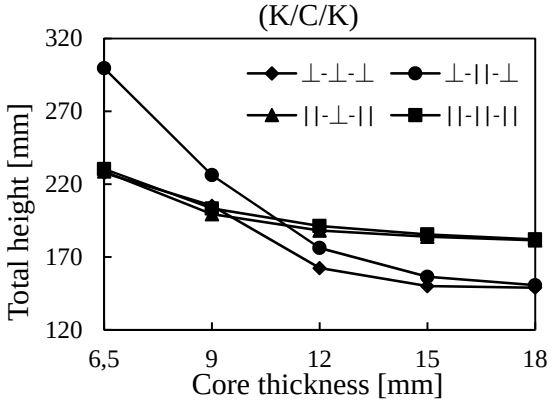
(K/C/K)
Total height [mm]
320
270
220
170
120
⊥-⊥-⊥
⊥-||-⊥
||-⊥-||
||-||-||
6,5
9
12
15
18
Core thickness [mm]

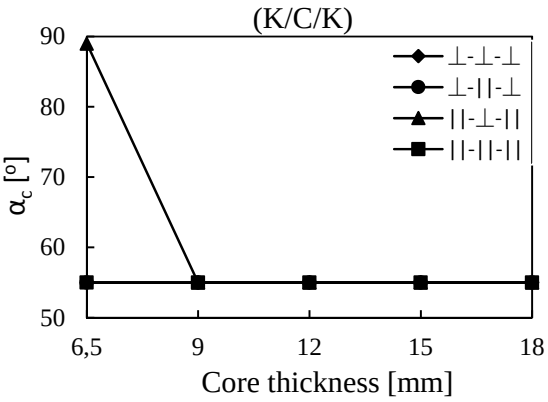
(K/C/K)
α_c [°]
90
80
70
60
50
⊥-⊥-⊥
⊥-||-⊥
||-⊥-||
||-||-||
6,5
9
12
15
18
Core thickness [mm]

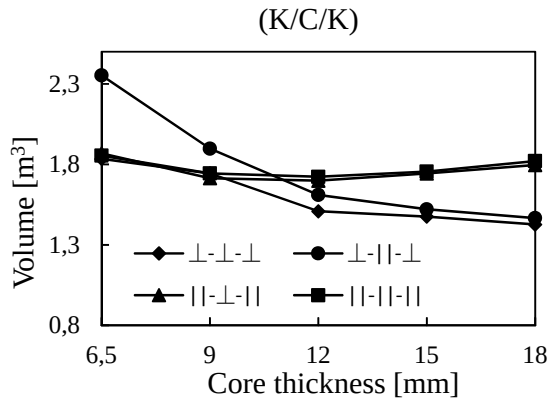
(K/C/K)
Volume [m³]
2,3
1,8
1,3
0,8
⊥-⊥-⊥
⊥-||-⊥
||-⊥-||
||-||-||
6,5
9
12
15
18
Core thickness [mm]

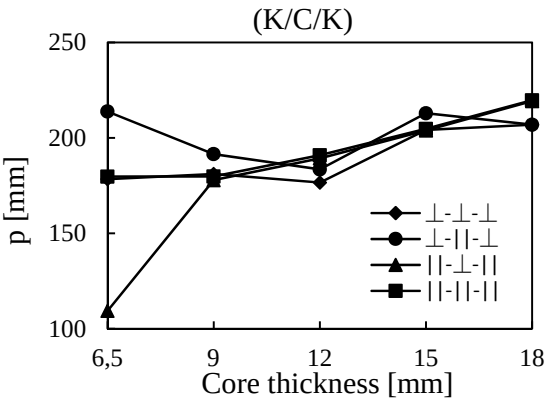
(K/C/K)
p [mm]
250
200
150
100
⊥-⊥-⊥
⊥-||-⊥
||-⊥-||
||-||-||
6,5
9
12
15
18
Core thickness [mm]

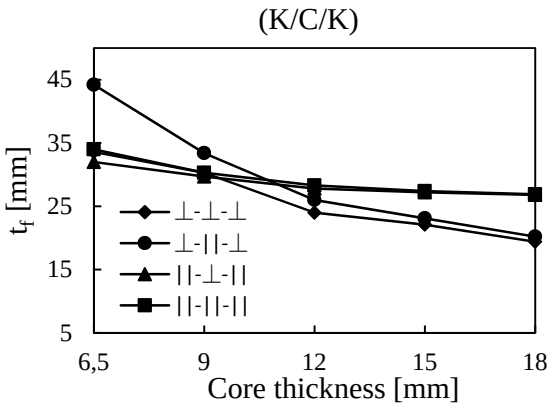
(K/C/K)
t_f [mm]
45
35
25
15
5
⊥-⊥-⊥
⊥-||-⊥
||-⊥-||
||-||-||
6,5
9
12
15
18
Core thickness [mm]

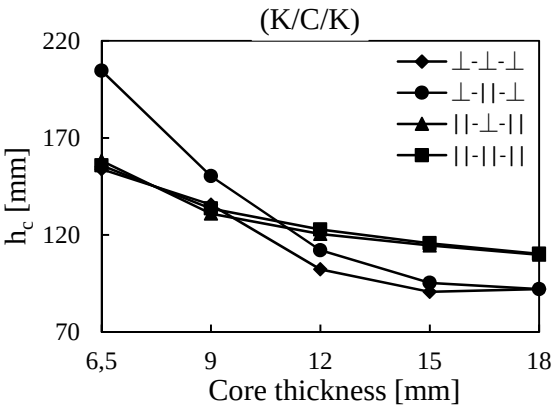
(K/C/K)
h_c [mm]
220
170
120
70
⊥-⊥-⊥
⊥-||-⊥
||-⊥-||
||-||-||
6,5
9
12
15
18
Core thickness [mm]

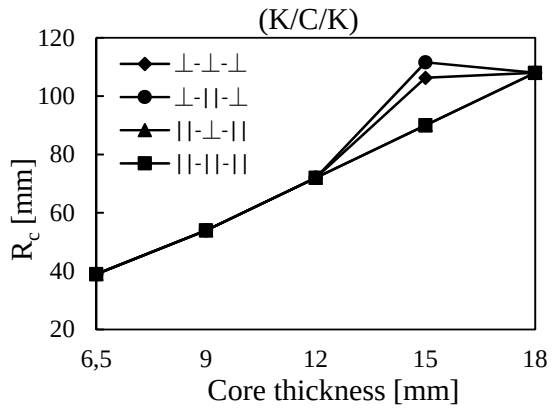
(K/C/K)
R_c [mm]
120
100
80
60
40
20
⊥-⊥-⊥
⊥-||-⊥
||-⊥-||
||-||-||
6,5
9
12
15
18
Core thickness [mm]

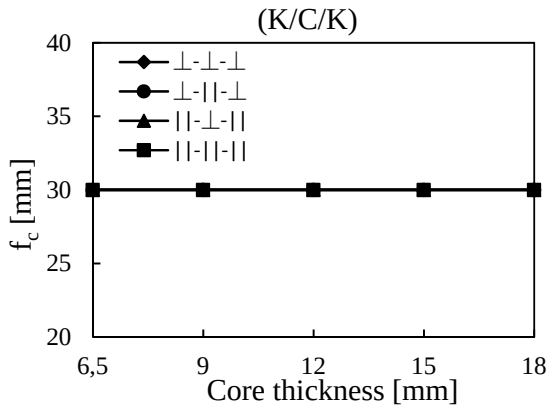
(K/C/K)
f_c [mm]
40
35
30
25
20
⊥-⊥-⊥
⊥-||-⊥
||-⊥-||
||-||-||
6,5
9
12
15
18
Core thickness [mm]

4x6 Floor

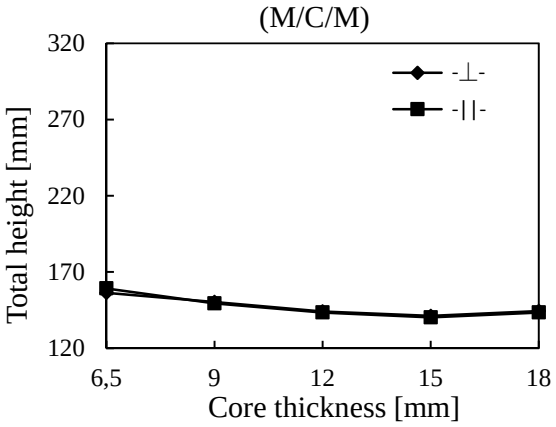
(M/C/M)
Total height [mm]
320
270
220
170
120
-⊥-
-||-
6,5
9
12
15
18
Core thickness [mm]

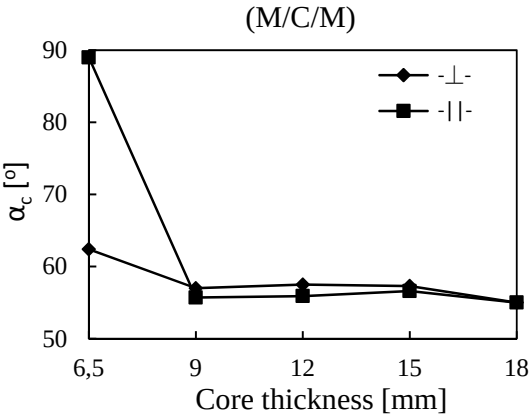
(M/C/M)
α_c [º]
90
80
70
60
50
-⊥-
-||-
6,5
9
12
15
18
Core thickness [mm]

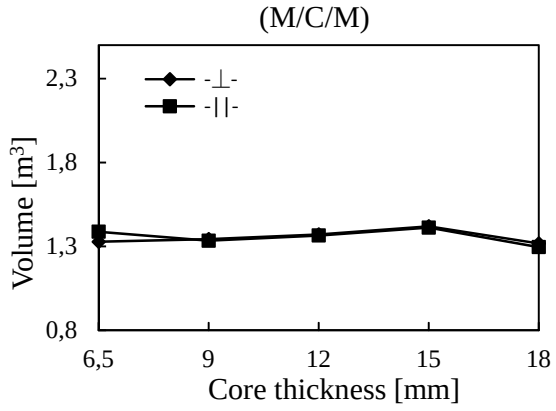
(M/C/M)
Volume [m^3]
2,3
1,8
1,3
0,8
-⊥-
-||-
6,5
9
12
15
18
Core thickness [mm]

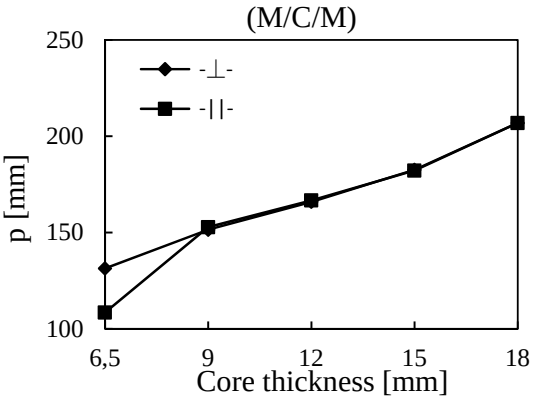
(M/C/M)
p [mm]
250
200
150
100
-⊥-
-||-
6,5
9
12
15
18
Core thickness [mm]

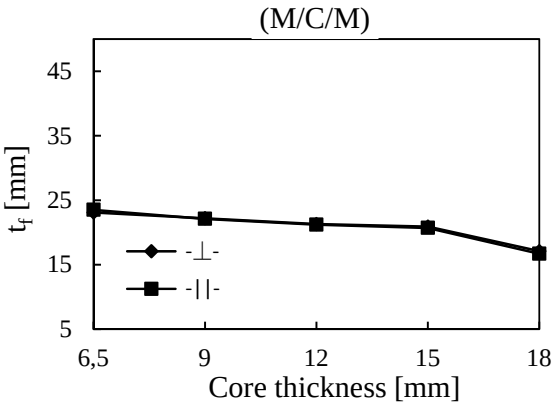
(M/C/M)
t_f [mm]
45
35
25
15
5
-⊥-
-||-
6,5
9
12
15
18
Core thickness [mm]

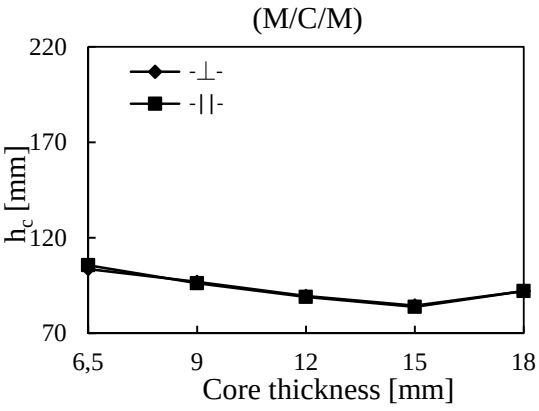
(M/C/M)
h_c [mm]
220
170
120
70
-⊥-
-||-
6,5
9
12
15
18
Core thickness [mm]

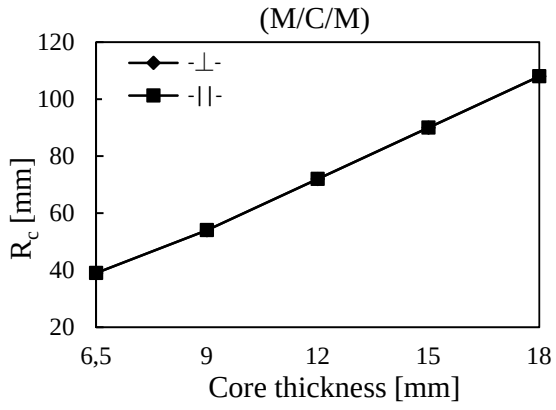
(M/C/M)
R_c [mm]
120
100
80
60
40
20
-⊥-
-||-
6,5
9
12
15
18
Core thickness [mm]

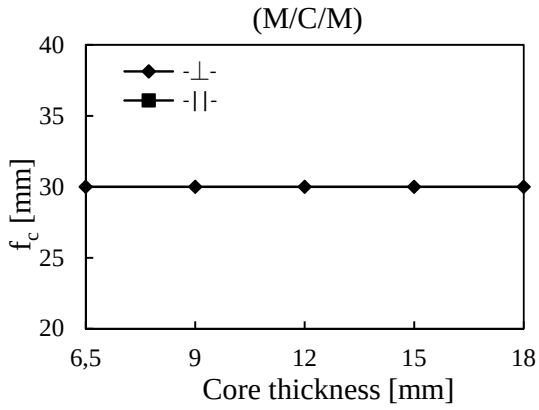
(M/C/M)
f_c [mm]
40
35
30
25
20
-⊥-
-||-
6,5
9
12
15
18
Core thickness [mm]

6x4 Floor

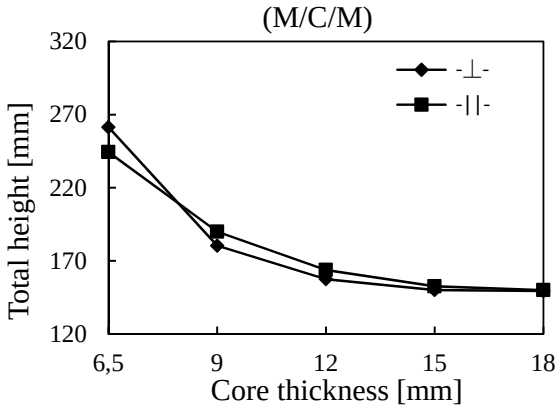
(M/C/M)
Total height [mm]
320
270
220
170
120
-⊥-
-||-
6,5
9
12
15
18
Core thickness [mm]

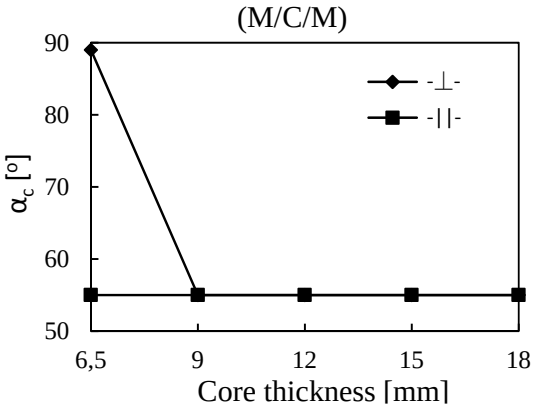
(M/C/M)
α_c [º]
90
80
70
60
50
-⊥-
-||-
6,5
9
12
15
18
Core thickness [mm]

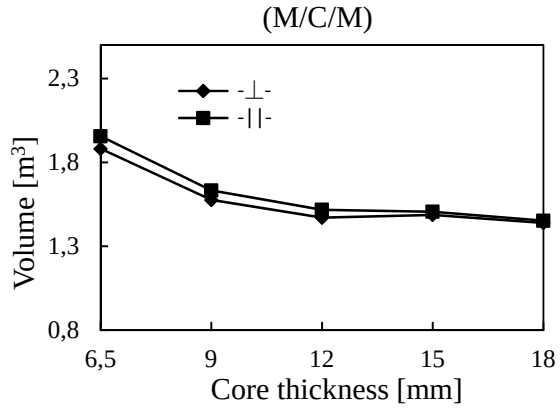
(M/C/M)
Volume [m^3]
2,3
1,8
1,3
0,8
-⊥-
-||-
6,5
9
12
15
18
Core thickness [mm]

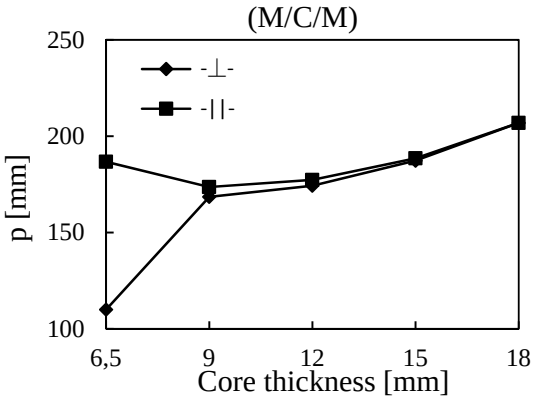
(M/C/M)
p [mm]
250
200
150
100
-⊥-
-||-
6,5
9
12
15
18
Core thickness [mm]

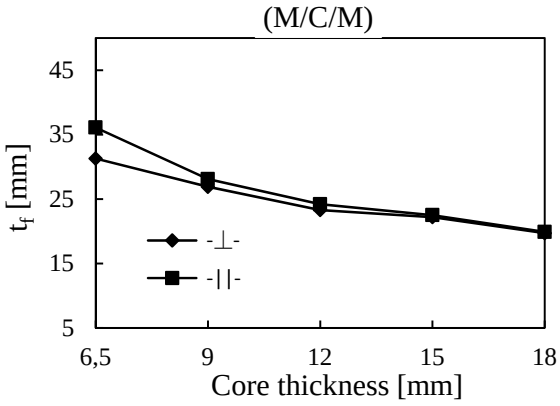
(M/C/M)
t_f [mm]
45
35
25
15
5
-⊥-
-||-
6,5
9
12
15
18
Core thickness [mm]

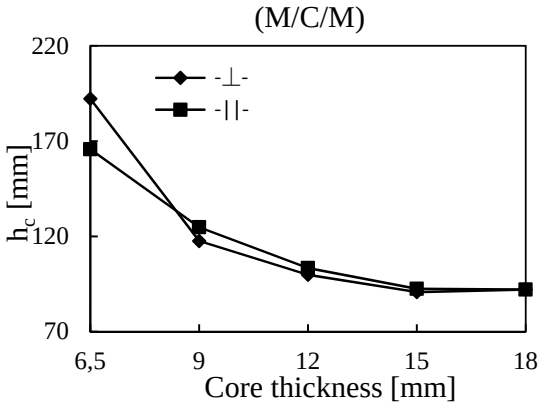
(M/C/M)
h_c [mm]
220
170
120
70
-⊥-
-||-
6,5
9
12
15
18
Core thickness [mm]

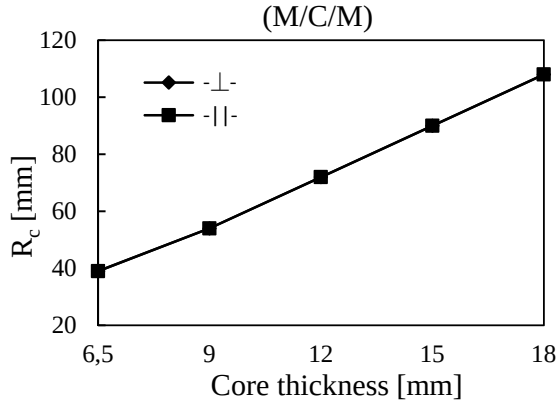
(M/C/M)
R_c [mm]
120
100
80
60
40
20
-⊥-
-||-
6,5
9
12
15
18
Core thickness [mm]

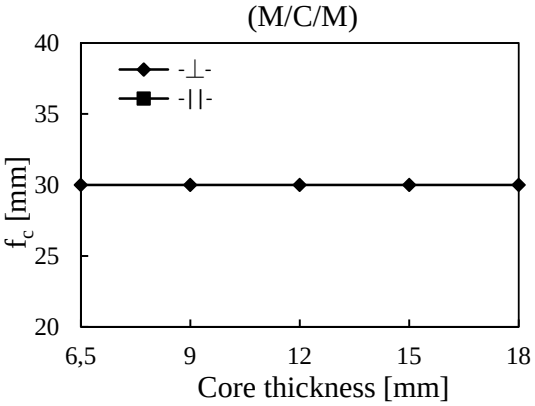
(M/C/M)
f_c [mm]
40
35
30
25
20
-⊥-
-||-
6,5
9
12
15
18
Core thickness [mm]

4x6 Floor

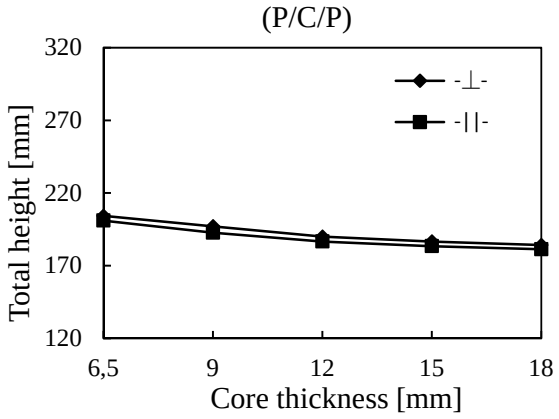
(P/C/P)
Total height [mm]
320
270
220
170
120
-⊥-
-||-
6,5
9
12
15
18
Core thickness [mm]

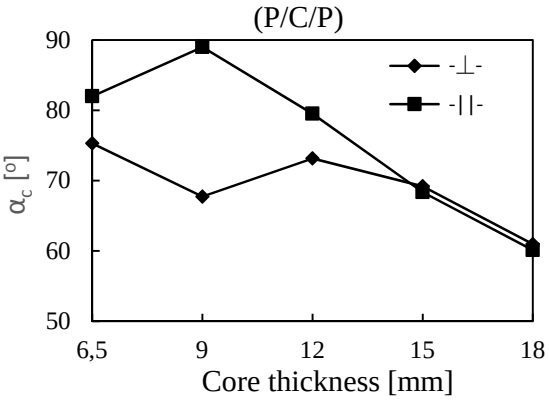
(P/C/P)
α_c [°]
90
80
70
60
50
-⊥-
-||-
6,5
9
12
15
18
Core thickness [mm]

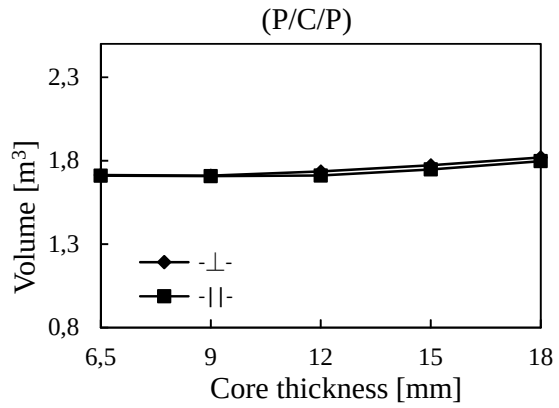
(P/C/P)
Volume [m³]
2,3
1,8
1,3
0,8
-⊥-
-||-
6,5
9
12
15
18
Core thickness [mm]

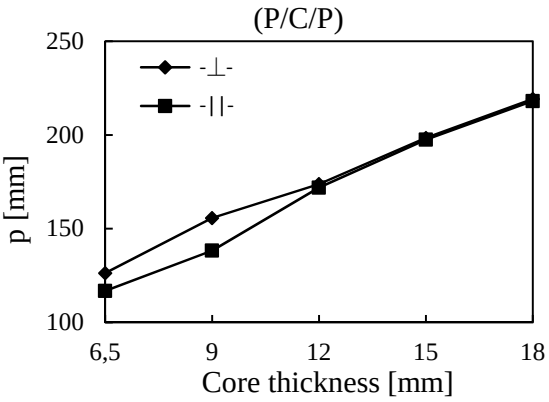
(P/C/P)
p [mm]
250
200
150
100
-⊥-
-||-
6,5
9
12
15
18
Core thickness [mm]

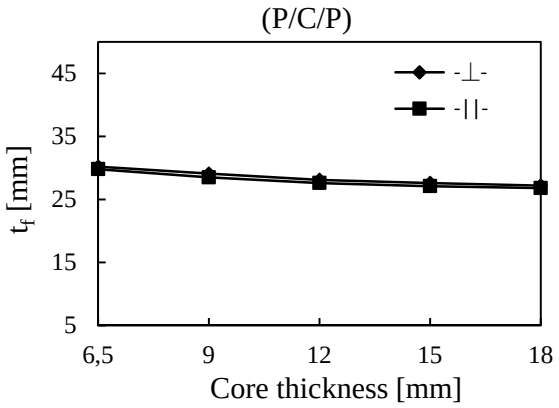
(P/C/P)
t_f [mm]
45
35
25
15
5
-⊥-
-||-
6,5
9
12
15
18
Core thickness [mm]

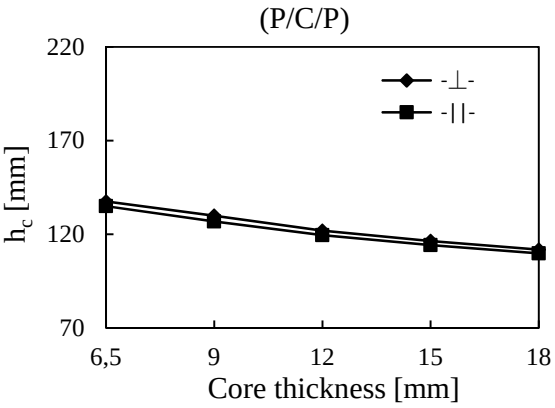
(P/C/P)
h_c [mm]
220
170
120
70
-⊥-
-||-
6,5
9
12
15
18
Core thickness [mm]

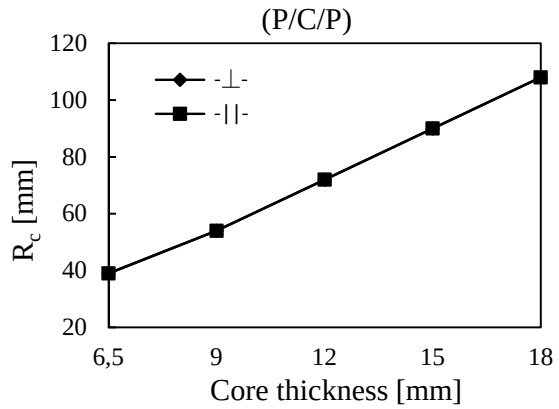
(P/C/P)
R_c [mm]
120
100
80
60
40
20
-⊥-
-||-
6,5
9
12
15
18
Core thickness [mm]

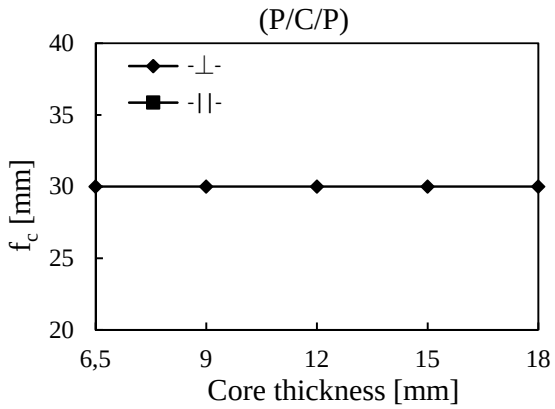
(P/C/P)
f_c [mm]
40
35
30
25
20
-⊥-
-||-
6,5
9
12
15
18
Core thickness [mm]

6x4 Floor

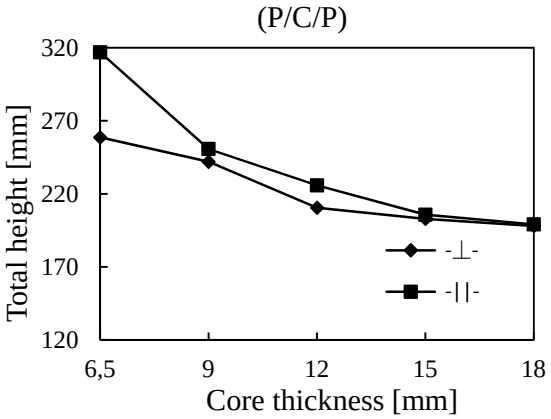
(P/C/P)
Total height [mm]
320
270
220
170
120
6,5
9
12
15
18
Core thickness [mm]
-⊥-
-||-

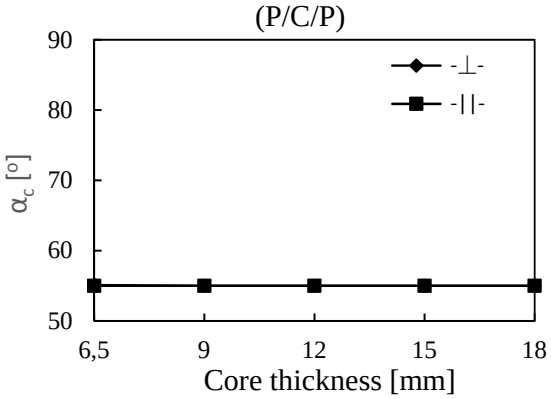
(P/C/P)
α_c [°]
90
80
70
60
50
6,5
9
12
15
18
Core thickness [mm]
-⊥-
-||-

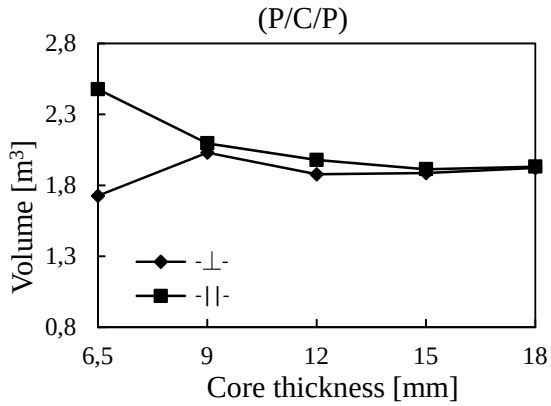
(P/C/P)
Volume [m³]
2,8
2,3
1,8
1,3
0,8
6,5
9
12
15
18
Core thickness [mm]
-⊥-
-||-

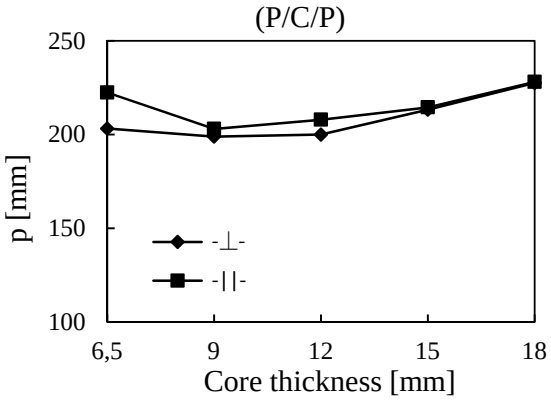
(P/C/P)
p [mm]
250
200
150
100
6,5
9
12
15
18
Core thickness [mm]
-⊥-
-||-

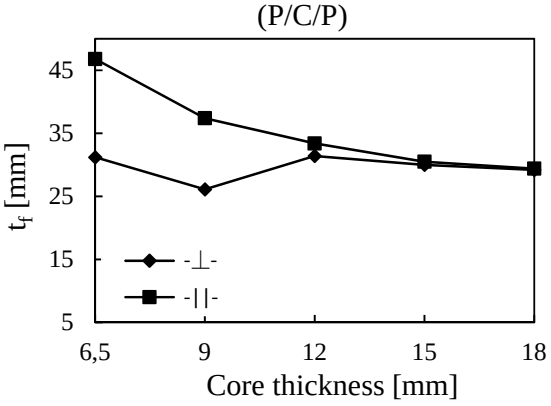
(P/C/P)
t_f [mm]
45
35
25
15
5
6,5
9
12
15
18
Core thickness [mm]
-⊥-
-||-

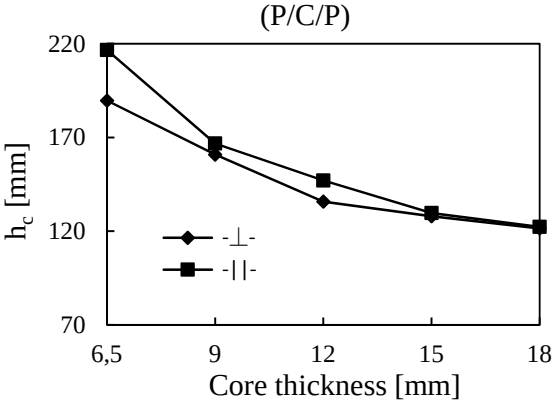
(P/C/P)
h_c [mm]
220
170
120
70
6,5
9
12
15
18
Core thickness [mm]
-⊥-
-||-

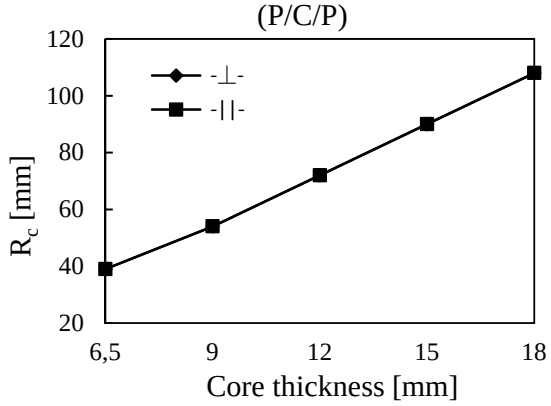
(P/C/P)
R_c [mm]
120
100
80
60
40
20
6,5
9
12
15
18
Core thickness [mm]
-⊥-
-||-

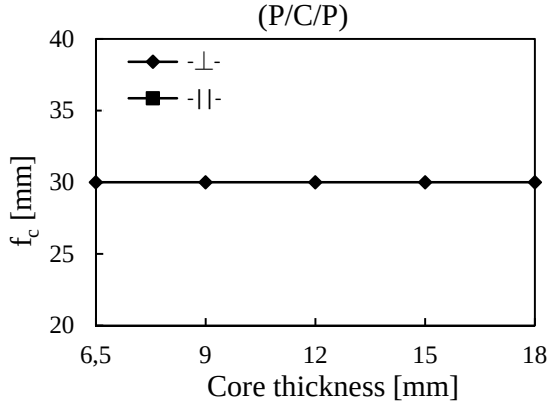
(P/C/P)
f_c [mm]
40
35
30
25
20
6,5
9
12
15
18
Core thickness [mm]
-⊥-
-||-

E Stresses

Controls of the 20 optimal cases in ultimate limit state where made in terms of maximum stresses in the face and in the core and also the Norris criteria. This is made in Abaqus/CAE 6.13-3 and is further explained in Section 7.1.3. Following tables are as follow:

- Maximum stresses in the face compared to its strength. Utilization ratio is shown for each case and also the maximum utilization ratio for each direction in both compression and tension.
- Maximum stresses in the corrugated core compared to its strength. Utilization ratio is shown for each case and also the maximum utilization ratio for each direction in both compression and tension.
- Norris criteria taken where the maximum von mises stress is obtain, which always occur in the core. Table also shows the utilization and the maximum utilization, which should be less then 1.

		Face											
		σ_{0t} [Pa]	σ_{0td} [Pa]	Uti	σ_{0c} [Pa]	σ_{0cd} [Pa]	Uti	σ_{90t} [Pa]	σ_{90td} [Pa]	%	σ_{90c} [Pa]	σ_{90cd} [Pa]	Uti
BBB	4x6	1,90E+06	2,61E+07	7,3%	-2,91E+06	1,81E+07	-16,0%	1,11E+06	2,39E+07	4,7%	-2,89E+06	1,65E+07	-17,5%
	6x4	2,03E+06	2,39E+07	8,5%	-2,93E+06	1,65E+07	-17,7%	1,14E+06	2,61E+07	4,4%	-1,64E+06	1,81E+07	-9,0%
CBC	4x6	1,70E+06	9,73E+06	17,5%	-2,47E+06	1,25E+07	-19,7%	1,05E+06	8,93E+06	11,8%	-1,58E+06	1,15E+07	-13,8%
	6x4	1,56E+06	9,00E+06	17,3%	-2,28E+06	1,15E+07	-19,8%	9,14E+05	9,67E+06	9,5%	-1,35E+06	1,25E+07	-10,8%
KBK	4x6	1,58E+06	1,17E+07	13,5%	-2,48E+06	1,27E+07	-19,6%	2,80E+05	4,00E+06	7,0%	1,53E+06	6,00E+06	25,5%
	6x4	1,83E+06	4,00E+06	45,8%	-2,81E+06	6,00E+06	-46,8%	2,28E+05	1,17E+07	1,9%	-3,37E+05	1,27E+07	-2,7%
PBP	4x6	6,64E+05	3,05E+06	21,8%	-9,77E+05	4,50E+06	-21,7%	3,88E+05	3,05E+06	12,7%	-5,88E+05	4,50E+06	-13,1%
	6x4	6,87E+05	3,05E+06	22,5%	-1,96E+06	4,50E+06	-43,6%	3,89E+05	3,05E+06	12,8%	-5,62E+05	4,50E+06	-12,5%
MBM	4x6	1,90E+06	-	-	-2,91E+06	-	-	1,01E+06	-	-	-2,89E+06	-	-
	6x4	1,33E+06	-	-	-2,56E+06	-	-	8,27E+05	-	-	-1,19E+06	-	-
BCB	4x6	1,87E+06	2,61E+07	7,2%	-2,88E+06	1,81E+07	-15,9%	9,47E+05	2,39E+07	4,0%	-1,96E+06	1,65E+07	-11,9%
	6x4	1,38E+06	2,40E+07	5,8%	-5,13E+06	1,67E+07	-30,8%	9,66E+05	2,60E+07	3,7%	-2,17E+06	1,80E+07	-12,1%
CCC	4x6	1,63E+06	9,73E+06	16,7%	-2,39E+06	1,25E+07	-19,1%	9,35E+05	8,93E+06	10,5%	-2,51E+06	1,15E+07	-21,9%
	6x4	1,24E+06	9,00E+06	13,8%	-2,02E+06	1,15E+07	-17,5%	8,42E+05	9,67E+06	8,7%	-1,28E+06	1,25E+07	-10,3%
KCK	4x6	1,59E+06	1,17E+07	13,6%	-2,48E+06	1,27E+07	-19,6%	2,15E+05	4,00E+06	5,4%	-8,15E+05	6,00E+06	-13,6%
	6x4	1,21E+06	4,00E+06	30,3%	-3,24E+06	6,00E+06	-54,0%	2,26E+05	1,17E+07	1,9%	-3,36E+05	1,27E+07	-2,7%
PCP	4x6	6,65E+05	3,05E+06	21,8%	-9,87E+05	4,50E+06	-21,9%	3,04E+05	3,05E+06	10,0%	-1,34E+06	4,50E+06	-29,8%
	6x4	5,32E+05	3,05E+06	17,4%	-2,60E+06	4,50E+06	-57,8%	3,74E+05	3,05E+06	12,3%	-6,71E+05	4,50E+06	-14,9%
MCM	4x6	1,20E+06	-	-	-1,83E+06	-	-	7,17E+05	-	-	-3,05E+06	-	-
	6x4	1,03E+06	-	-	-4,87E+06	-	-	7,93E+05	-	-	-1,87E+06	-	-
MAX				45,8%			-57,8%			12,8%			-29,8%

		Core											
		σ_{0t} [Pa]	σ_{0td} [Pa]	Uti	σ_{0c} [Pa]	σ_{0cd} [Pa]	Uti	σ_{90t} [Pa]	σ_{90td} [Pa]	Uti	σ_{90c} [Pa]	σ_{90cd} [Pa]	Uti
BBB	4x6	2,15E+06	2,72E+07	7,9%	-3,07E+06	1,89E+07	-16,3%	3,73E+06	2,28E+07	16,4%	-6,43E+06	1,58E+07	-40,7%
	6x4	3,14E+06	2,33E+07	13,5%	-7,23E+06	1,62E+07	-44,6%	1,05E+06	2,67E+07	3,9%	-2,29E+06	1,85E+07	-12,4%
CBC	4x6	1,41E+06	2,67E+07	5,3%	-2,18E+06	1,85E+07	-11,8%	2,46E+06	2,33E+07	10,5%	-2,94E+06	1,62E+07	-18,1%
	6x4	3,41E+06	2,33E+07	14,6%	-5,65E+06	1,62E+07	-34,9%	1,14E+06	2,67E+07	4,3%	-1,80E+06	1,85E+07	-9,7%
KBK	4x6	2,09E+06	2,72E+07	7,7%	-2,58E+06	1,89E+07	-13,7%	3,43E+06	2,28E+07	15,0%	-4,76E+06	1,58E+07	-30,1%
	6x4	3,71E+06	2,33E+07	15,9%	-4,13E+06	1,62E+07	-25,5%	1,24E+06	2,67E+07	4,7%	-1,32E+06	1,85E+07	-7,1%
PBP	4x6	2,04E+06	2,67E+07	7,7%	-3,09E+06	1,85E+07	-16,7%	2,98E+06	2,33E+07	12,8%	-3,02E+06	1,62E+07	-18,6%
	6x4	5,32E+06	2,33E+07	22,8%	-8,02E+06	1,62E+07	-49,5%	1,85E+06	2,67E+07	6,9%	-2,60E+06	1,85E+07	-14,1%
MBM	4x6	2,15E+06	2,67E+07	8,1%	-3,07E+06	1,85E+07	-16,6%	3,73E+06	2,33E+07	16,0%	-6,43E+06	1,62E+07	-39,7%
	6x4	4,09E+06	2,33E+07	17,5%	-5,71E+06	1,62E+07	-35,2%	1,36E+06	2,67E+07	5,1%	-1,82E+06	1,85E+07	-9,9%
BCB	4x6	1,97E+06	1,01E+07	19,4%	-2,50E+06	1,31E+07	-19,1%	3,51E+06	8,53E+06	41,1%	-5,06E+06	1,09E+07	-46,3%
	6x4	4,26E+06	8,73E+06	48,8%	-5,86E+06	1,12E+07	-52,3%	1,41E+06	9,93E+06	14,2%	-1,91E+06	1,28E+07	-14,9%
CCC	4x6	1,35E+06	9933333	13,6%	-2,36E+06	12800000	-18,4%	2,09E+06	8,73E+06	23,9%	-5,12E+06	1,12E+07	-45,7%
	6x4	3,62E+06	8,73E+06	41,5%	-6,01E+06	1,12E+07	-53,7%	1,21E+06	9,93E+06	12,2%	-1,91E+06	1,28E+07	-14,9%
KCK	4x6	1,43E+06	1,01E+07	14,1%	-1,64E+06	1,31E+07	-12,6%	2,53E+06	8,53E+06	29,6%	2,73E+06	1,09E+07	25,0%
	6x4	4,35E+06	8,73E+06	49,8%	-7,38E+06	1,12E+07	-65,9%	1,47E+06	9,93E+06	14,8%	-2,32E+06	1,28E+07	-18,1%
PCP	4x6	1,81E+06	9933333	18,2%	-2,38E+06	12800000	-18,6%	2,53E+06	8,73E+06	29,0%	-4,99E+06	1,12E+07	-44,6%
	6x4	4,90E+06	8,73E+06	56,1%	-7,44E+06	1,12E+07	-66,4%	1,73E+06	9,93E+06	17,4%	-2,52E+06	1,28E+07	-19,7%
MCM	4x6	1,69E+06	9933333	17,0%	-2,11E+06	12800000	-16,5%	2,99E+06	8,73E+06	34,2%	-3,97E+06	1,12E+07	-35,4%
	6x4	4,57E+06	8,73E+06	52,3%	-7,74E+06	1,12E+07	-69,1%	1,56E+06	9,93E+06	15,7%	-2,54E+06	1,28E+07	-19,8%
MAX				56,1%			-69,1%			41,1%			-46,3%

Material	LxB	σ_x [Pa]	f_x [Pa]	σ_y [Pa]	f_y [Pa]	τ_{xy} [Pa]	f_v [Pa]	Norris [-]
BBB	4x6	-3,07E+06	2,83E+07	-6,43E+06	2,37E+07	0	9,50E+06	0,039
	6x4	-7,23E+06	2,77E+07	-2,29E+06	2,43E+07	0	9,50E+06	0,071
CBC	4x6	-1,53E+06	2,77E+07	-2,94E+06	2,43E+07	0	9,50E+06	0,009
	6x4	-5,65E+06	2,77E+07	-1,80E+06	2,43E+07	0	9,50E+06	0,043
KBK	4x6	-2,58E+06	2,83E+07	-4,76E+06	2,37E+07	0	9,50E+06	0,022
	6x4	-4,13E+06	2,77E+07	-1,32E+06	2,43E+07	0	9,50E+06	0,023
PBP	4x6	-3,09E+06	2,77E+07	-1,23E+06	2,43E+07	0	9,50E+06	0,012
	6x4	-8,02E+06	2,77E+07	-2,60E+06	2,43E+07	0	9,50E+06	0,087
MBM	4x6	-3,07E+06	2,77E+07	-6,43E+06	2,43E+07	0	9,50E+06	0,040
	6x4	-5,71E+06	2,77E+07	-1,82E+06	2,43E+07	0	9,50E+06	0,044
BCB	4x6	-2,50E+06	1,96E+10	-5,06E+06	1,64E+07	0	7,00E+06	0,023
	6x4	-5,86E+06	1,92E+07	-1,91E+06	1,68E+07	0	7,00E+06	0,097
CCC	4x6	-2,36E+06	1,92E+07	-5,12E+06	1,68E+07	0	7,00E+06	0,053
	6x4	-6,01E+06	1,92E+07	-1,91E+06	1,68E+07	0	7,00E+06	0,102
KCK	4x6	-1,64E+06	1,96E+10	-2,73E+06	1,64E+07	0	7,00E+06	0,010
	6x4	-7,38E+06	1,92E+07	-2,32E+06	1,68E+07	0	7,00E+06	0,154
PCP	4x6	-2,38E+06	1,92E+07	-5,00E+06	1,68E+07	0	7,00E+06	0,051
	6x4	-7,44E+06	1,92E+07	-2,52E+06	1,68E+07	0	7,00E+06	0,155
MCM	4x6	-2,11E+06	1,92E+07	-3,97E+06	1,68E+07	0	7,00E+06	0,033
	6x4	-7,76E+06	1,92E+07	-2,54E+06	1,68E+07	0	7,00E+06	0,170